

TARGETING TELOMERASE IN HER2 POSITIVE BREAST CANCER:

ROLE OF CANCER STEM CELLS

Jillian Elizabeth Koziel

Submitted to the faculty of the University Graduate School  
in partial fulfillment of the requirements  
for the degree  
Doctor or Philosophy  
in the Department of Medical and Molecular Genetics,  
Indiana University

February 2015

Accepted by the Graduate Faculty, Indiana University, in partial fulfillment of the requirements for the degree of Doctor of Philosophy.

---

Brittney-Shea Herbert, Ph.D., Chair

Doctoral Committee

---

Rebecca J. Chan, M.D., Ph.D.

---

Bryan P. Schneider, M.D.

October 21, 2014

---

Hiroshi Tanaka, Ph.D.

## ACKNOWLEDGEMENTS

I would first and foremost like to thank my mentor, Dr. Brittney-Shea Herbert, for all the advice, support, motivation, and encouragement over the last five years. Dr. Herbert provided endless insight and ideas into helping me complete this project and allowed me to develop as a young scientist throughout my time in her laboratory, both pushing me to achieve my goals and providing the time and space to do so. She truly cares about the well-being of the students under her supervision, as well as all the graduate students she advises in the Medical and Molecular Genetics Department, for which I will always be grateful.

I sincerely thank each of my committee members, Dr. Rebecca Chan, Dr. Bryan Schneider, and Dr. Hiromi Tanaka, for sharing of their time and knowledge with me. Their constructive criticisms, insightful comments, and encouragements helped to shape my research for the better and I am truly appreciative. I also thank my former committee members, Dr. Linda Malkas and Dr. Brenda Grimes, for their insight and expertise while they were at Indiana University.

I am grateful for my fellow lab mates, past and present, Melanie Fox, Amruta Phatak, Elizabeth Phipps, Alyssa Sprouse, and Catherine Steding. They provided technical assistance and advice, but most importantly friendship and encouragement throughout this journey. My time here would not have been the same without them. I thank Dr. Susan Clare and the members of her laboratory for a wonderful collaboration and friendship. I would also like to thank the Genetics Department administrative staff, especially Mrs. Peggy Knople, Mrs. Margie Day, Mrs. Jean Good, and Mrs. Susan Steele-Moore for all of their assistance with administrative duties.

This work would not have been possible without the generous gifts and sharing of resources and expertise by so many. I thank Dr. Francisco Esteva for kindly sharing the SKBR3 and trastuzumab-resistant SKBR3 cell lines used in parts of this study, as well as Dr. Harikrishna Nakshatri for kindly sharing the TMD-231 cell line derived in his laboratory. I am indebted to Geron Corporation for generously providing us with imetelstat and the control oligonucleotides essential to this project. I am also very appreciative of the Indiana University Simon Cancer Center (IUSCC) Infusion Pharmacy for saving and generously sharing extra trastuzumab with me. I thank Dr. Harlan Shannon for his help with the combination studies and Dr. George Sandusky for his help with the histology examinations. I am grateful for many laboratories on campus providing technical assistance, equipment use, and reagents, as well as the IUSCC flow cytometry core for their expertise. I thank the IUSCC for providing me a predoctoral cancer biology training fellowship and Dr. Hal Broxmeyer for providing me a predoctoral fellowship from his NIH T32 training grant. I also thank Susan G. Komen for the Cure for supporting our work.

I owe a huge thank you to my family and friends for their love and support throughout this journey. I thank my parents for their never-ending encouragement and unwavering confidence in me. I thank my niece and nephew (and I guess my brother and sister-in-law ☺) for always putting a smile on my face, especially when I need it the most. I wouldn't be who I am today and where I am today without the constant support, encouragement, and inspiration of those I cherish most, for which I am eternally grateful.

TARGETING TELOMERASE IN HER2 POSITIVE BREAST CANCER:  
ROLE OF CANCER STEM CELLS

Cancer stem cells (CSCs) are proposed to play a major role in tumor progression, metastasis, and recurrence. The Human Epidermal growth factor Receptor 2 (HER2) gene is amplified and/or its protein product overexpressed in approximately 20% of breast cancers. HER2 overexpression is associated with increased CSCs, which may explain the aggressive phenotype and increased likelihood of recurrence for HER2<sup>+</sup> breast cancers. Telomerase is reactivated in tumor cells, including CSCs, but has limited activity in normal tissues, providing support for the use of telomerase inhibition in anti-cancer therapy. Telomerase inhibition via an antagonistic oligonucleotide, imetelstat (GRN163L), has been shown to be effective in limiting cell growth *in vitro* and limiting tumor growth. Moreover, we have previously shown imetelstat can decrease metastases to the lungs, leading us to question if this is due to imetelstat targeting the CSC population. In this thesis, we investigated the effects of imetelstat on CSC and non-CSC populations of HER2<sup>+</sup> breast cancer cell lines, as well as a triple negative breast cancer cell line, which lacks HER2 overexpression. Imetelstat inhibited telomerase activity in both CSC and non-CSC subpopulations. Moreover, imetelstat treatment alone and in combination with trastuzumab significantly reduced the CSC fraction and inhibited CSC functional ability, as shown by a significant decrease in mammosphere counts and invasive potential. Tumor growth rate was slower in combination treated mice compared to either drug alone. Additionally, there was a trend toward decreased CSC marker expression in imetelstat treated xenograft cells

compared to vehicle control. The decrease in CSC marker expression we observed occurred prior to and after telomere shortening, suggesting imetelstat acts on the CSC subpopulation in telomere length dependent and independent mechanisms. Our study suggests addition of imetelstat to trastuzumab may enhance the effects of HER2 inhibition therapy.

Brittney-Shea Herbert, Ph.D., Chair

## TABLE OF CONTENTS

LIST OF TABLES .....	x
LIST OF FIGURES .....	xi
ABBREVIATIONS .....	xiv
CHAPTER ONE .....	1
Introduction and Literature Review .....	1
Breast Cancer Statistics and Subtypes .....	1
HER2 Positive Breast Cancer .....	2
Telomeres and Cancer .....	10
Telomerase and Cancer .....	15
Targeting Telomerase for Anti-Cancer Therapy .....	18
Cancer Stem Cell Hypothesis .....	22
Overall Objective and Hypothesis .....	27
Significance .....	29
CHAPTER TWO .....	30
Materials and Methods .....	30
Reagents .....	30
Cell Culture .....	30
Treatment with Imetelstat and/or Trastuzumab .....	31
Flow Cytometry and Fluorescence Activated Cell Sorting .....	34
Telomerase Activity Determination .....	34
Telomere Length Determination .....	35
Methylene Blue Cell Proliferation Assay for Combination Studies .....	36
Mammosphere Culture Assays .....	38
Invasion Assays .....	38

Western Immunoblotting .....	39
Xenograft Mice Studies .....	39
Statistical Analyses .....	42
CHAPTER THREE .....	43
Results .....	43
Long-term Treatment with Imetelstat Inhibits Cellular Proliferation and Telomerase Activity .....	43
CSCs Have Active Telomerase and Are Sensitive to Telomerase Inhibition via Imetelstat .....	49
Telomerase Inhibition via Imetelstat Can Decrease CSCs and Limit Mammosphere Formation .....	53
Imetelstat Augments the Effects of Trastuzumab in HER2 <sup>+</sup> Breast Cancer Cell Lines.....	63
Imetelstat in Combination with Trastuzumab Decreases the CSC Population....	68
Imetelstat in Combination with Trastuzumab Inhibits Self-renewal and Invasive Potential of CSCs.....	76
Imetelstat and trastuzumab Combination Treatment Decreases Primary Tumor Growth <i>In Vivo</i> .....	79
Imetelstat Treated Xenograft Cells Have Decreased CSC Features .....	87
CHAPTER FOUR.....	92
Discussion.....	92
CHAPTER FIVE .....	98
Conclusions and Future Directions .....	98

REFERENCES..... 104  
CURRICULUM VITAE

## LIST OF TABLES

Table 3.1. Panel of Cell Lines Studied .....	44
Table 3.2. HCC1569 Combination Index .....	65
Table 3.3. HCC1954 Combination Index .....	67
Table 3.4. Summary of Pilot Studies to Determine Metastatic Capability <i>In Vivo</i> .....	83
Table 3.5. Xenograft HCC1954 Study Lung Metastases Observations .....	88

## LIST OF FIGURES

Figure 1.1. HER2 Signaling Pathway .....	4
Figure 1.2. HER2 Targeted Therapies .....	7
Figure 1.3. Proposed Mechanisms of Trastuzumab Resistance.....	8
Figure 1.4. Telomeres Protect Chromosome Ends.....	11
Figure 1.5. Senescence and Crisis are Initiated by Telomere Shortening .....	14
Figure 1.6. The Telomerase Enzyme Complex.....	16
Figure 1.7. Imetelstat Structure .....	20
Figure 1.8. Imetelstat Binds to the Template Region of hTR .....	21
Figure 1.9. Rationale for Targeting Cancer Stem Cells.....	24
Figure 2.1. Experimental Set-up for Cumulative Population Doubling Graphs .....	32
Figure 2.2. Experimental Set-up for Long-term Culture .....	33
Figure 2.3. Isobologram Method to Quantitate Drug Interactions .....	37
Figure 2.4. Xenograft HCC1954 Animal Study Set-up.....	40
Figure 2.5. TMD-231 Animal Study Set-up .....	41
Figure 3.1. Certain Cell Lines Overexpress HER2 Protein .....	45
Figure 3.2. Long-term Treatment with Imetelstat Inhibits Cellular Proliferation.....	46
Figure 3.3. Continued Treatment with Imetelstat Inhibits Telomerase Activity.....	48
Figure 3.4. Flow Sorting Gating Strategy .....	50
Figure 3.5. CSCs have Active Telomerase that can be Inhibited by Imetelstat .....	51
Figure 3.6. Average Telomere Length is Similar in all Subpopulations with Imetelstat Treatment Leading to Telomere Shortening .....	52
Figure 3.7. Longer Telomeres are Shortened with Imetelstat Treatment.....	54
Figure 3.8. Cell Lines have Variable CSC Marker Expression.....	55
Figure 3.9. Cell Lines have Variable ALDH1 Protein Expression.....	57

Figure 3.10. Imetelstat, but not the Sense Oligonucleotide Control, Decreases the Percentage of CSCs .....	58
Figure 3.11. Imetelstat Inhibits Mammosphere Formation .....	59
Figure 3.12. Imetelstat Decreases the Percentage of CSCs in the TNBC Cell Line TMD-231 .....	60
Figure 3.13. Imetelstat Inhibits Mammosphere Formation in TMD-231 Cells .....	61
Figure 3.14. Imetelstat Inhibits Telomerase Activity in both Adherent and Spheroid TMD-231 Cell Cultures.....	62
Figure 3.15. Imetelstat Augments the Effects of Trastuzumab in HCC1569 Cells.....	64
Figure 3.16. Imetelstat Augments the Effects of Trastuzumab in HCC1954 Cells.....	66
Figure 3.17. Imetelstat Alone and in Combination with Trastuzumab Decreases the CD44 <sup>+</sup> /CD24 <sup>-</sup> CSC Population.....	69
Figure 3.18. Trastuzumab, Imetelstat, and Combination Treatment Decrease the ALDH <sup>+</sup> CSC Population in HCC1569 Cells .....	70
Figure 3.19. Trastuzumab, Imetelstat, and Combination Treatment Decrease the ALDH <sup>+</sup> CSC Population in HCC1954 Cells .....	72
Figure 3.20. Trastuzumab, Imetelstat, and Combination Treatment Decrease the ALDH <sup>+</sup> CSC Population in SKBR3 Cells .....	73
Figure 3.21. Trastuzumab Limits Cellular Proliferation in SKBR3 Cells, But Not SKBR3-R Cells.....	74
Figure 3.22. Trastuzumab, Imetelstat, and Combination Treatment Decrease the ALDH <sup>+</sup> CSC Population in SKBR3-R Cells.....	75
Figure 3.23. Trastuzumab, Imetelstat, and Combination Treatment Inhibit Mammosphere Formation of HCC1569 Cells .....	77
Figure 3.24. Imetelstat Alone and in Combination with Trastuzumab Limits Invasion Potential of HCC1569 Cells .....	78

Figure 3.25. Xenograft HCC1954 Cells have Similar Morphology to Parental Cells.....	80
Figure 3.26. Xenograft HCC1954 Cells Overexpress HER2 Protein .....	81
Figure 3.27. Xenograft HCC1954 Cells Metastasize to the Lungs.....	84
Figure 3.28. Trastuzumab and Combination Treatment Inhibits Xenograft HCC1954 Primary Tumor Growth.....	85
Figure 3.29. Imetelstat, Trastuzumab, and Combination Treatment Decreases Xenograft HCC1954 Tumor Growth Rates.....	86
Figure 3.30. Imetelstat Decreases TMD-2331 Primary Tumor Growth and Lung Metastases.....	89
Figure 3.31. Imetelstat Decreases TMD-231 CSC Features.....	91

## ABBREVIATIONS

ABCB1	ATP-binding cassette, sub-family B, Member 1
ABCG2	ATP-binding cassette, sub-family G, Member 2
AKT	v-akt murine thymoma viral oncogene
ALDH	Aldehyde dehydrogenase
ALT	Alternative Lengthening of Telomeres
AML	Acute Myeloid Leukemia
ANOVA	Analysis of Variance
ATCC	American Type Culture Collection
a.u.	Arbitrary Units
bp	Base pair
BRCA1	breast cancer 1, early onset
BRCA2	breast cancer 2, early onset
CI	Combination Index
CSC	Cancer Stem Cell
DAPI	4',6-diamidino-2-phenylindole
DEAB	Diethylaminobenzaldehyde
DIG	Digoxigenin
DMEM	Dulbecco's Modified Eagle's Medium
DMEM/F12	DMEM and Ham's F 12 50/50 Mix
EGFR	Epidermal Growth Factor Receptor
EMP	Epithelial Mesenchymal Plasticity
EMT	Epithelial Mesenchymal Transition
ER	Estrogen Receptor
FBS	Fetal Bovine Serum
FDA	Food and Drug Administration
FISH	Fluorescence In Situ Hybridization
FMO	Fluorescence Minus One
GRN163L	Imetelstat
H&E	Hematoxylin and Eosin
HBSS	Hank's Balanced Salt Solution
HER2	Human Epidermal Growth Factor Receptor 2
HER3	Human Epidermal Growth Factor Receptor 3
HER4	Human Epidermal Growth Factor Receptor 4
HSC	Hematopoietic Stem Cell
hTERT	human Telomerase Reverse Transcriptase
hTR	human Telomerase RNA component
IC	Internal control
IGF1R	Insulin-like Growth Factor 1 Receptor
IHC	Immunohistochemistry
Kb	kilobase
LB	Lysis Buffer
MAPK	Mitogen-Activated Protein Kinase
MET	Mesenchymal to Epithelial Transition
MM	Mismatch Control Oligonucleotide
MMP	Matrix Metalloproteinase
MTA	Metastasis Associated Protein
mTOR	Mechanistic Target of Rapamycin
MUC4	Mucin-4

NF- $\kappa$ B	Nuclear Factor Kappa-light-chain-enhancer of activated B cells
NK	Natural Killer
NOD/SCID	Non-obese Diabetic/Severe Combined Immunodeficient
NSG	NOD/LtSz-scid IL2Rgamma-null
PBS	Phosphate Buffered Saline
PBS-T	Phosphate Buffered Saline with Tween 20
PI3K	Phosphatidylinositol 3-Kinase
PIK3CA	Phosphatidylinositol 3-Kinase, Catalytic subunit Alpha
POT1	Protection Of Telomeres 1
PR	Progesterone Receptor
PTEN	Phosphatase and Tensin
PVDF	Polyvinylidene Difluoride
RAP1	Repressor Activator Protein 1
RIPA	Radioimmunoprecipitation Assay Buffer
RPMI	Roswell Park Memorial Institute Medium
RTA	Relative Telomerase Activity
SD	Standard Deviation
SDS-PAGE	Sodium Dodecyl Sulfate Polyacrylamide Gel Electrophoresis
SEM	Standard Error of the Mean
siRNA	Small Interfering RNA
SSC	Saline Sodium Citrate
T-DM1	ado-trastuzumab emtansine
TIN2	TRF1-interacting nuclear factor 2
TNBC	Triple Negative Breast Cancer
TRAP	Telomeric Repeat Amplification Protocol
TPP1	tripeptidyl peptidase I
TRF	Terminal Restriction Fragment
TRF1	Telomeric Repeat Binding Factor 1
TRF2	Telomeric Repeat Binding Factor 2
UT	Untreated
Wnt	Wingless-type MMTV integration sites

## CHAPTER ONE

### INTRODUCTION AND LITERATURE REVIEW

#### **Breast Cancer Statistics and Subtypes**

Accounting for nearly 1 in every 4 deaths, cancer remains the second leading cause of death in the United States. An estimated 1.65 million new cancer cases will be diagnosed and 585,000 people will die of cancer in 2014 in the United States alone. The lifetime probability of developing cancer is 1 in 2 for men and 1 in 3 for women. Although 5-year survival rates have drastically improved since the 1970s due to advances in early detection and treatment, metastatic and recurrent disease remain difficult to treat (American Cancer Society, [www.cancer.org](http://www.cancer.org)).

Breast cancer is one of the most commonly diagnosed cancers in women, second to skin cancers. During their lifetime, about 1 in 8 (12%) of women will develop invasive breast cancer. An estimated 232,000 new cases of invasive breast cancer and 62,000 new cases of non-invasive carcinoma *in situ* will be diagnosed this year. Breast cancer is the second leading cause of cancer deaths in women, accounting for 15% of cancer fatalities and claiming an estimated 40,000 lives this year. Survival rates correlate with disease stage at diagnosis. Localized disease (Stage 0 or I) has a 5-year relative survival rate of nearly 100%. Relative 5-year survival rates for regional disease (Stage II and III) are 93% and 72%, respectively. The 5-year relative survival rate dramatically decreases when cancer is detected in distant organs or lymph nodes (Stage IV) to 22% (American Cancer Society, [www.cancer.org](http://www.cancer.org)).

Many factors have been linked to an increased risk of breast cancer. These factors include lifestyle factors such as weight, exercise level, smoking, alcohol use, contraceptive use, pregnancy history, and hormone replacement therapy. Other personal risk modifiers include race, age, high breast tissue density, and family history of breast cancer. An estimated 5-10% of breast cancers are due to inherited mutations, such as *BRCA1* and *BRCA2* mutations in familial breast and ovarian cancer and *p53* mutations in Li-Fraumeni syndrome (American Cancer Society, [www.cancer.org](http://www.cancer.org)).

Breast cancer is traditionally classified based on receptor expression status of estrogen receptor (ER), progesterone receptor (PR), and human epidermal growth factor receptor 2 (HER2). While receptor status remains fundamental to classification and treatment determination in breast cancer, seminal work by Perou and colleagues expanded our understanding of the heterogeneity and complexity of this disease. Based on hierarchical clustering analysis of cDNA microarray data, Perou and collaborators discovered five distinct molecular subtypes of breast cancer: basal-like, HER2, normal-like, Luminal A, and Luminal B (Perou et al., 2000). Further work showed the intrinsic subtypes highly correlated with clinical outcomes, including poor prognosis in the basal-like and HER2<sup>+</sup> cancer subtypes, as well as significant differences in survival between the luminal subtypes (Sorlie et al., 2001).

### **HER2 Positive Breast Cancer**

The *HER2* (Human Epidermal Growth Factor Receptor 2) gene, also known as *ERBB2* and *neu*, encodes a 185 kDa receptor tyrosine kinase (Akiyama et al., 1986). HER2 is a member of the human epidermal growth factor receptor family, including EGFR (also known as HER1), HER3, and HER4. HER receptors exist as monomers at

the cell surface and dimerize upon ligand binding. HER2 does not have a known ligand, but it is the preferential heterodimerization partner for all HER family receptors (Yarden, 2001). Upon dimerization, the receptors auto and cross-phosphorylate, which activates many downstream signaling molecules, including the ras-MAPK and PI3K-AKT pathways, leading to cell cycle progression, cell survival, and proliferation (Reese and Slamon, 1997). Figure 1.1 shows the signaling pathways activated upon receptor dimerization.

The *HER2* gene is found amplified and/or its protein product the HER2 receptor overexpressed based upon IHC and FISH analyses in approximately 20% of all breast cancers, with the classification as the HER2 positive (HER2<sup>+</sup>) breast cancer subtype. HER2 amplification/overexpression is a predictor of decreased overall survival, decreased time to relapse, increased early metastases, and poor prognosis (Slamon et al., 1987; Slamon et al., 1989; Tiwari et al., 1992). Additionally, HER2 expression level positively correlates with tumor grade, S-phase (dividing) cell fraction, and aneuploidy (Ross et al., 2009). Tumors with HER2 overexpression are oncogene addicted due to their dependency on HER2 function, shown by knockdown of HER2 receptor by siRNA, kinase-dead HER2, and anti-HER2 antibodies *in vitro* and inducible tumor models *in vivo* leading to apoptosis and tumor regression in HER2 overexpressing cancer cells, but not tumor cells without HER2 overexpression (reviewed in (Moasser, 2007)).

The oncogene addiction and poor clinical prognosis of HER2<sup>+</sup> breast cancers necessitated therapeutic targeting of the HER2 receptor. Trastuzumab (Herceptin™, Genentech) was the first available HER2-targeted therapy. Trastuzumab is a humanized murine monoclonal antibody that binds to the extracellular domain of the HER2 receptor. While its mechanism of action is not completely established, trastuzumab is thought to exert its antitumor activity through activation of antibody-

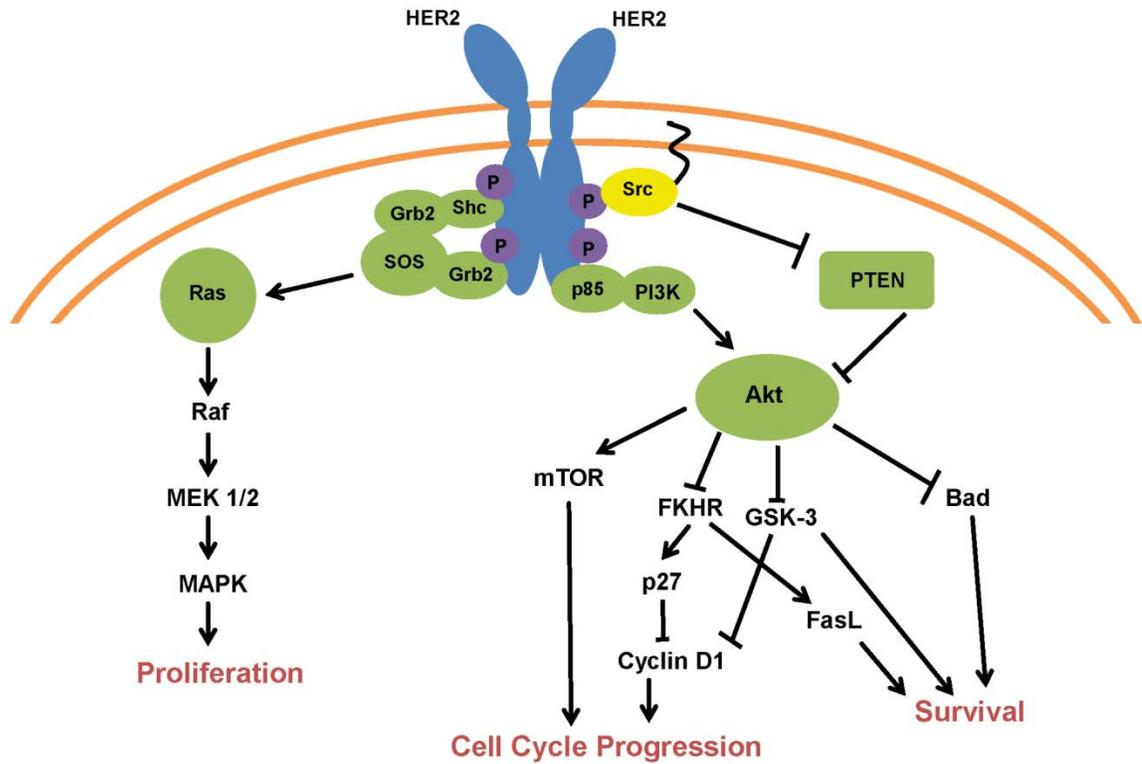


**Figure 1.1. HER2 Signaling Pathway.** Upon receptor dimerization and phosphorylation, ras-MAPK and PI3K-Akt pathways are activated, leading to proliferation, cell cycle progression, and survival. Adapted from (Lin and Winer, 2007).

dependent cell cytotoxicity, abrogation of intracellular signaling, inhibition of proteolytic cleavage of the extracellular domain, decreased DNA damage repair, and reduction of tumor angiogenesis (Bianchini and Gianni, 2014; Spector and Blackwell, 2009).

Pertuzumab (Perjeta™, Genentech) is another monoclonal antibody targeting the extracellular domain of HER2, but at a different epitope than trastuzumab. Pertuzumab blocks receptor dimerization and gained FDA approval in 2012 for first line HER2<sup>+</sup> metastatic breast cancer treatment when used in combination with trastuzumab and docetaxel due to prolonged progression free survival (Baselga et al., 2012).

Ado-trastuzumab emtansine (Kadcyla™, Genentech), abbreviated T-DM1, is a novel antibody-drug conjugate consisting of the monoclonal antibody trastuzumab stably linked to the cytotoxic microtubule inhibitor DM1 (derivative of maytansine). T-DM1 improves the therapeutic index and minimizes exposure to normal tissue by specifically delivering the cytotoxic drug to HER2 overexpressing cells. T-DM1 gained FDA approval as a second line HER2<sup>+</sup> metastatic breast cancer therapy in 2013 based on prolonged progression free survival and overall survival (Verma et al., 2012).

Lapatinib (Tykerb™, GlaxoSmithKline) was the first available tyrosine kinase inhibitor for HER2<sup>+</sup> breast cancer. Lapatinib is a small molecule inhibitor of both HER2 and EGFR that reversibly binds to the receptor's intracellular ATP-binding pocket and prevents downstream signaling by inhibiting receptor autophosphorylation (Li and Li, 2013).

The novel next-generation tyrosine kinase inhibitors, neratinib (HKI-272, Puma Biotechnology) and afatinib (Gilotrif, Boehringer Ingelheim Pharmaceuticals), are irreversible pan-HER kinase inhibitors that covalently bind cysteine residues in the ATP-binding pockets of EGFR and HER2, as well as HER4 with neratinib, and inhibit receptor autophosphorylation. While monotherapy clinical trials of these agents have been promising, combination therapies have not proven more efficacious thus far and both

agents lack FDA approval for treatment of HER2<sup>+</sup> breast cancer (Zhang and Munster, 2014). Figure 1.2 summarizes the HER2 targeted therapy options.

While HER2 targeted therapy revolutionized outcomes in HER2<sup>+</sup> breast cancer, many patients are either initially resistant or acquire resistance to trastuzumab leading to disease progression. Many mechanisms of trastuzumab resistance have been proposed (See Figure 1.3). One such mechanism involves a disrupted interaction between HER2 and trastuzumab through either glycoprotein Mucin-4 (MUC4) overexpression which sterically hinders antibody binding to HER2 extracellular domain or overexpression of p95 HER2, a truncated HER2 receptor that lacks the extracellular domain and thus the trastuzumab binding site (Mukohara, 2011; Nahta et al., 2006). Another mechanism of trastuzumab resistance is through compensatory signaling from other HER family members, such that inhibition of PI3K and MAPK by trastuzumab blocking HER2 may be bypassed by activating signals from HER1 and HER4 (Awada et al., 2012). Overexpression of insulin-like growth factor 1 receptor (IGF1R), which also activates the PI3K pathway, leads to trastuzumab resistance (Lu et al., 2001; Nahta et al., 2005). Additionally, loss of PTEN function, PIK3CA mutations, cyclin E amplification/overexpression, and p27 downregulation may also contribute to trastuzumab resistance (Mohd Sharial et al., 2012; Nahta and Esteva, 2006; Scaltriti et al., 2011). ER signaling is thought to be involved in lapatinib resistance (Xia et al., 2006). Resistance remains a serious concern and many strategies for overcoming it are being investigated, including combining HER2 inhibitors, combination with endocrine therapy in ER<sup>+</sup> patients, and inhibitors of the PI3K/AKT/mTOR pathway (Mohd Sharial et al., 2012).

Additional challenges of HER2 targeted therapy relate to cardiotoxicity and the blood-brain barrier. HER2 has been shown essential to normal heart ventricle

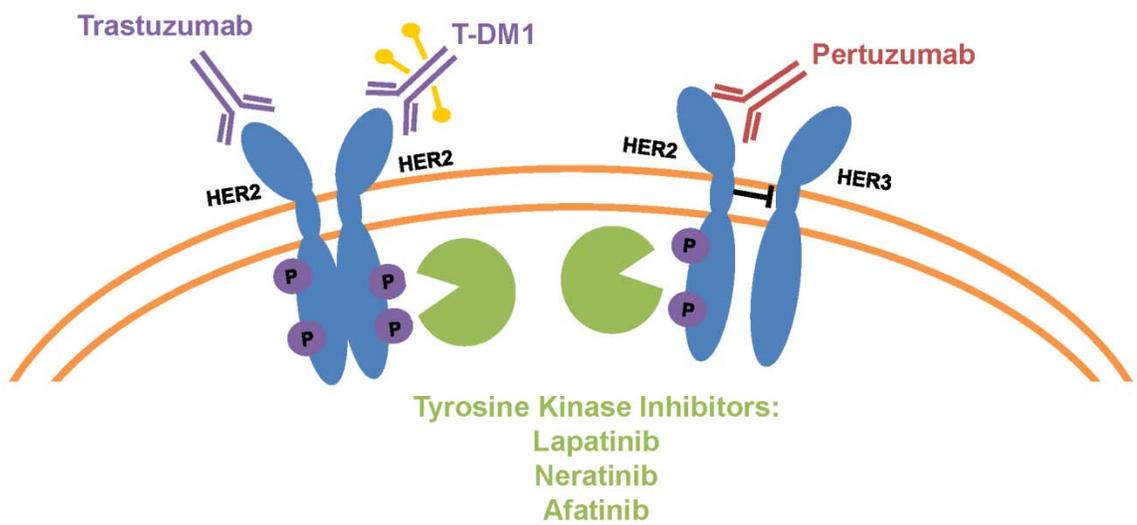


**Figure 1.2. HER2 Targeted Therapies.** HER2 can be inhibited many ways, including use of monoclonal antibodies (trastuzumab, pertuzumab, and T-DM1) and tyrosine kinase inhibitors (lapatinib, neratinib, and afatinib). Adapted from (Zelnak and Wisinski, 2014).

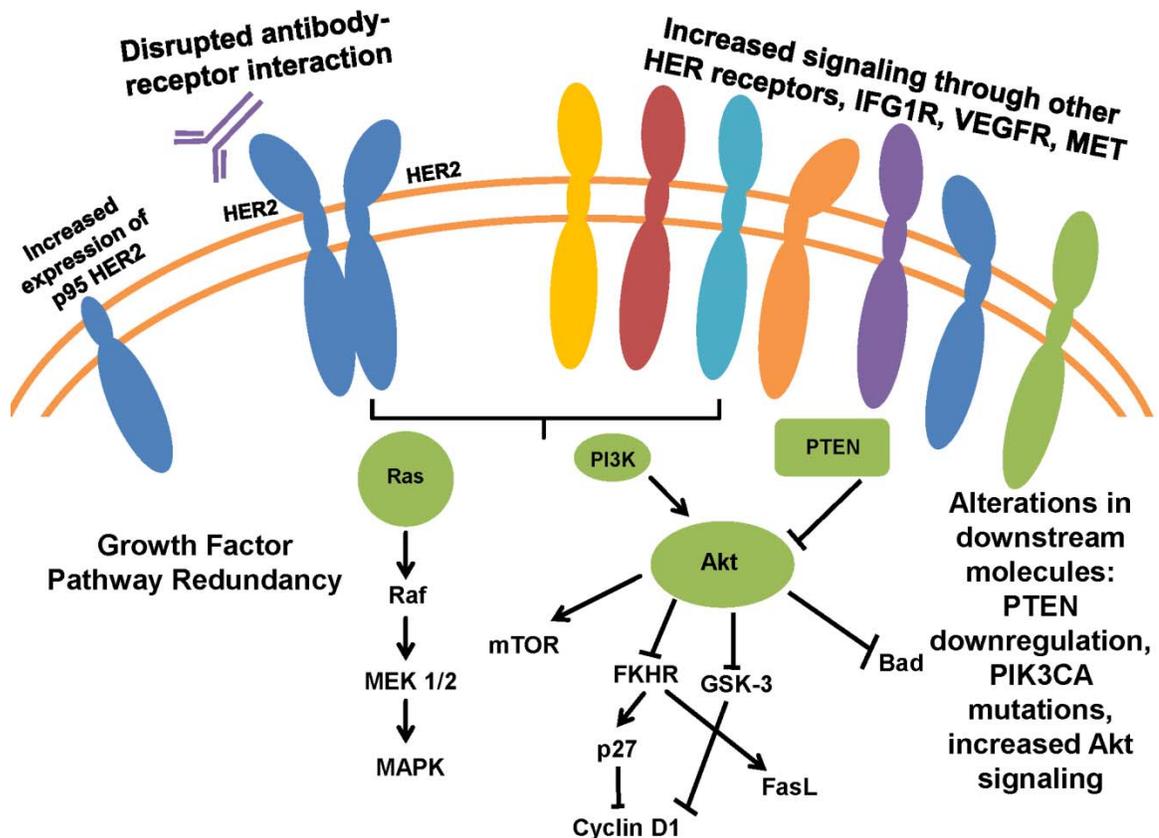


**Figure 1.3. Proposed Mechanisms of Trastuzumab Resistance.** Disrupted interaction of antibody and receptor, increased signaling through other growth factor receptors, and alterations in downstream signaling molecules are all possible mechanisms of resistance. Adapted from (Mohd Shariyal et al., 2012).

development and conditional mutant mice develop severe dilated cardiomyopathy, suggesting the importance of HER2 in normal cardiac function and potential cardiac toxicities with HER2 targeted therapy (Ozcelik et al., 2002). Indeed, the pivotal phase III trial leading to trastuzumab FDA approval found asymptomatic or symptomatic cardiac dysfunction occurred in 27% of patients receiving trastuzumab plus anthracycline and cyclophosphamide versus 8% in anthracycline and cyclophosphamide alone and 13% of the group given trastuzumab plus paclitaxel versus 1% of patients given paclitaxel alone (Slamon et al., 2001). A meta-analysis of five randomized clinical trials of trastuzumab therapy in HER2<sup>+</sup> breast cancer revealed a significant increased risk of congestive heart failure and significant increased risk of grade significant left ventricular ejection fraction reduction in the trastuzumab arm (Bria et al., 2008). Trastuzumab related cardiac toxicities appear to largely be reversible, with one study finding mean time to recovery of left ventricular ejection fraction was 1.5 months following cessation of trastuzumab and increases in left ventricular ejection fraction in 37 out of 38 patients (84% of which underwent medical treatment for left ventricular dysfunction) (Ewer et al., 2005). The most important risk factors for developing trastuzumab-induced cardiomyopathy include age, previous exposure to anthracyclines, and borderline ejection fraction before treatment (Guglin et al., 2008). Clinical trial data have demonstrated HER2 positive metastatic breast cancer patients are two to four times more likely than HER2 negative disease patients to develop brain metastases (Mehta et al., 2013). Additionally, a large retrospective trial of early stage breast cancer patients found HER2 positive disease is a significant risk factor for central nervous system relapse. Patients with HER2<sup>+</sup> tumors had a 2.7% 10-year cumulative incidence of central nervous system disease as the site of first relapse compared to 1.0% in HER2 negative tumors and 6.8% cumulative incidence of central nervous system metastases compared to 3.5% in HER2 negative patients (Pestalozzi et al., 2006). Studies indicate trastuzumab does not itself increase

the risk of brain metastasis, but is likely a consequence of prolonged survival, revealing the central nervous system as a sanctuary site due to the inability of trastuzumab to penetrate the blood-brain barrier (Lin and Winer, 2007; Mehta et al., 2013). Indeed, one study found the median trastuzumab level ratio in serum to cerebrospinal fluid was 420:1 and 76:1 after whole brain radiotherapy, which is thought to disrupt the blood-brain barrier (Stemmler et al., 2007). With improvements in patient survival, resistance and central nervous system disease remain key challenges of HER2 targeted therapies. While HER2<sup>+</sup> tumors have an oncogene dependence on HER2, these tumors, like all cancers, must also achieve limitless replicative potential to continue to grow and thrive. The potential for replicative immortality is mainly achieved by telomerase reactivation and maintenance of telomere length. Inhibiting telomerase activity and thus decreasing telomere length could aid in anti-HER2 treatment by blocking another dependence of these tumor cells.

### **Telomeres and Cancer**

Telomeres are DNA-protein complexes that cap and protect the ends of linear chromosomes (Figure 1.4) (Blackburn, 1991). A repetitive TTAGGG sequence, up to 20 Kb in length, followed by a 3' single-stranded G-rich overhang comprise the DNA component of human telomeres (Makarov et al., 1997; Moyzis et al., 1988). A T-loop structure is formed by invasion of the single-stranded overhang into the double-stranded telomeric repeats, protecting the telomere from unregulated nuclease digestion of the 3' overhang and end-to-end fusions (Griffith et al., 1999; Wei and Price, 2003). The protein component of human telomeres is comprised of six proteins (TRF1, TRF2, POT1, TIN2,

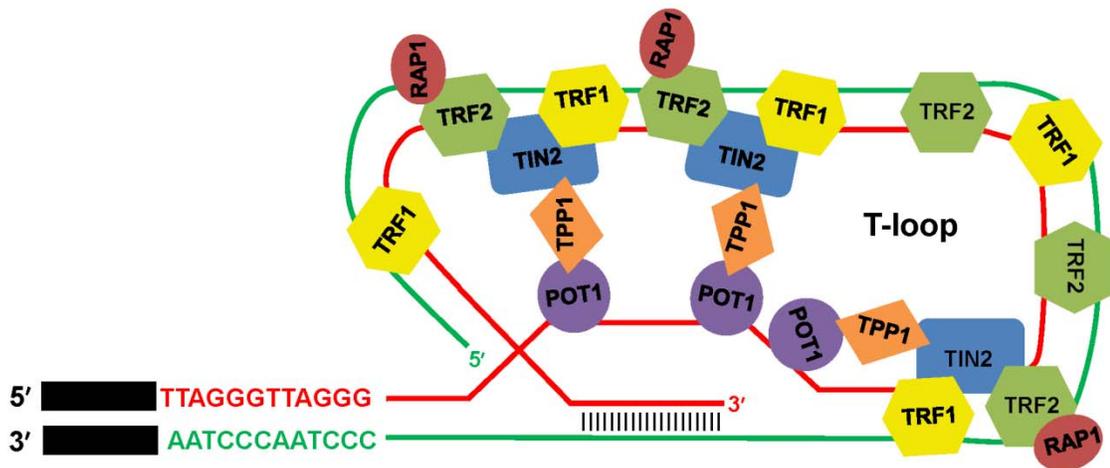


**Figure 1.4. Telomeres Protect Chromosome Ends.** Telomeres are comprised of TTAGGG telomeric repeats ending with a 3' G-rich overhang that invades into the double stranded repeats to form a T-loop structure. Telomeric DNA, along with the shelterin proteins (TRF1, TRF2, TIN2, TPP1, POT1, and RAP1), cap the ends of linear chromosomes and prevent them from being recognized as double-strand breaks. Adapted from (Denchi, 2009).

TPP1, and RAP1) that form the shelterin complex, which is responsible for t-loop formation and telomere protection against DNA repair machinery recognizing telomeres as double-strand breaks (de Lange, 2005). TRF1 and TRF2 show specificity for binding double-stranded TTAGGG replicative DNA, while POT1 shows specificity for single-stranded TTAGGG repeats (Palm and de Lange, 2008). TIN2, TPP1, and RAP1 are recruited to the telomere by TRF1 and TRF2 and act as tethering proteins to keep the shelterin complex stable (de Lange, 2005). TIN2 joins TRF1 and TRF2; TPP1 links TIN2 to POT1; and Rap1 interacts with TRF2 and represses homology-directed repair at chromosome ends (Denchi, 2009; Kabir et al., 2010). Conditional deletion of *TRF1* and *TRF2* in murine models reveals the shelterin complex protects telomeres from ATM (ataxia telangiectasia mutated) and ATR (ataxia telangiectasia and Rad 3 related) signaling, homologous recombination, classical non-homologous end joining, microhomology-mediated alternative non-homologous end joining, and resection (Sfeir and de Lange, 2012).

DNA polymerases are incapable of completely replicating the linear ends of DNA due to the requirement of primers to initiate synthesis and the unidirectional addition of nucleotides, leading to the phenomenon known as the “end-replication problem” and erosion of telomeric DNA with each cell division (Harley et al., 1990; Levy et al., 1992). Human leukocytes lose approximately 25 base pairs of telomeric DNA per year, with reports of up to 45 bp per year (Muezzinler et al., 2013). Normal somatic cells have a finite replicative capacity and enter into a senescent phase of terminal growth arrest once they reach their limited number of doublings (Hayflick and Moorhead, 1961). Telomere length acts as a mitotic clock in that once dividing cells reach a certain telomere length, senescence is signaled to protect from the loss of critical genes during replication (Allsopp and Harley, 1995; Harley et al., 1992). Ultimately, telomere erosion

triggers a DNA damage response leading to growth arrest, called the M1 stage (d'Adda di Fagagna et al., 2003). Cells can bypass M1 senescence in the absence of cell-cycle checkpoint pathways p53 and/or Rb and cells continue to proliferate until telomeres become critically short, resulting in crisis (M2 stage) (Wright and Shay, 1992). Crisis is characterized by many uncapped chromosome ends, chromosome breakage fusion bridge cycles, end fusions, and mitotic catastrophe leading to apoptosis (Shay and Wright, 2005). In a rare M2 cell, telomerase can become reactivated leading to indefinite cellular proliferation and this escaping crisis is thought to be a hallmark of cancer (Figure 1.5) (Hanahan and Weinberg, 2000).

Short, dysfunctional telomeres are a common feature of cancer cells (Maser and DePinho, 2002). Telomere attrition promotes genomic instability and cancer development by inducing chromosome fusions and breakage (Gunes and Rudolph, 2013). Artandi and colleagues showed telomerase deficient, p53 mutant mice developed epithelial cancers through this process of breakage fusion bridge cycles forming complex non-reciprocal translocations and this model of telomere dysfunction may explain the massive ploidy changes associated with tumorigenesis (Artandi et al., 2000). Additional work in telomerase deficient mice and studies of human disease suggest telomere dysfunction plays a role in early stages of carcinogenesis (Boulton et al., 1997; Chin et al., 1999; Meeker and Argani, 2004; Meeker et al., 2004; Roger et al., 2013; Rudolph et al., 1999; Rudolph et al., 2001; Tanaka et al., 2012). Additionally, work from the Rudolph Lab provides evidence supporting the hypothesis that telomere dysfunction induces chromosomal instability and increases tumor initiation, but telomerase is needed for genome stabilization and tumor progression following initiation (Bergus-Nahrman et al., 2012).

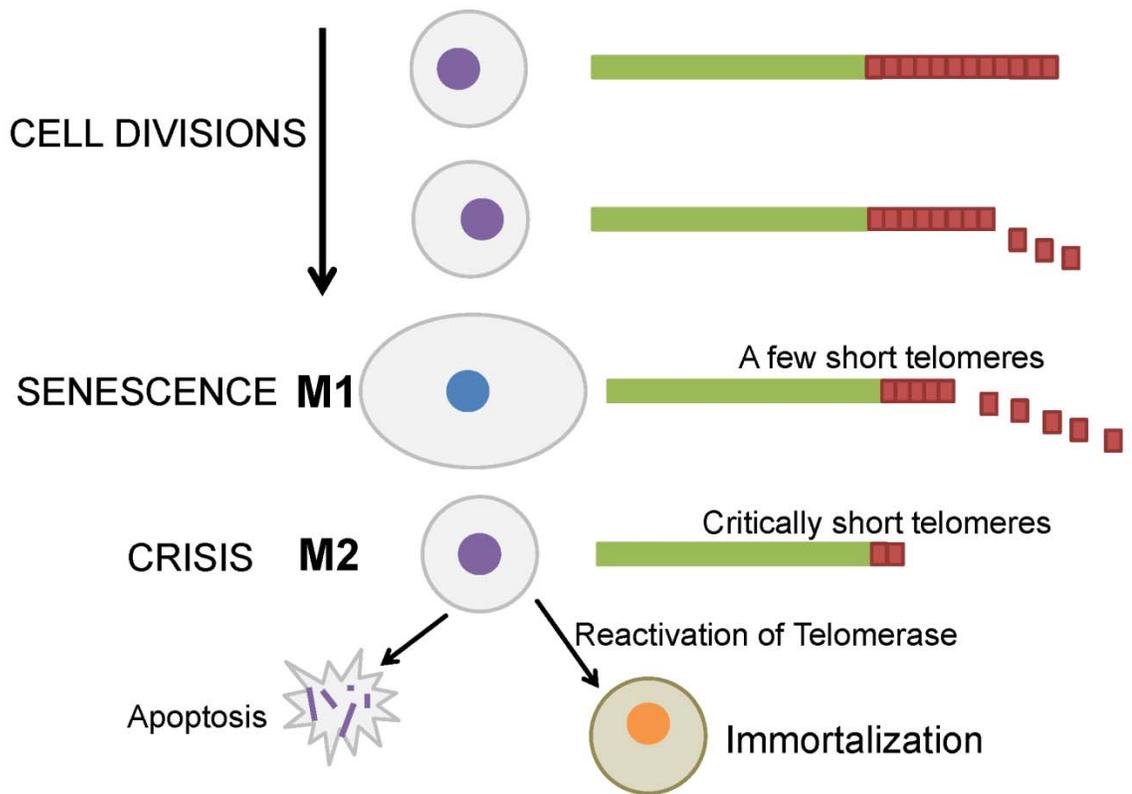


**Figure 1.5 Senescence and Crisis are Initiated by Telomere Shortening.** Telomeres progressively shorten with each cell division until a few short telomeres signal a growth arrest, known as senescence (M1). In the absence of important cell cycle checkpoint pathways, cells can bypass senescence and continue dividing until telomeres become critically short, triggering crisis (M2). At this point, most cells undergo apoptosis, but rarely cells can reactivate telomerase and become immortal. Adapted from (Shay and Wright, 2010).

## Telomerase and Cancer

Complete replication of telomeres is accomplished by telomerase, a specialized enzyme capable of reverse transcribing DNA (Blackburn, 2005). Telomerase is comprised of the protein hTERT, which contains a reverse transcriptase domain capable of catalyzing the addition of a six nucleotide repeat (TTAGGG) onto the ends of telomeres, and an RNA component (termed hTR), which contains a template region that is complementary to the human telomere sequence (Figure 1.6) (Feng et al., 1995; Greider and Blackburn, 1987; Morin, 1989). Other telomere/telomerase associated proteins (such as TEP1, HSP90, p23, dyskerin, NOP10, NHP2, and GAR1) are required for assembly of a functional telomerase holoenzyme complex (Cong et al., 2002). Telomerase expression is low or absent in normal human somatic cells, which have a limited replicative capacity; however, telomerase is expressed in embryonic development, germ line cells, and stem cells of proliferating tissues (Chiu et al., 1996; Kim et al., 1994; Wright et al., 1996). Transfection of normal somatic cells with vectors containing *TERT* can elongate telomeres and extend the lifespan of normal cells *in vitro* (Bodnar et al., 1998). The addition of telomerase to normal cells does not cause tumorigenicity despite conferring cellular immortality. To create tumorigenic cells, SV40 large T-antigen and oncogenic H-ras are required in addition to ectopic expression of TERT (Hahn et al., 1999).

Approximately 90% of cancers have telomerase reactivation, enabling cancer cells to maintain their telomere length just above the critically short threshold and thereby avoid senescence and apoptosis and acquire indefinite replicative/proliferative capacity (Hanahan and Weinberg, 2011; Kim et al., 1994). The remaining 10% of cancers, mainly soft tissue sarcomas and osteosarcomas, maintain telomere length through the alternative lengthening of telomeres (ALT) pathway (Henson et al., 2005).



The ALT pathway is thought to rely on homologous recombination between telomeres and is characterized by highly heterogeneous telomere lengths and the formation of ALT-associated promyelocytic leukemia (PML) bodies (APB) (Nabetani and Ishikawa, 2011). A significant correlation has been shown between telomerase activity and tumor size, lymph node status, and stage in carcinomas with telomerase activity increasing as tumor progression occurs (Hoos et al., 1998; Looi et al., 2007; Watanabe et al., 2002). Additionally, increased telomerase activity is associated with increased risk of death, disease recurrence, and decreased disease-free survival (Clark et al., 1997; Liu, 2011).

Interestingly, work has shown an association between HER receptors and their downstream signaling pathways and hTERT expression and telomerase activity. One study found in cells with EGFR overexpression EGF activates the hTERT promoter through MAPK signaling and MEK inhibitors blocked the activation of hTERT mRNA expression (Maida et al., 2002). Another group reported hTERT promoter activity was stimulated by HER2, Ras, and Raf via ERK-MAP-kinase dependent phosphorylation of the transcription factor ER81. Furthermore, hTERT expression was increased in HER2<sup>+</sup> breast cancer cell lines and tumor samples relative to HER2<sup>-</sup> counterparts (Goueli and Janknecht, 2004). Moreover, the results from this study were confirmed with breast cancer patient samples again showing hTERT transcriptional activation in specimens with increased HER2 and ER81 expression (Vageli et al., 2009). Additionally, HER2 was found to mediate hTERT transcription through NF- $\kappa$ B and c-myc activation (Papanikolaou et al., 2011). Furthermore, histone 3 phosphorylation by MAPK induces hTERT expression and telomerase activity (Ge et al., 2006). These reports support a role for HER2 signaling in the induction of telomerase activity and provided the rationale for the work in our laboratory studying the effect of pharmacological inhibition of telomerase in HER2<sup>+</sup> breast cancer cells (Goldblatt et al., 2009a).

## Targeting Telomerase for Anti-Cancer Therapy

Telomerase is an attractive target for cancer therapeutics for a variety of reasons. Primarily, telomerase activity is required for nearly all tumors (90% reactivate telomerase) to achieve limitless replicative potential. Telomerase is encoded by non-redundant (unique) genes, having significant therapeutic implications in that tumors are less likely to develop resistance to anti-telomerase therapies than other cancer targets that are members of a gene family (Harley, 2008). Additionally, telomerase expression is absent or low in normal tissues, which generally have longer telomeres than cancer cells, providing a degree of tumor specificity for telomerase targeted therapeutics (Ouellette et al., 2011). This differential expression between normal and cancer cells provide a therapeutic window in which cancer cells can efficiently be targeted by telomerase inhibitors while normal cells remain largely unaffected (Shay and Wright, 2006).

Various strategies have been employed in targeting telomeres and telomerase. The most advanced anti-telomerase therapeutic is the RNA template antagonistic oligonucleotide imetelstat (GRN163L) and the focus of this thesis (See below) (Roth et al., 2010). Telomerase enzymatic activity can also be inhibited by small molecule inhibitors that bind to the active site of hTERT (BIBR1532) (Ruden and Puri, 2013). Telomerase immunotherapy can be used to elicit cytotoxic T cell immune responses to kill cells expressing the hTERT peptide (GV1001 and GRN-VAC1) (Harley, 2008). Another approach involves using gene therapy to drive expression of a lytic virus from the TERT promoter leading to cell lysis (Telomelysin) (Ouellette et al., 2011). G-quadrex stabilizers prevent telomerase from binding to the telomeres and uncap telomeres through displacement of TRF2 and POT1 (Telomestatin) (Kelland, 2007).

As mentioned, imetelstat is the most advanced telomerase inhibitor to date. Imetelstat has been studied in 17 Phase I/II clinical trials, one of which is recruiting pediatric patients with recurrent brain tumors and two of which were done in the metastatic breast cancer setting ([www.clinicaltrials.gov](http://www.clinicaltrials.gov)). Using the hTR template region sequence (5'-CUAACCCUACC-3') as their target, Geron Corporation developed a thio-phosphoramidate 13-mer oligonucleotide telomerase inhibitor, termed GRN163 (Asai et al., 2003). Subsequently, addition of a 5' terminal lipophilic (palmitoyl) group improved cellular uptake and enhanced potency of the telomerase inhibitor (lipid modification designated by an "L", termed GRN163L) (Figure 1.7) (Herbert et al., 2005). GRN163L, clinically known as imetelstat, binds with high affinity to the template region of the RNA component of human telomerase resulting in competitive inhibition of telomerase enzymatic activity by preventing telomerase from binding to and extending the telomere (Figure 1.8) (Gryaznov, 2010). Our group and others have shown imetelstat alone, and in combination with chemotherapeutic agents including paclitaxel, doxorubicin, trastuzumab, and ATM kinase inhibitors or irradiation, can inhibit telomerase in a wide variety of tumor cells and compromise cancer cell viability and growth, both *in vitro* and *in vivo* (Agarwal et al., 2008; Burchett et al., 2014; Dikmen et al., 2005; Dikmen et al., 2008; Djojsubroto et al., 2005; Goldblatt et al., 2009a; Goldblatt et al., 2009b; Gomez-Millan et al., 2007; Hochreiter et al., 2006; Shamma et al., 2008; Tamakawa et al., 2010).

A potential concern of telomerase inhibition therapy is the long lag time from start of treatment to cell death or senescence due to their mechanism of action. While cancer cells have shorter telomeres than normal cells, these cells must still undergo a large number of cell divisions before telomeres become critically short and signal a DNA damage response or growth arrest (Shay and Wright, 2006). This suggests telomerase

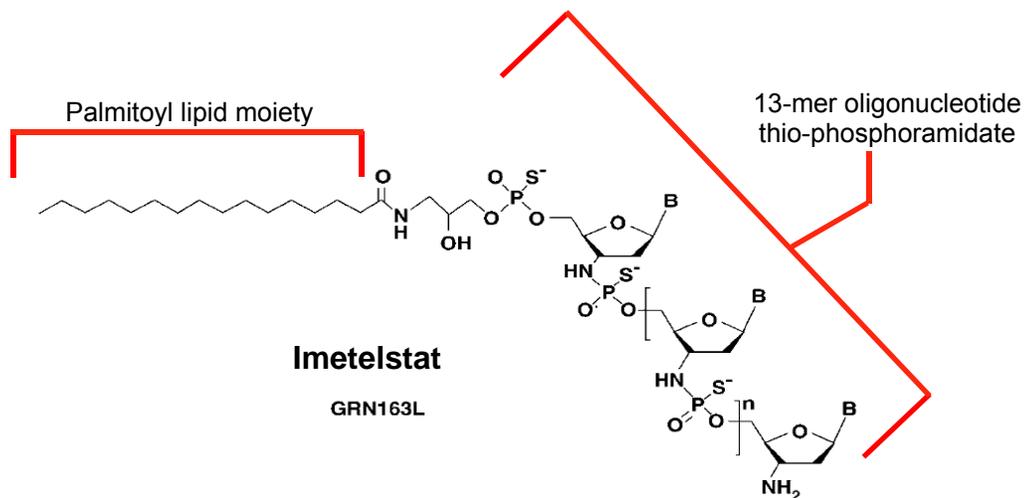


**Figure 1.7 Imetelstat Structure.** Imetelstat (GRN163L) is a telomerase template antagonist, consisting of a 13-mer thio-phosphoramidate oligonucleotide backbone covalently bound to a palmitoyl lipid moiety, which improves cellular uptake. Adapted from (Gryaznov, 2010).

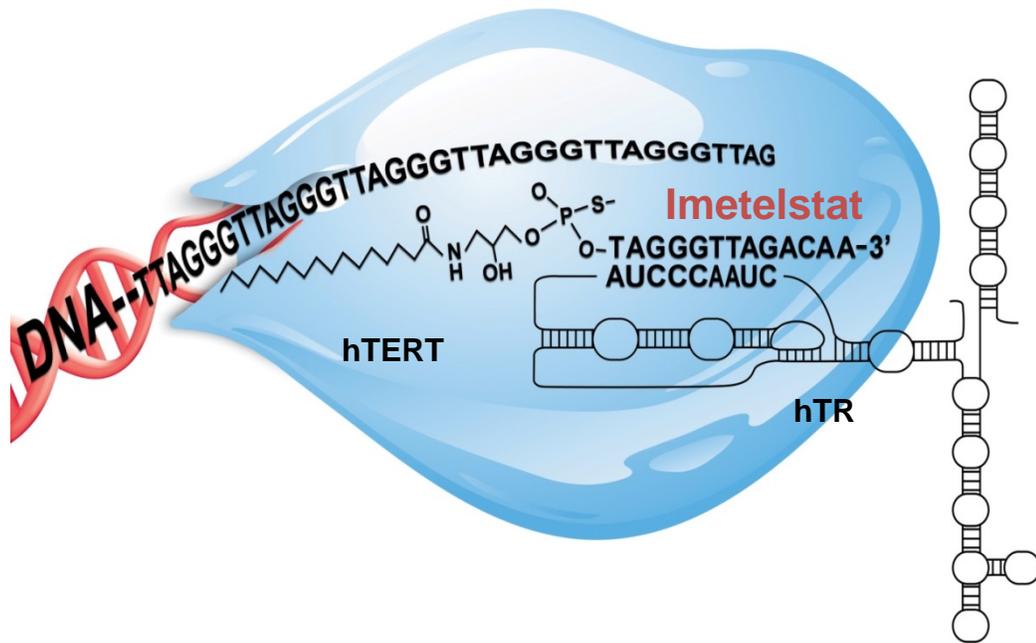


**Figure 1.8 Imetelstat Binds to the RNA Template of hTR.** Imetelstat prevents telomerase from binding telomeric DNA, leading to telomerase inhibition and telomere shortening. Adapted from (Gryaznov, 2010; Harley, 2008)

inhibitors would be most effective when used in combination with standard therapies that have a quick effect on tumor cells. Combination therapy may increase drug efficacy, leading to critical telomere shortening, extensive tumor reduction, and lower drug doses helping to reduce normal cell toxicity (Ruden and Puri, 2013). Furthermore, telomerase inhibitors, like imetelstat, will be best tolerated when used in combination with agents that have different dose-limiting toxicities, such as targeted therapies like trastuzumab that have very few hematological side effects.

### **Cancer Stem Cell Hypothesis**

The cancer stem cell (CSC) hypothesis postulates that many cancers are hierarchically organized and a subpopulation of cells within the tumor possess the basic properties of stem cells, the ability to self-renew and differentiate (Cho and Clarke, 2008). CSCs also have other stem cell-like properties including the active expression of telomerase, anti-apoptotic pathway activation, increased activity of membrane transporters, and an increased ability to migrate (Wicha et al., 2006). Evidence suggests that CSCs may be responsible for tumor progression, metastasis, chemotherapy and radiotherapy resistance, and subsequent tumor recurrence (Balic et al., 2006; Li et al., 2008; Ponti et al., 2005; Visvader and Lindeman, 2008). Indeed, breast CSCs have increased expression of proinvasive genes, increased invasion *in vitro*, and an invasiveness gene signature derived from these cells is strongly correlated with metastasis-free survival and overall survival (Liu et al., 2007; Sheridan et al., 2006). Additionally, epithelial-mesenchymal transition activation has been shown to generate CSCs and is associated with increased motility and acquisition of invasive and metastatic properties (Gupta et al., 2009; Mani et al., 2008; Morel et al., 2008).

Moreover, glioma stem cells are resistant to ionizing radiation due to enhanced DNA damage repair (Bao et al., 2006). Hepatic cancer cells are resistant to the chemotherapeutic agents doxorubicin, 5-fluorouracil, and gemcitabine due to upregulation of *ABCG2* and *ABCB1* encoding efflux pumps (Haraguchi et al., 2006). Additionally, paired breast cancer cores pre and post neoadjuvant chemotherapy (docetaxel or doxorubicin and cyclophosphamide) had an increased CSC population following chemotherapy, showing CSCs are intrinsically resistance to conventional chemotherapy (Li et al., 2008). These resistant tumorigenic cells may drive tumor recurrence by regenerating the bulk of the tumor following therapy (Figure 1.9) (Dontu et al., 2003). This supports the need and extensive ongoing effort to find agents that target the CSC population.

Cancer stem cells were first identified in seminal work from Dr. John Dick's laboratory studying Acute Myeloid Leukemia (AML). Using methods developed to isolate and characterize normal hematopoietic stem cells (Baum et al., 1992; Spangrude et al., 1988), the authors found only a subset of cells from AML patients were able to recapitulate the disease in severe combined immunodeficient (SCID) recipient mice. These leukemia stem cells were characterized as CD34<sup>+</sup>/CD38<sup>-</sup> and had extensive proliferative capacity, self-renewal potential, and were able to differentiate into leukemic blasts *in vivo* (Bhatia et al., 1997; Bonnet and Dick, 1997; Lapidot et al., 1994). Lineage tracing has shown a single leukemia stem cell can give rise to various populations of leukemic cells due to heterogeneity in self-renewal potential and these functional differences reflect a hierarchical arrangement of leukemia cells similar to the normal hematopoietic compartment (Hope et al., 2004).

The first evidence of CSCs in solid tumors came from work in breast cancer. Al-Hajj and colleagues identified breast CSCs from patient tumors using surface marker

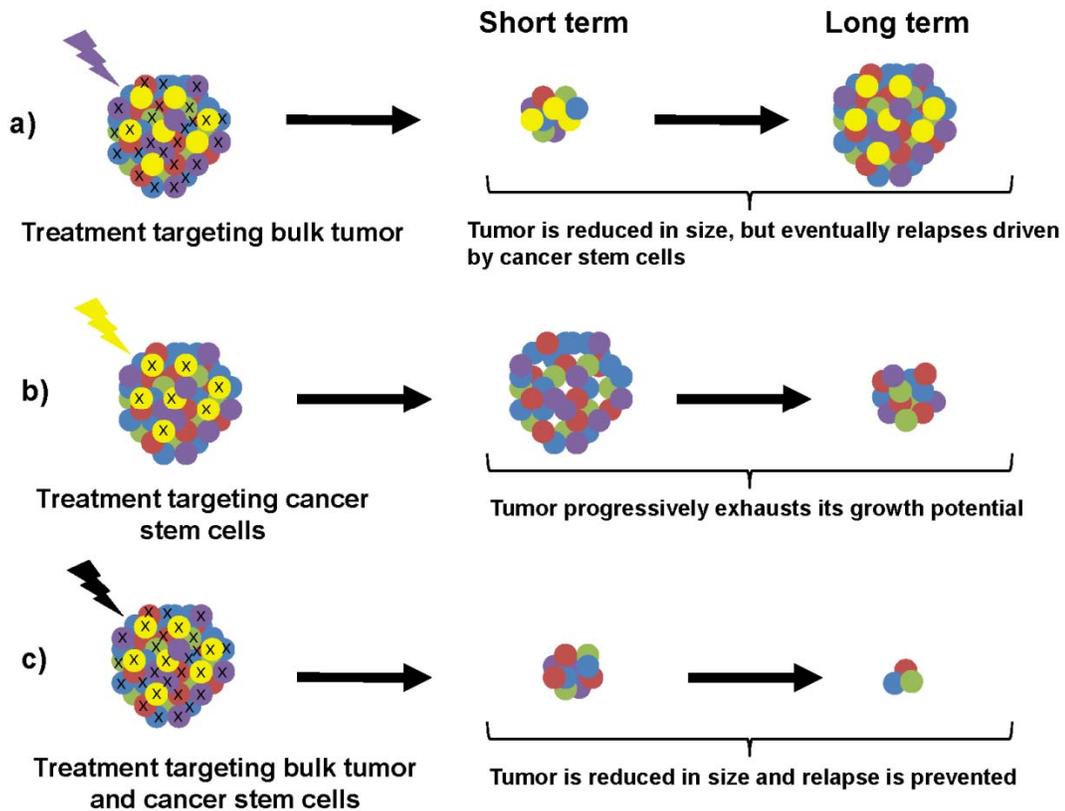


**Figure 1.9 Rationale for Targeting Cancer Stem Cells.** A) Standard chemotherapy drugs target rapidly dividing cells, leading to tumor size reduction, but leaving the CSC population, which can drive a recurrence. B) Targeting the CSC population leads to progressive tumor reduction due to exhaustion of growth potential. C) Treating both bulk tumor cells and the CSCs reduces tumor size and prevents a relapse. Adapted from (Dalerba et al., 2007)

expression and tumor regeneration potential upon mammary fat pad implantation of these cells in nonobese diabetic/severe combined immunodeficient (NOD/SCID) mice (Al-Hajj et al., 2003). As few as 200 breast CSCs, defined by the phenotype  $CD44^+/CD24^-$ , were able to consistently form tumors upon transplantation, whereas 100 fold as many (20,000)  $CD44^+/CD24^+$  cells did not form any tumors. Moreover, secondary and tertiary transplantation of the breast CSCs remained capable of generating the phenotypic heterogeneity of the initial tumor, demonstrating the self-renewal capacity of this population as well as the ability to differentiate into bulk tumor cells. Ginestier and collaborators identified another marker for breast CSCs- cells with high levels of aldehyde dehydrogenase 1 (ALDH1) enzymatic activity (Ginestier et al., 2007). ALDH1 is a detoxifying enzyme responsible for intracellular aldehyde oxidation and may play a role in differentiation of stem cells through oxidation of retinol into retinoic acid (Chute et al., 2006). As few as 500 ALDH<sup>+</sup> cells were able to generate tumors in the mammary fat pad of NOD/SCID mice and displayed CSC properties, notably the ability to self-renew, differentiate into ALDH<sup>-</sup> cells, and recapitulate the heterogeneity of the parental tumor (Ginestier et al., 2007). Subsequently, CSCs have been identified and isolated in a number of other malignancies, including brain cancers, melanoma, ovarian cancer, prostate cancer, bone sarcomas, colon cancer, multiple myeloma, pancreatic cancer, and head and neck cancers (Bapat et al., 2005; Collins et al., 2005; Fang et al., 2005; Gibbs et al., 2005; Li et al., 2007; Matsui et al., 2004; Prince et al., 2007; Ricci-Vitiani et al., 2007; Singh et al., 2003).

The expression of cell surface CSC markers is heterogeneous. High variability in the CSC phenotype has been observed between patients with some tumors having few CSCs and in others CSCs are a substantial proportion of the tumor mass (Tirino et al., 2013). Moreover, tumors may harbor multiple genetically or phenotypically distinct

CSCs (Visvader and Lindeman, 2012). The oncogenic events and mutations that contribute to transformation are thought to influence the CSC phenotype (Badve and Nakshatri, 2012). This may explain why one tumor or tumor-derived cell line displays a certain CSC population (for example, CD44<sup>+</sup>/CD24<sup>-</sup> in MDA-MB 231 breast cancer cells) and another has a different CSC population (ALDH<sup>+</sup> in SKBR3 breast cancer cells). Thus, a variety of markers must be used and functional assays tested when studying CSCs.

Multiple studies suggest Human Epidermal Growth Factor Receptor 2 (HER2) plays an important role in regulating the CSC population in HER2<sup>+</sup> breast cancer. HER2 overexpression and ALDH expression are significantly correlated in human breast cancer patient samples (Ginestier et al., 2007). The CSC population in HER2 overexpressing breast cancer cell lines expresses the highest levels of HER2 protein without HER2 gene amplification changes (Magnifico et al., 2009). Additionally, HER2 overexpression expands the normal breast epithelial stem/early progenitor cell population, as well as the CSC population in malignant breast cells, resulting in increased tumorigenicity and invasiveness with HER2 amplification (Korkaya et al., 2008). HER2 blockade via trastuzumab or HER2/EGFR blockade via lapatinib decreases the CSC population (Korkaya et al., 2008; Magnifico et al., 2009). Neoadjuvant trastuzumab significantly increases pathologic complete response rate compared to chemotherapy alone, suggesting a reduction in the CSC population (Buzdar et al., 2005; Korkaya and Wicha, 2013). Moreover, in contrast to chemotherapy, lapatinib reduced the CSC population in the neoadjuvant setting, although this decrease was not statistically significant (Li et al., 2008).

Telomerase is expressed in both bulk cancer cells and CSCs, suggesting CSCs could be sensitive to telomerase inhibition therapy (Ju and Rudolph, 2006; Ponti et al.,

2005). Imetelstat has been shown to target the CSC population in a number of tumor types including glioblastoma, neuroblastoma, prostate, breast, and pancreatic cancer (Castelo-Branco et al., 2011; Joseph et al., 2010; Marian et al., 2010a; Marian et al., 2010b). While these studies investigated changes in marker expression, spheroid formation, and tumor growth *in vivo* after imetelstat treatment, the effect of telomerase inhibition on invasion and metastases was not addressed nor the effect of imetelstat in combination with standard therapies on the CSC population. Telomerase inhibitors are most effective when used in combination with standard therapies, likely due to the long lag time to achieve telomere shortening (Ruden and Puri, 2013). Our laboratory has shown that imetelstat can augment the effects of trastuzumab and restore sensitivity in trastuzumab-resistant breast cancer cell lines (Goldblatt et al., 2009a).

### **Overall objective and hypothesis**

Finding therapeutics to target the CSC population is an active area of research due to their role in metastasis, tumor recurrence, and resistance to conventional chemotherapies. Telomerase activity is present in both the CSC and bulk populations of cancer cells, suggesting CSCs may be sensitive to telomerase inhibition as a potential therapeutic target. Our laboratory has previously reported imetelstat can decrease lung metastases in a breast cancer xenograft model (Hochreiter et al., 2006), prompting us to question whether the decreased lung metastases were due in part to imetelstat targeting the CSC population. Moreover, we have found imetelstat can augment the effects of trastuzumab in HER2<sup>+</sup> breast cancers and can resensitize resistant cells to trastuzumab (Goldblatt et al., 2009a). HER2 overexpression increases the CSC population, which

may explain the aggressive, metastatic phenotype associated with this breast cancer subtype.

The goals of this project were to better understand the effect of telomerase inhibition on the CSC population in HER2<sup>+</sup> breast cancer cells. Additionally, we wanted to expand our studies on the effects of trastuzumab and imetelstat combination treatment. This thesis specifically addresses the following hypotheses:

1. HER2<sup>+</sup> CSCs have active telomerase that can be inhibited by imetelstat treatment, leading to telomere length shortening.
2. Imetelstat alone, and in combination with trastuzumab, can decrease the CSC population and their functional ability.
3. Imetelstat, trastuzumab, and combination therapy can decrease tumor growth *in vivo* and metastases.

To address the hypotheses presented in this thesis, a variety of cellular and molecular biology techniques, as well as animal model studies, were performed. HER2<sup>+</sup> breast cancer cell lines underwent Fluorescently Activated Cell Sorting to separate CSCs from the bulk, non-CSC population to determine telomerase activity and telomere length before and after imetelstat treatment in each subpopulation. To determine the effect of imetelstat, trastuzumab, and combination treatment on the CSC population, pretreated cells underwent flow cytometry analysis of CSC marker expression. Mammosphere and invasion assays were used to test the functional ability of CSCs from HER2<sup>+</sup> breast cancer cell lines following treatment. Additionally, preclinical animal models were used to study the effect of combination treatment on tumor growth *in vivo* and to investigate the xenograft CSC population and metastasis to the lungs after imetelstat treatment.

## **Significance**

Despite its success, not all patients respond to trastuzumab and those that initially do frequently develop resistance and have disease progression within one year (Miller, 2004; Wu et al., 2011). Treatment options for refractory patients are limited and mortality high requiring the development of suitable treatment strategies. We expect our contribution here to determine whether targeting telomerase through imetelstat treatment in combination with trastuzumab can provide a successful treatment regimen for HER2<sup>+</sup> breast cancer patients. This research is significant because development of better course of therapy provides a strong clinical impact on patients with HER2<sup>+</sup> disease. The addition of imetelstat to trastuzumab may slow disease progression, delaying or possibly preventing patient mortality. Moreover, this research will improve our knowledge of the effect of telomerase inhibitors on CSCs, specifically HER2<sup>+</sup> CSCs, which has not been previously studied.

## CHAPTER TWO

### MATERIALS AND METHODS

#### Reagents

The telomerase template antagonist, imetelstat (GRN163L, 5'-Palm-TAGGGTTAGACAA-3'), its complimentary control oligonucleotide (Sense, 5'-Palm-ATCCAATCTGTT-3'), and a mismatch oligonucleotide (5'-Palm-TAGGTGTAAGCAA-3', mismatched bases underlined) were kindly provided by Geron Corporation (Menlo Park, CA) and were prepared as previously described (Herbert et al., 2005). Trastuzumab was kindly provided by the Indiana University Simon Cancer Center (IUSCC) Infusion Pharmacy. All other chemicals were purchased from Sigma-Aldrich unless otherwise noted.

#### Cell Culture

HCC1569 and HCC1954 HER2<sup>+</sup> breast cancer cell lines were purchased from American Type Culture Collection (ATCC CRL-2330 and CRL-2338) and cultured in RPMI media (Corning cellgro) containing 10% fetal bovine serum (FBS, Fisher Scientific). SUM225 cells were purchased from Asterand, Inc. and were cultured in Ham's F12 media supplemented with 5% FBS, 5 µg/mL insulin, and 1 µg/mL hydrocortisone. SKBR3 and trastuzumab-resistant SKBR3-R pool 1 HER2<sup>+</sup> cells were a generous gift from Dr. Francisco Esteva (MD Anderson Cancer Center) and were cultured in DMEM/F12 media containing 10% FBS. Trastuzumab-resistant SKBR3 cells (SKBR3-R) were cultured with the addition of 4 µg/mL trastuzumab (Nahta and Esteva, 2004). TMD-231 TNBC cells were a generous gift from Dr. Harikrishna Nakshatri

(Indiana University School of Medicine) (Helbig et al., 2003) and were cultured in DMEM media containing 10% FBS. All cells were cultured at 37°C with 5% CO<sub>2</sub> and routinely checked for mycoplasma contamination. Cells were passaged weekly and media was changed two-three times per week.

### **Treatment with Imetelstat and/or Trastuzumab**

Cells were allowed to attach overnight prior to any drug treatment. For the cumulative population doubling experiments, cells were plated in triplicate in 6-well culture plates and media was replaced the following day with fresh media containing a serial dilution of imetelstat (1.25 μM, 2.5 μM, and 5 μM) or 5 μM sense oligonucleotide. To refresh drug, media was spiked with additional drug every 3 days and cells were counted and passaged every 7 days for up to 18 weeks (See Figure 2.1 for experimental set-up). Population doubling was calculated as the log of the (number cells counted divided by number cells plated) divided by log of 2. For the long term treatment studies to look at CSC marker expression, cells were plated in T75 culture flasks and media was replaced the following day with fresh media containing 2.5 μM imetelstat and/or trastuzumab [0.625 μM (1 trastuzumab: 4 imetelstat ratio) for HCC1954 and SKBR3 cells and 0.3125 μM (1 trastuzumab: 8 imetelstat ratio) for HCC1569 cells]. Media was spiked with additional imetelstat every 3 days and cells were counted and passaged after 6 days of treatment for up to 26 weeks (See Figure 2.2 for experiment set-up). For the cell sorting experiments to determine telomerase activity, cells were treated with 2.5 μM imetelstat or sense oligonucleotide for 3 days prior to sorting. For the cell sorting experiments to determine telomere length, cells were treated with 2.5 μM imetelstat or

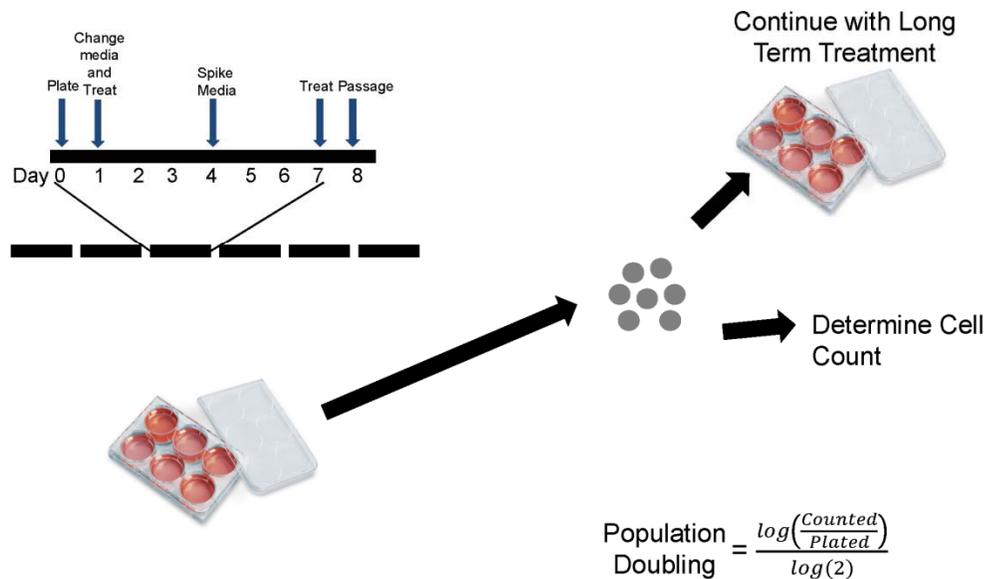


**Figure 2.1. Experimental Set-up for Cumulative Population Doubling Graphs.** Cells were plated and allowed to attach overnight. Media was changed the next day with media containing varying concentrations of imetelstat or the sense oligonucleotide control. Media was spiked with drug every 3 days and cells were counted and passaged every 7 days.

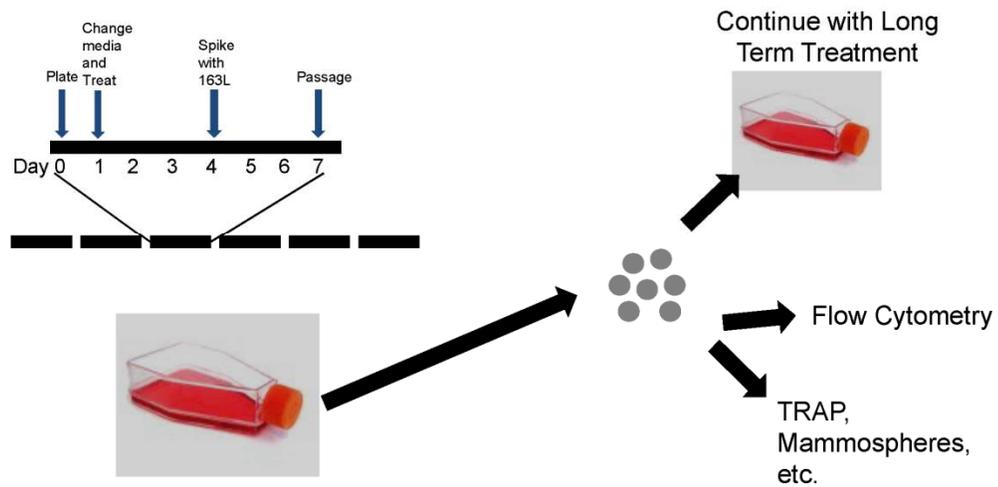


**Figure 2.2. Experimental Set-up for Long-term Culture.** Cells were plated and allowed to attach overnight. Media was changed the next day to media containing imetelstat, trastuzumab, or combination. Media was spiked with imetelstat after 3 days and passaged after 6 days of treatment.

sense oligonucleotide for 6 weeks (same experimental set-up as Figure 2.2) prior to sorting.

### **Flow Cytometry and Fluorescence Activated Cell Sorting (FACS)**

Flow cytometry analysis was performed using an LSRII 407 nm laser cytometer (BD Biosciences) and cell sorting using a Special Order Research Product FACSAria sorter (BD Biosciences) through the IUSCC Flow Cytometry Core. Cells were stained with APC-H7-conjugated CD44, PE-Cy7- conjugated CD24, and violet LIVE/DEAD fixable dead cell stain (all antibodies from BD Biosciences and viability stain from Life Technologies). BD CompBeads and ArC Amine reactive compensation beads (BD biosciences and Life Technologies, respectively) were used to determine appropriate compensation. FMO (fluorescence minus one) controls were used to determine appropriate gates for positive and negative populations. The Aldefluor assay was used to measure and separate cells based on ALDH activity according to manufacturer's guidelines (StemCell Technologies). Control samples treated with DEAB (diethylaminobenzaldehyde) were used for gating the negative population. FlowJo software (Tree Star) was used for all analyses.

### **Telomerase Activity Determination**

Telomerase activity was determined using the telomeric repeat amplification protocol (TRAP). The TRAP assay was performed using the TRAPeze Telomerase Detection kit (Millipore) and a Cy5 fluorescently labelled TS primer according to established protocols (Herbert et al., 2006; Wright et al., 1995). Briefly, cells were lysed

in NP-40 lysis buffer (10 mM Tris-HCl, 1% NP-40, 150 mM NaCl, 0.25 mM Na deoxycholate, 1 mM MgCl<sub>2</sub>, 1 mM EGTA, 5 mM β-mercaptoethanol, and 10% glycerol in DEPC-treated H<sub>2</sub>O) at 1000 cells/μL and incubated at room temperature for 30 minutes with kit reagents to allow telomerase extension. Extended products were amplified via PCR and run on 10% nondenaturing acrylamide gels at 200 Volts for 120 minutes. Gels were visualized using a PhosphorImager. Densitometry of the 6-bp telomerase-specific ladder and 36-bp internal control standard was quantified using ImageJ (<http://imagej.nih.gov/ij>). Relative telomerase activity (RTA) was calculated as the ratio of the telomerase ladder to the internal control standard.

### **Telomere Length Determination**

Average telomere length was determined using the TeloTAGGG telomere length assay (Roche Diagnostics) to measure terminal restriction fragments (TRF). Genomic DNA was isolated using the DNeasy Blood and Tissue Kit (Qiagen) according to the manufacturer's protocol. The TeloTAGGG assay was performed according to the manufacturer's guidelines with minor changes (Roche). Briefly, 1 μg genomic DNA was digested overnight using *Rsa I*/*Hinf I* restriction enzymes. Digested DNA fragments were separated by electrophoresis using a 0.8% agarose gel, transferred to a nylon membrane (Roche) via capillary transfer and 20X SSC buffer (Invitrogen). Following overnight southern transfer, DNA was UV-crosslinked to the membrane (Spectrolinker) and a non-radioactive DIG-labeled telomere probe was hybridized to the membrane for 6 hours. The blot was exposed to X-ray film for 5–10 minutes. Chemiluminescent detection of TRF's was quantified by densitometry using ImageQuant TL (GE Healthcare

Life Sciences) and average telomere length was calculated using TELORUN as previously described (Herbert et al., 2003).

### **Methylene Blue Cell Proliferation Assay for Combination Studies**

Cells were plated in 96 well microplates and treated for 5 days with a 1:2 serial dilution of imetelstat or trastuzumab. To determine the effects of combination therapy, additional microplates were treated in parallel with 1:2 serial dilutions of imetelstat and trastuzumab, in which the two agents were at constant ratios of 1:1, 1:2, 1:4, 1:8, and vice versa to each other. Cell proliferation was determined via methylene blue staining as previously described (Oliver et al., 1989) with minor changes. In brief, cells were fixed with 100% methanol for 15 minutes, stained with 0.05% methylene blue stain (Ricca Chemical) for 15 minutes, washed, dried and de-stained with 0.5 M HCl. Optical density readings were collected at 610 nm using an absorbent plate reader (BioTek). Nonlinear regression sigmoidal curves were used to determine IC<sub>50</sub> values and calculated using GraphPad Prism4. Drug interactions were quantitated using both the isobologram approach (Tallarida, 2011) and combination index (CI) using the Chou Talalay method (Chou and Talalay, 1984) calculated using CalcuSyn (BIOSOFT). Values that fell below the line of additivity on the isobologram are considered synergistic (Figure 2.3). CI < 1 is considered synergistic; CI = 1 is considered additive; CI > 1 is considered antagonistic.

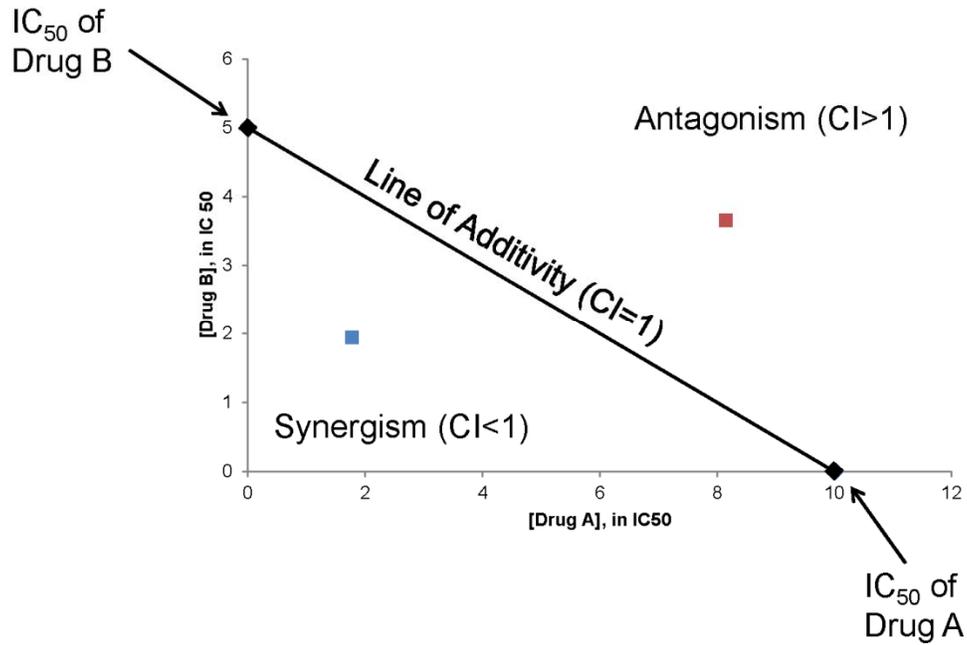


**Figure 2.3. Isobologram Method to Quantitate Drug Interactions.** IC<sub>50</sub> values of drug A and B are plotted on the X and Y axes. A line is drawn to connect the 2 values, known as the line of additivity. Next, the IC<sub>50</sub> values of various combination ratios of drug A:B are graphed. If the point falls below the line of additivity (blue dot above), the combination is synergistic. If the point lies above the line of additivity (red dot above), the combination is antagonistic.

## **Mammosphere Culture Assays**

One hundred thousand pretreated cells were seeded onto ultra-low attachment 100 mm dishes or 15,000 cells in ultra-low attachment 6-well plates for counting spheroids and cultured in MammoCult Medium (StemCell Technologies) supplemented with 4 µg/mL heparin sulfate and 0.48 µg/mL hydrocortisone . After 7 to 10 days in culture, mammospheres were collected and quantified using a Z1 dual threshold Coulter Particle Counter (Beckman Coulter). To generate secondary mammospheres, mammospheres were collected, trypsinized, replated at a density of 15,000 cells per well, analyzed microscopically for single cellularity, and grown under mammosphere conditions.

## **Invasion Assay**

Invasive potential was determined using the Cell Invasion Assay (Millipore) per manufacturer's instructions. In brief, cells were pretreated with imetelstat, trastuzumab, and/or combination treatment to decrease CSC marker expression. 75,000 cells in serum-free media were seeded onto the top of the 24-well insert containing 8 µm pores and coated with ECMatrix™. Media containing 10% FBS was placed in the bottom of the well. Cells were allowed to invade for 72 hours at which point the media and cells that had not invaded were removed by cotton swabs. Bottom of the inserts were stained, rinsed, and analyzed under light microscope. Ten random fields per well were counted.

## **Western Immunoblotting**

Cells were harvested and lysed in RIPA buffer (50 mM Tris-HCl pH 7.5, 150 mM NaCl, 37 mM  $\beta$ -glycerol phosphate, 47 mM NaF, 1% NP40, 0.1% SDS, 0.5% Sodium deoxycholate, 10% glycerol, and protease inhibitor cocktail). 25  $\mu$ g protein was loaded into a 10% SDS-PAGE gel and ran for 90–120 minutes at 100 Volts. Proteins were transferred to PVDF membrane at 12 Volts overnight at 4°C. Membranes were blocked for 60 minutes in 5% instant nonfat dry milk in PBS-T. HER2 antibody (Calbiochem) was used at 1:1000 in 5% milk in PBS-T and 1:10,000 secondary antibody (goat anti-mouse, Pierce). ALDH antibody (BD biosciences) was used at 1:1000 in 5% milk in PBS-T and 1:3000 secondary antibody. Beta-actin antibody (Sigma) served as a loading control and was used at 1:1000 in 5% milk in PBS-T and 1:10,000 secondary antibody. Primary antibodies were incubated overnight at 4°C and secondary antibodies were incubated for 60–75 minutes at room temperature.

## **Xenograft mice studies**

All animal experiments were approved and carried out in strict accordance by the Institutional Animal Care and Utilization Committee (Study number 3715 and 10711) at the Indiana University School of Medicine. 750,000 Xenograft HCC 1954 (1:1 mixture of serum-free media and Matrigel® (BD Biosciences)) or 1 million TMD-231 (in serum free media) cells were implanted into the mammary fat pad of 5–7 week old female NOD/LtSz-scid IL2Rgamma-null (NSG) mice. Surgery was performed under isoflurane anesthesia and 0.05 mg/kg buprenorphine was given for pain management. Animals were treated with saline vehicle (thrice weekly), trastuzumab (20 mg/kg, twice weekly), and/or imetelstat (30 mg/kg, thrice weekly) by intraperitoneal injection. Tumor volume

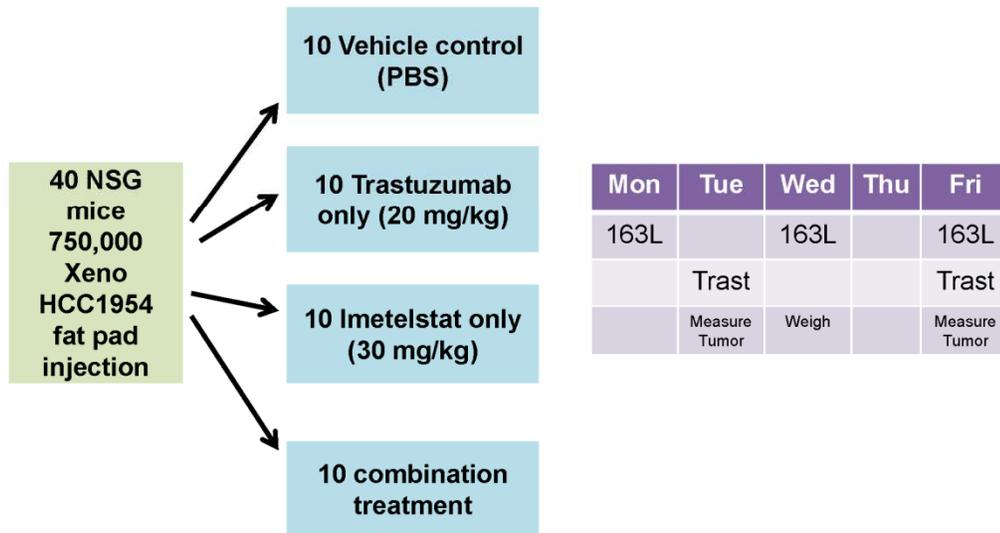


**Figure 2.4. Xenograft HCC1954 Animal Study Set-up.** Forty NSG mice underwent mammary fat pad injection surgery and were divided equally into 4 treatment groups- vehicle control, imetelstat, trastuzumab, and combination. Imetelstat was administered by intraperitoneal injection three times per week; trastuzumab was also administered by intraperitoneal injection twice weekly. Animals were weighed once a week and tumor volume was measured by calipers twice weekly. Animals were sacrificed after 10 weeks of treatment.

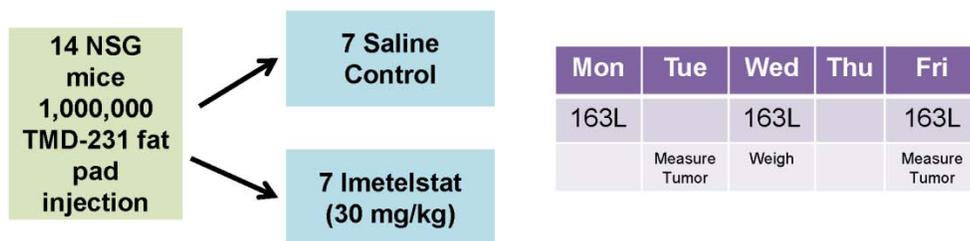


**Figure 2.5. TMD-231 Animal Study Set-up.** Fourteen NSG mice underwent mammary fat pad injection surgery and were divided equally into 2 groups-vehicle control (saline) and imetelstat. Imetelstat was administered by intraperitoneal injection three times per week. Animals were weighed once a week and tumor volume was measured by calipers twice weekly. Animals were sacrificed after 7 weeks of treatment.

was calculated as  $(\text{length} \times \text{width}^2) / 2$  (in mm) by caliper measurements twice weekly. See Figures 2.4 and 2.5 for experimental set-up. After 7 weeks for TMD-231 and 10 weeks for HCC 1954, animals were euthanized and lungs and primary tumor were resected. Lungs were formalin fixed, paraffin embedded, sectioned, and stained with hematoxylin and eosin (H&E) for analysis. Primary tumor tissue was mechanically and enzymatically digested with collagenase/hyaluronidase solution (StemCell Technologies), incubated for 2 hours, and passed through a 40  $\mu\text{m}$  cell strainer to ensure single cellularity prior to cell culture or flow cytometry analysis.

### **Statistical Analysis**

GraphPad Prism4 (GraphPad Software, Inc.) was used to complete all statistical analyses. Student's t-test, one-way ANOVA with Tukey's multiple comparisons post-tests, and two-way repeated measures ANOVA with Bonferroni post-tests were used to determine p-values. In all experiments,  $p < 0.05$  was considered statistically significant.

## CHAPTER THREE

### RESULTS

#### **Long-term Treatment with Imetelstat Inhibits Cell Growth and Telomerase Activity in HER2<sup>+</sup> Breast Cancer Cell Lines**

We utilized a panel of six breast cancer cell lines, five of which are reported to have HER2 protein overexpression and the other is triple negative (ER<sup>-</sup>, PR<sup>-</sup>, HER2<sup>-</sup>), for the experiments conducted in these studies (Table 3.1)(Neve et al., 2006). To verify HER2 protein is overexpressed in these cell lines, we performed Western blot analysis. We found HER2 is indeed overexpressed in the HCC1569, HCC1954, SKBR3, SKBR3-R, SUM225, BT474, BT474-R, and MCF7 HER2 cell lines and HER2 expression is low in the TMD-231, MCF7 pcDNA, and HCC1937 breast cancer cell lines (Figure 3.1). We chose to focus our work mainly on the HCC1569 and HCC1954 cell lines, as these lines are ER<sup>-</sup> (response rates to anti-HER2 therapy vary depending on ER status (Nahta and O'Regan, 2012)) and have not previously been studied with telomerase inhibitors. We also included work on the SKBR3, SKBR3-R, and TMD-231 cells, which are also ER<sup>-</sup> but our laboratory has investigated the use of telomerase inhibition in these cell lines previously.

To study the effects of imetelstat treatment in HER2<sup>+</sup> breast cancer cell lines, cumulative population doublings were measured in two HER2<sup>+</sup> cell lines not previously studied for telomerase inhibition, HCC1569 and HCC1954. Imetelstat treatment inhibited proliferation in both cell lines as measured by cumulative population doublings (Figure 3.2). Cumulative population doublings of the HCC1569 cell line statistically significantly differed between imetelstat and untreated cells after 35, 42, and 63 days of treatment for 5  $\mu$ M, 2.5  $\mu$ M, and 1.25  $\mu$ M imetelstat, respectively, and remained different

**Table 3.1. Panel of Cell Lines Studied.**

<b>Cell Line</b>	<b>HER2</b>	<b>ER</b>	<b>Trastuzumab Sensitive</b>
HCC1569	+	-	+
HCC1954	+	-	+
TMD-231	-	-	-
SKBR3	+	-	+
SKBR3-R	+	-	-
Sum225	+	-	+

Six Cell Lines were obtained from ATCC or as described in Materials and Methods. Five cell lines are from HER2<sup>+</sup> breast cancer patients and one is from a TNBC patient. With the exception of the SKBR3-R cell line, all HER2<sup>+</sup> cell lines respond to trastuzumab treatment in our studies.

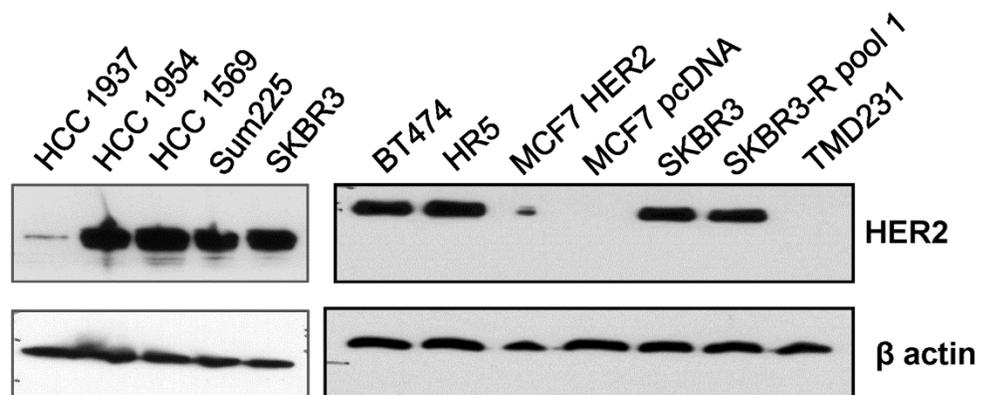
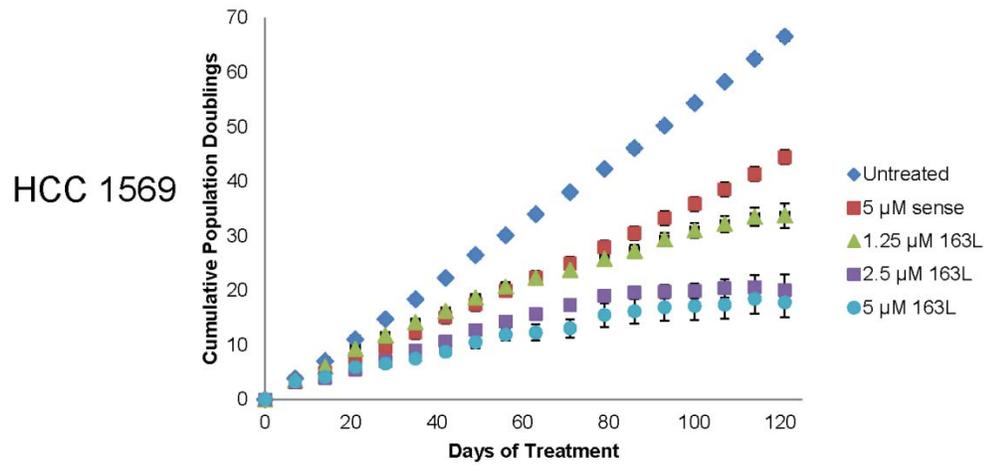


**Figure 3.1. Certain Breast Cancer Cell Lines Overexpress HER2 Protein.** Western blot analysis of various breast cancer cell lines shows HCC1954, HCC1569, SUM225, SKBR3, BT474, BT474-R (HR5), MCF7-HER2, SKBR3, and SKBR3-R cell lines overexpress HER2 protein, as previously reported.

**A**



**B**

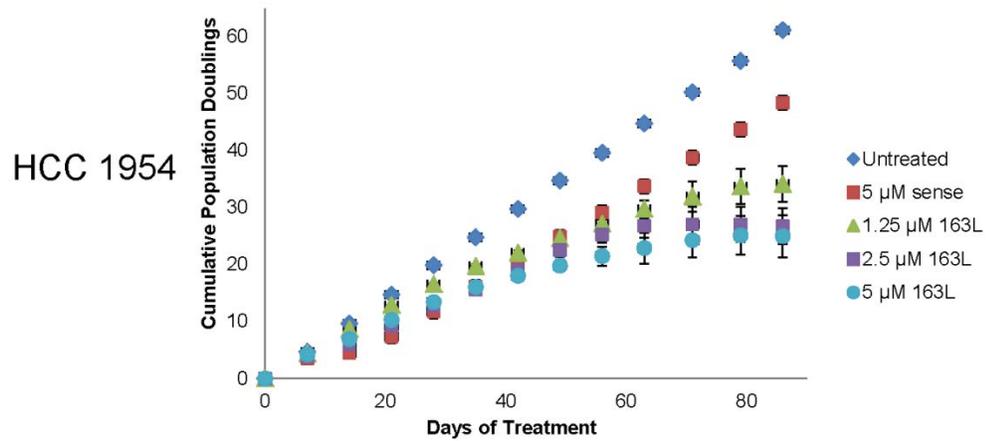


**Figure 3.2. Long-term Treatment with Imetelstat Inhibits Cellular Proliferation.** Cumulative Population doubling graphs of HCC1569 (A) and HCC1954 (B) cell lines. UT= untreated, 163L= imetelstat

throughout the remainder of the experiment (Figure 3.2 A, two-way repeated measures ANOVA,  $p < 0.05$ ). HCC1569 cells stopped doubling and reached the stationary phase or plateau of the population doubling graph after 17 weeks of treatment. Cumulative population doublings of the HCC1954 cell line statistically significantly differed between imetelstat and untreated cells after 56, 63, and 71 days of treatment for 5  $\mu\text{M}$ , 2.5  $\mu\text{M}$ , and 1.25  $\mu\text{M}$  imetelstat, respectively, and remained different throughout the remainder of the experiment (Figure 3.2 B, two-way repeated measures ANOVA,  $p < 0.05$ ). HCC1954 reached the stationary phase after 10 weeks of treatment. The sense oligonucleotide control had a minor effect on cell proliferation, which is likely an unrelated oligonucleotide effect, but it occurred much later than imetelstat and did not inhibit cells from continuing to proliferate. Although cumulative population doublings began to significantly differ sooner in the HCC1569 cells, it took longer to reach the plateau than in HCC1954 cells. The HCC1569 cells were slower growing, doubling about 4 times per week versus 5 times in the HCC1954 cells, and have longer baseline telomere length, which may explain why a longer treatment regimen is required to reach the stationary phase in this cell line. We also measured telomerase activity during long-term treatment with imetelstat by the TRAP assay. As expected, imetelstat was able to inhibit telomerase activity for all time points studied (up to 6 weeks of treatment) with the control sense oligonucleotide having no effect on telomerase activity (Figures 3.3), suggesting cells remained sensitive to telomerase inhibition and did not become resistant to imetelstat treatment.

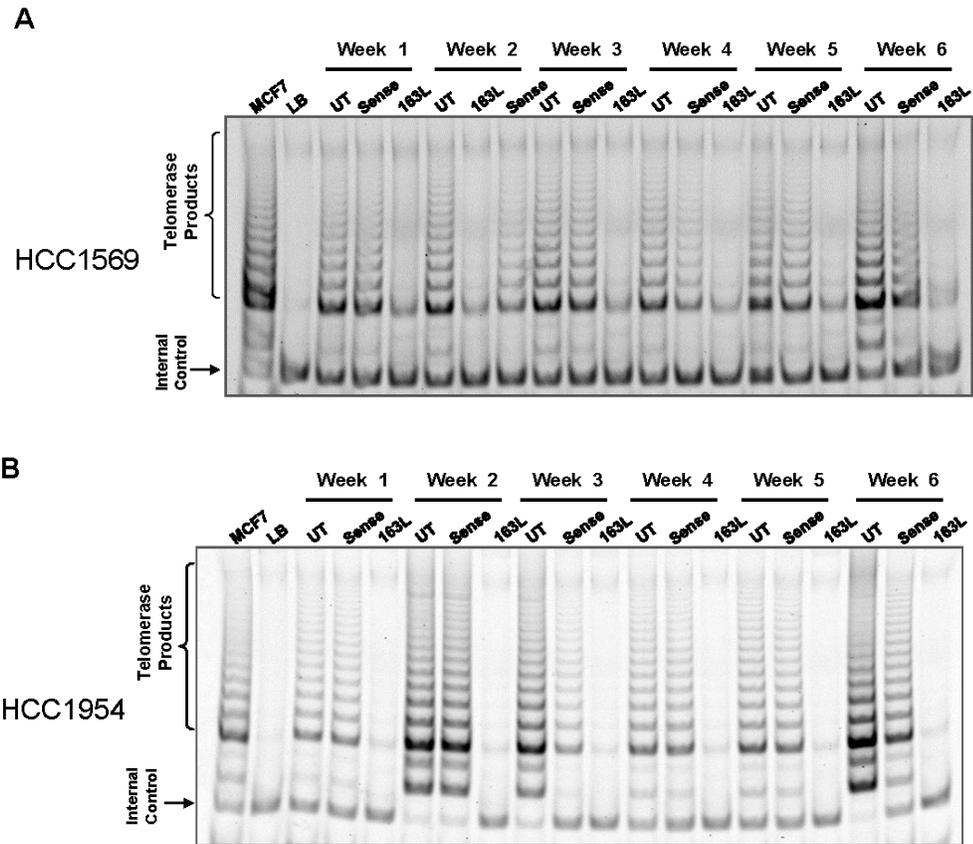


**Figure 3.3. Continued Treatment with Imetelstat Inhibits Telomerase Activity.** TRAP assay to determine telomerase activity of A) HCC1569 and B) HCC1954 cells continually treated with 2.5  $\mu$ M imetelstat or sense control for up to 6 week, telomerase activity determined weekly. LB= lysis buffer, UT= untreated, 163L= imetelstat

## **HER2<sup>+</sup> CSCs Have Active Telomerase and Are Sensitive to Telomerase**

### **Inhibition via Imetelstat**

Previous studies have reported similar telomerase activity between CSCs and their bulk tumor cell counterparts, as well as similarities in telomere length (Joseph et al., 2010; Ponti et al., 2005). We wanted to determine whether our HER2<sup>+</sup> cell lines also had similar telomerase activity and telomere length in the CSC, non-CSC (bulk tumor cells), and unsorted populations. HCC1569 cell line was flow sorted based on CD44/CD24 expression and ALDH enzymatic activity. ALDH enzymatic activity was used to sort the SKBR3 and HCC1954 cell lines. See Figure 3.4 for representative sorting gates used in these experiments. Unsorted, non-CSC, and CSC populations all had active telomerase, as visualized by the robust ladder formation of telomerase products in the TRAP assay (Figure 3.5 A, C) and relative telomerase activity quantification (Figure 3.5 B, D). There was no difference in relative telomerase activity between CSC, non-CSC, and unsorted cells in the HCC1569 cell line based on CD44/CD24 expression (one-way ANOVA,  $p > 0.05$ ). All other samples were only sorted twice so statistical analysis could not be performed. We also tested whether imetelstat can inhibit telomerase activity in the different subpopulations. Imetelstat (labelled 163L) was able to abolish telomerase activity in both the CSC and non-CSC populations; again, the sense oligonucleotide control did not affect telomerase activity (Figure 3.5 A–D).

In line with the previous reports, we found similar average telomere length between the CSC and non-CSC populations in our HER2<sup>+</sup> breast cancer cell lines (Figure 3.6). Six weeks of imetelstat treatment decreased average telomere length in the HCC1954 cell line, but not the HCC1569 cell line (Figure 3.6 B). HCC1569 cells had a longer baseline telomere length than HCC1954, possibly explaining why we did not

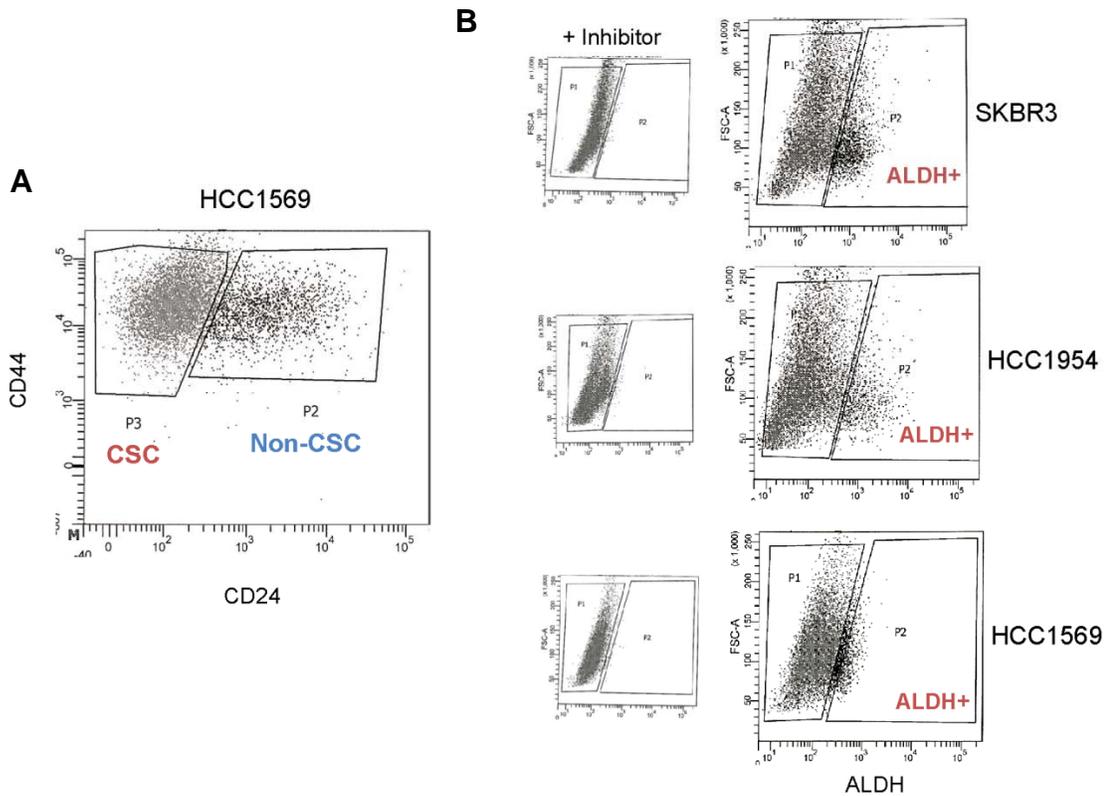


**Figure 3.4. Flow Sorting Gating Strategy.** A) HCC1569 cells were sorted based on CD44/CD24 expression into CSC and non-CSC populations. B) SKBR3, HCC1954, and HCC1569 cells were sorted based on ALDH activity. Aliquots were also incubated with ALDH inhibitor diethylamino benzaldehyde (DEAB) to gate ALDH<sup>-</sup> (non-CSC) and ALDH<sup>+</sup> (CSC) populations.

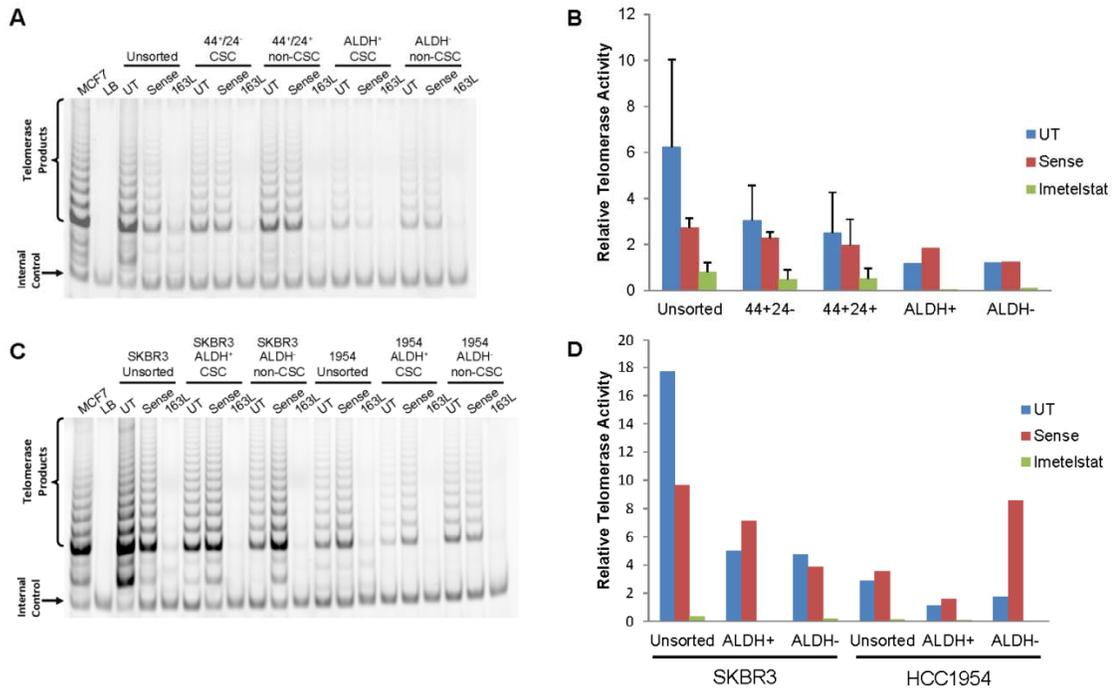


**Figure 3.5. CSCs Have Active Telomerase That Can Be Inhibited by Imetelstat.**  
 A) Detection of telomerase activity by TRAP assay of HCC1569 flow sorted CSCs and non-CSCs by marker expression following 3 day treatment of 2.5  $\mu$ M imetelstat or sense oligonucleotide. B) Average quantification of relative telomerase activity from representative image A) and 1-2 additional experiments using ratio of telomerase products to internal standard. Standard deviation bars in CD44/CD24 samples, as this was repeated 3 times with no significant difference. C) TRAP assay of SKBR3 and HCC1954 flow sorted CSCs and non-CSCs following 3 day treatment of 2.5  $\mu$ M imetelstat or sense oligonucleotide. D) Average quantification of relative telomerase activity from representative image C) and 1 additional experiment. UT= untreated cells, 163L= imetelstat treated cells

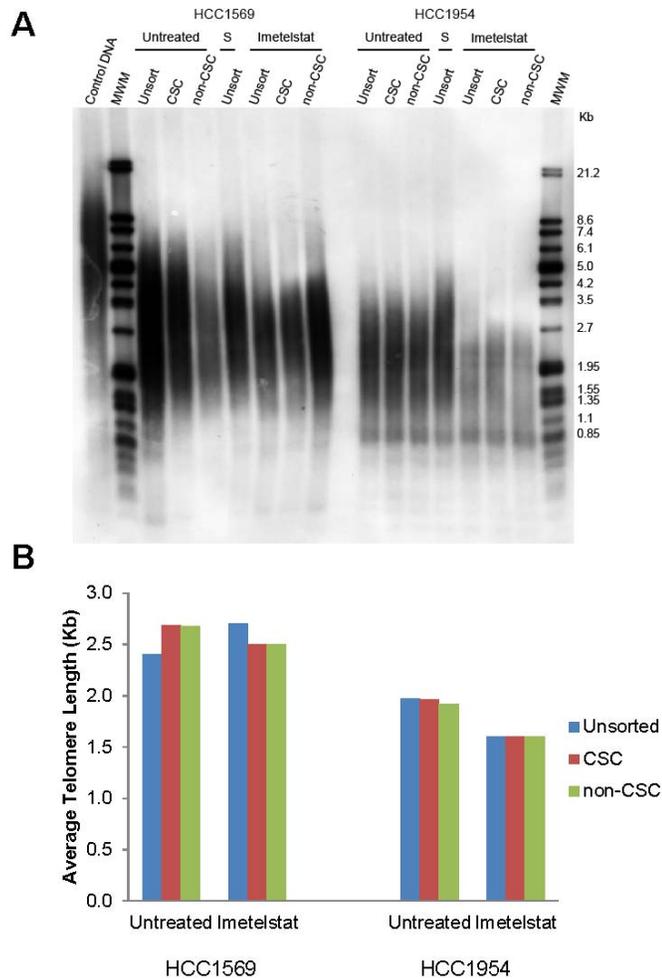


**Figure 3.6. Average Telomere Length is Similar in all Subpopulations with Imetelstat Treatment Leading to Telomere Shortening.** A) Telomere length determination by Terminal restriction fragment analysis of HCC1569 and HCC1954 flow sorted cells following 6 weeks of treatment of 2.5  $\mu$ M imetelstat or sense oligonucleotide. MWM= molecular weight marker, Unsort= unsorted cells, S= sense oligonucleotide control, HCC1569 CSC= CD44<sup>+</sup>/CD24<sup>-</sup>, HCC1569 non-CSC= CD44<sup>+</sup>/CD24<sup>+</sup>, HCC1954 CSC= ALDH<sup>+</sup>, HCC1954 non-CSC= ALDH<sup>-</sup>. B) Average telomere length quantified using TELORUN. Kb=kilobase

see differences in average telomere length at this time point of treatment. However, there appeared to be a shortening of the longer telomeres in both cell lines with imetelstat treatment, shown by a shift down in the telomere smear on the membrane (Figure 3.6 A). Indeed, examination of the densitometry of the telomere smears revealed shortening of longer telomeres in both cell lines with imetelstat treatment, shown by a shift in the curve toward a smaller molecular weight (Figure 3.7). The longer baseline telomere length of HCC1569 may also explain why longer treatment duration is needed to achieve the stationary phase or plateau of the population doubling graph (Figure 3.2). Due to the fact the TRF analysis determined average telomere length, we cannot rule out the possibility of a few short telomeres in the CSC population or cells after treatment with imetelstat.

### **Telomerase Inhibition Can Decrease CSCs and Limit Mammosphere Formation**

The use of breast cancer cell lines to study CSCs has been validated (Charafe-Jauffret et al., 2009; Fillmore and Kuperwasser, 2008). HCC1569, HCC1954, SKBR3, SUM225, and TMD-231 cell lines were subjected to flow cytometry analysis of CD44 and CD24 marker expression, as well as ALDH enzymatic activity. The HCC1569 cell line was positive for CD44 expression and contained both positive and negative CD24 expressing cells, allowing us to use this cell line to measure the CD44<sup>+</sup>/CD24<sup>-</sup> CSC population (Figure 3.8 A). Additionally, TMD-231 cells stained almost entirely CD44<sup>+</sup>/CD24<sup>-</sup>, but did not exhibit ALDH enzymatic activity (Figure 3.8 E). HCC1954, SKBR3, and SUM225 cell lines did not have a measureable CD44<sup>+</sup>/CD24<sup>-</sup> population (Figure 3.8 B–D). As predicted by the correlation of HER2 and ALDH, HCC1569, HCC1954, and SKBR3 cells had ALDH<sup>+</sup> CSC subpopulations (Figure 3.8 A–C)

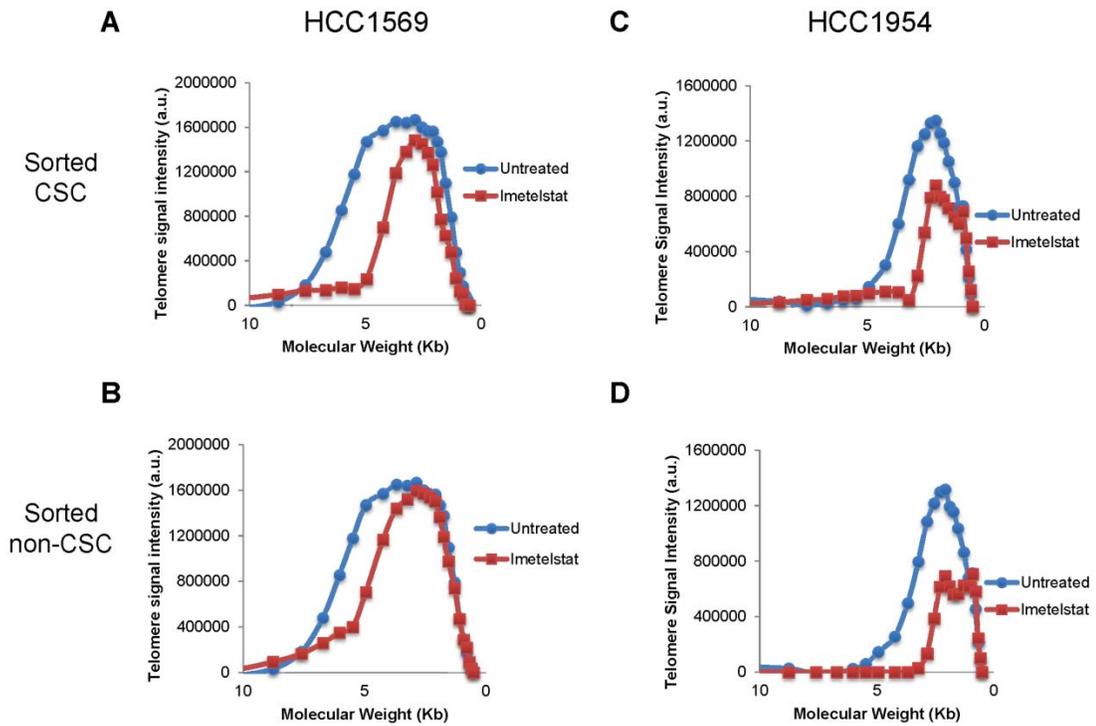


**Figure 3.7. Longer Telomeres are Shortened with Imetelstat Treatment.** Telomere length quantification using TELORUN of sorted HCC1569 (A-B) and HCC1954 (C-D) cells pretreated with imetelstat or untreated for 6 weeks prior to sorting CSC (top panels) and non-CSC (bottom panels) populations. Shift in Molecular Weight (telomere length in Kb) after imetelstat treatment (red lines) shows telomere shortening of the longer telomeres within each sample. a.u. = arbitrary units

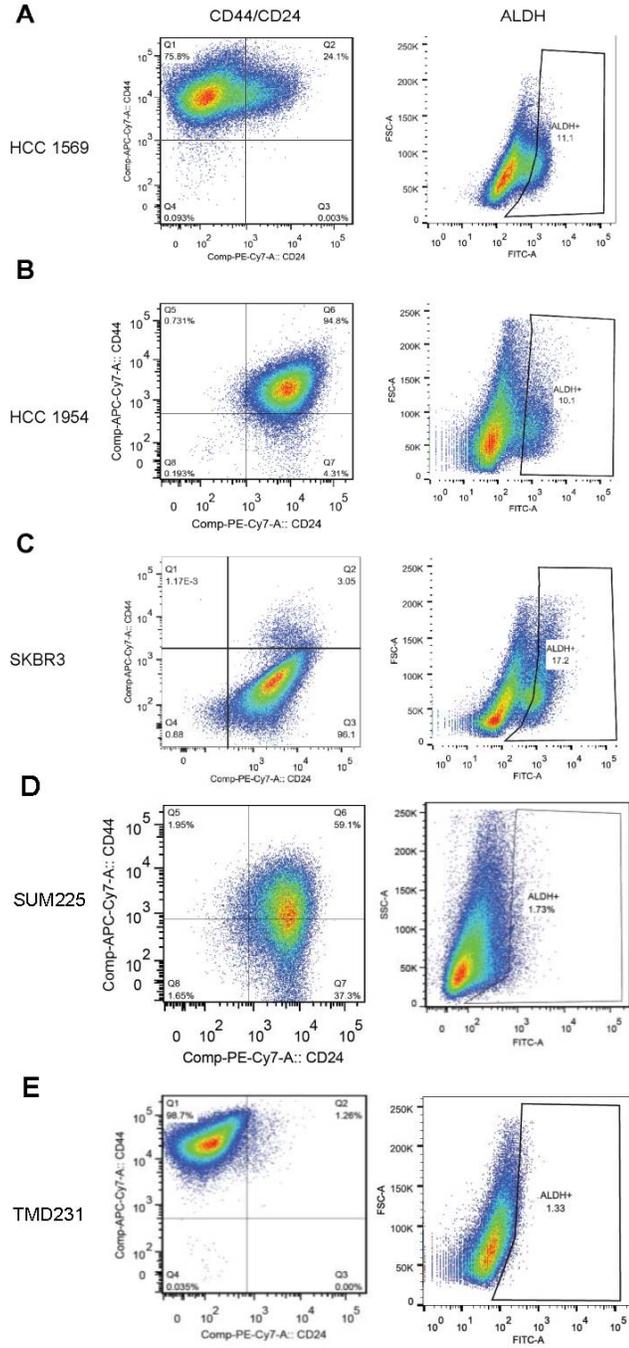


**Figure 3.8. Cell Lines have Variable CSC Marker Expression.** Flow cytometry analysis of CD44/CD24 (left panels) and ALDH enzymatic activity (right panels) of HCC1569 (A), HCC1954 (B), and SKBR3 (C), SUM225 (D), and TMD-231 (E) cell lines.

(Ginestier et al., 2007). We were not able to detect substantial ALDH enzymatic activity in the HER2<sup>+</sup> SUM225 cell line despite this cell line had the highest protein expression of ALDH (Figure 3.9), suggesting protein expression does not predict enzymatic activity.

To determine the effect of telomerase inhibition on the CSC population, we measured CD44<sup>+</sup>/CD24<sup>-</sup> expression in the HCC1569 cell line with and without imetelstat treatment. Imetelstat decreased the CSC population by more than 25% (62.9% in imetelstat treated versus 88.7% in untreated, 1.41 fold decrease), whereas the sense oligonucleotide control had no effect (Figure 3.10). Furthermore, imetelstat pretreatment statistically significantly decreased mammosphere count, an *in vitro* assessment of stem cell function, compared to untreated and sense controls (Figure 3.11 B–C). Spheroids also appeared smaller after imetelstat pretreatment (Figure 3.11 A), suggesting imetelstat inhibited proliferation of the CSCs.

Additionally, we wanted to follow-up on our previous work showing imetelstat decreased lung metastases *in vivo* by using the same cell line as that study (Hochreiter et al., 2006). In a pilot experiment, imetelstat decreased the CSC population of the TNBC cell line TMD-231 by 1.45 fold (98.7% in the untreated vs 68.3% with imetelstat treatment), whereas the mismatch oligonucleotide had no effect (Figure 3.12), suggesting imetelstat can target the CSC population of other breast cancer subtypes as well. Moreover, imetelstat decreased the functional ability of these CSCs, as shown by decreased spheroid formation efficiency, 9.36% in the untreated vs 1.5% with imetelstat pretreatment (Figure 3.13). Furthermore, imetelstat inhibited telomerase activity in both adherent and mammosphere cultures in this experiment (Figure 3.14), indicating imetelstat is able to infiltrate a mass of cells similar to tumors in patients.

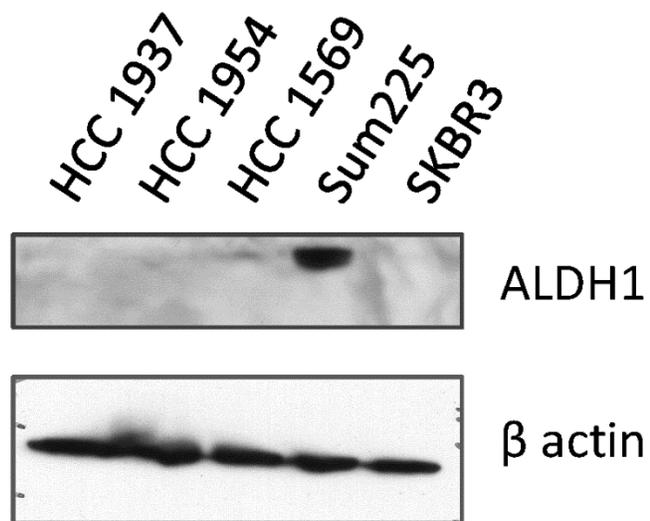


**Figure 3.9. Cell Lines have Variable ALDH1 Protein Expression.** Western immunoblotting for ALDH1 protein expression from HCC1937, HCC1954, HCC1569, Sum225, and SKBR3 cell lines.

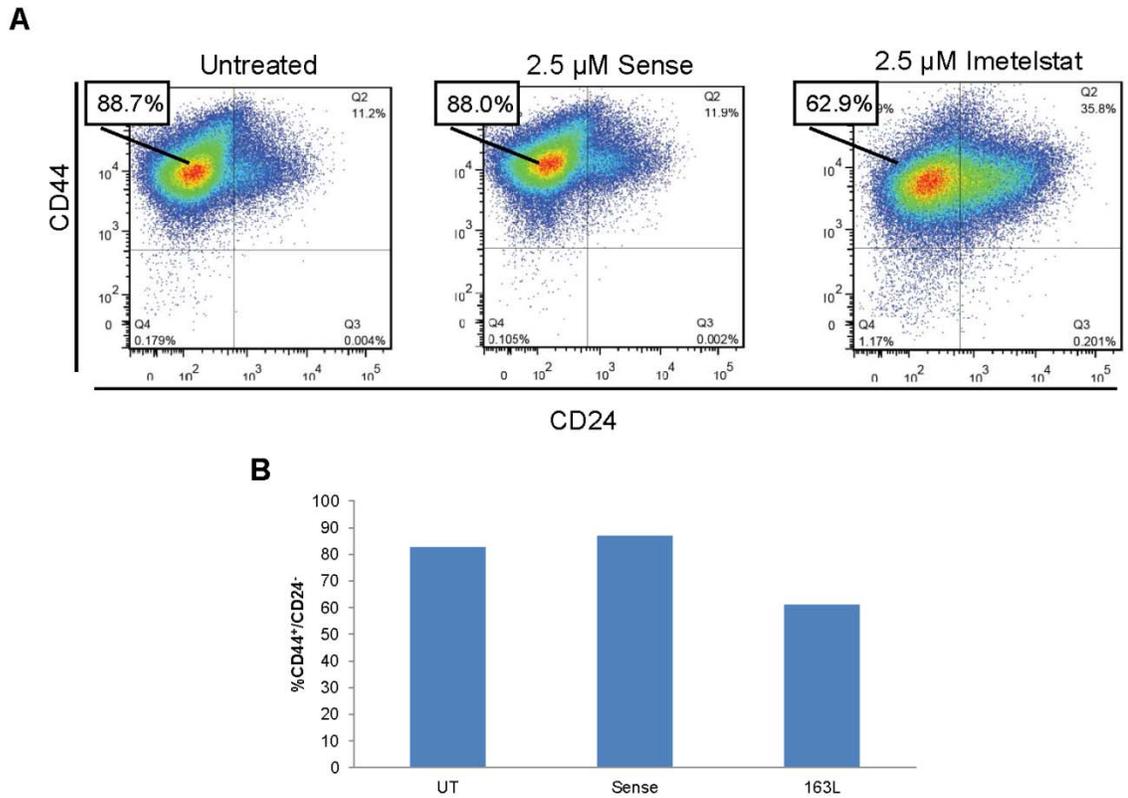


**Figure 3.10. Imetelstat, but not the Sense Oligonucleotide Control, Decreases the Percentage of CSCs.** A) Representative flow cytometry analysis of CSC marker expression of HCC1569 cells following imetelstat or sense treatment. B) Average percent CSC (n=2) after 144 days of treatment.

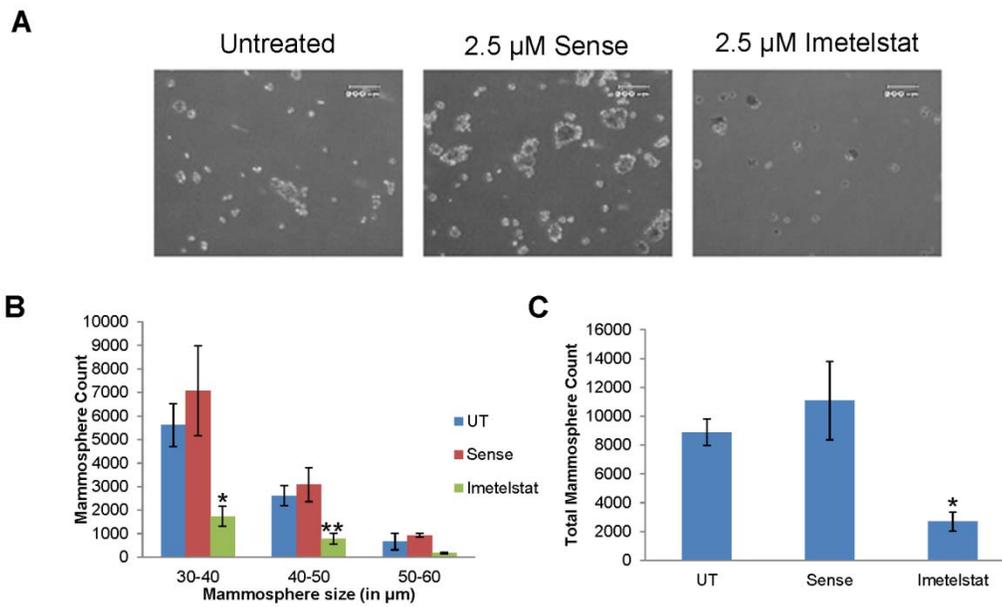


**Figure 3.11. Imetelstat Inhibits Mammosphere Formation.** A) Representative images of primary mammosphere cultures from HCC1569 cells pretreated for 150 days and cultured for 8 days as mammospheres without additional treatment, 4X Magnification, 200  $\mu$ m scale bar. B) Primary mammosphere count grouped by mammosphere size (n=3), average  $\pm$  SD, one-way ANOVA, \*  $p < 0.05$ , \*\*  $p < 0.01$  compared to untreated. C) Sum of mammosphere size groups graphed as total mammosphere count, average  $\pm$  SD, one-way ANOVA, \*  $p < 0.05$  compared to untreated.

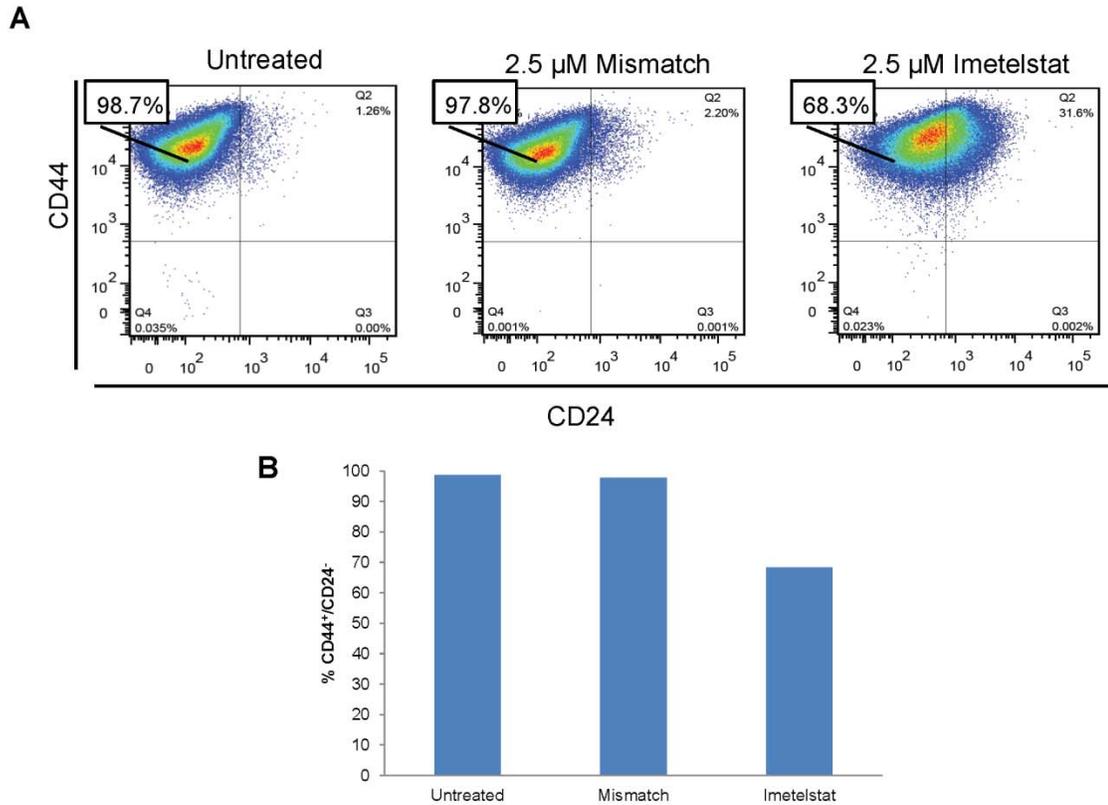


**Figure 3.12. Imetelstat Decreases the Percentage of CSCs in the TNBC Cell Line TMD-231.** A) Flow cytometry analysis of TMD-231 cells treated with 2.5  $\mu$ M imetelstat or mismatch control oligonucleotide for 56 days. B) Bar graph of %CD44<sup>+</sup>/CD24<sup>-</sup> CSC population following 56 days of treatment, n=1.

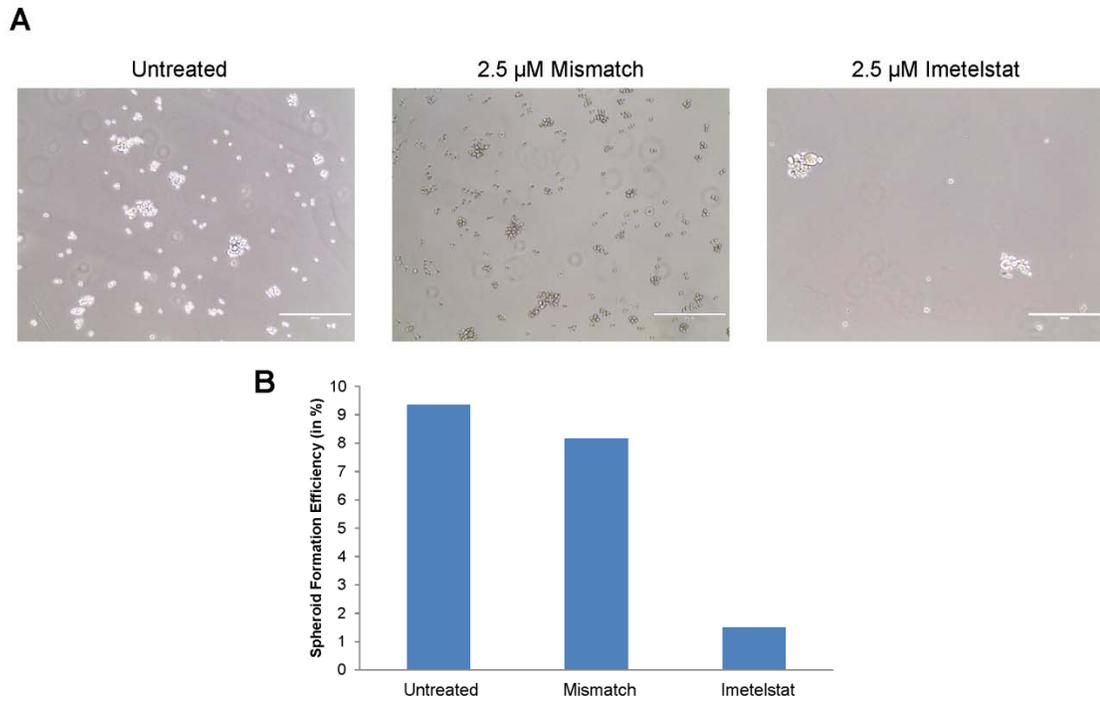


**Figure 3.13. Imetelstat Inhibits Mammosphere Formation in TMD-231 Cells.**  
 A) Representative images of primary mammosphere cultures from TMD-231 cells pretreated for 98 days and cultured as mammospheres for 7 days without additional treatment, 10X Magnification, 400  $\mu$ m scale bar. B) Graph of Spheroid formation efficiency (Mammosphere count/ number plated), n=1.

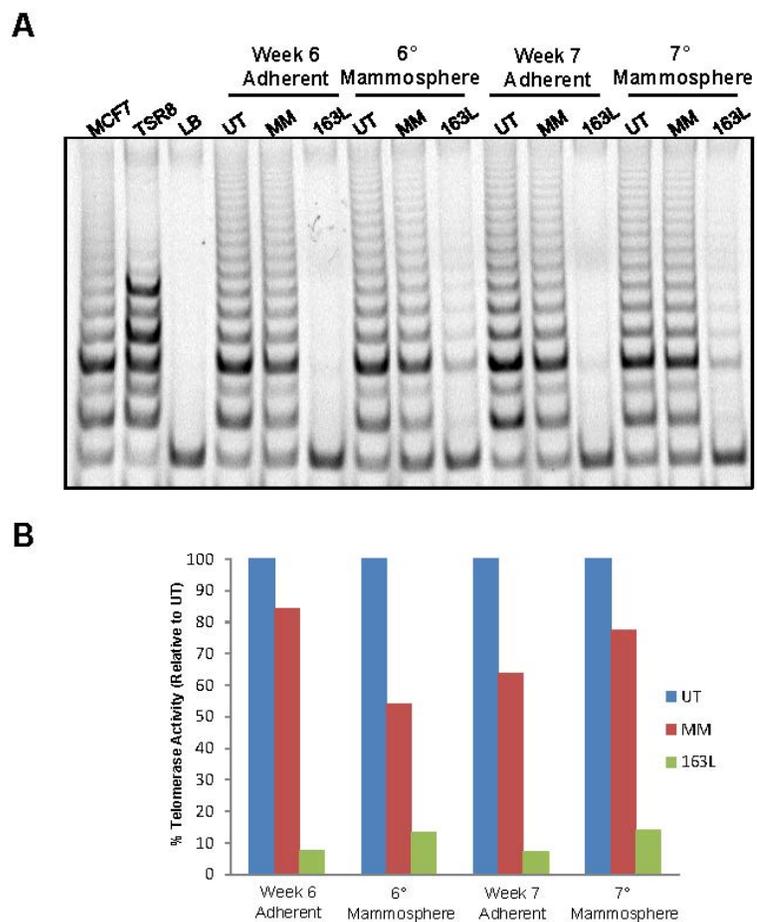


**Figure 3.14. Imetelstat Inhibits Telomerase Activity in Both Adherent and Spheroid TMD-231 Cell Cultures.** A) Telomerase activity as determined by the TRAP assay for TMD-231 cells cultured as adherent monolayers or non-adherent spheroids and treated with 2.5  $\mu$ M imetelstat or mismatch control oligonucleotide for 6 or 7 weeks. B) Quantification of A) and graphed as percent telomerase activity relative to the untreated.

## **Imetelstat Augments the Effects of Trastuzumab in HER2<sup>+</sup> Breast Cancer Cell Lines**

Our laboratory has previously reported a synergistic effect of imetelstat and trastuzumab combination therapy *in vitro* (Goldblatt et al., 2009a). Moreover, we also found imetelstat is able to resensitize trastuzumab-resistant cells to trastuzumab. We next wanted to verify this effect also applied to the HCC1569 and HCC1954 cell lines. The HCC1569 and HCC1954 cell lines have previously been classified as having a *de novo* resistance to trastuzumab, due to not decreasing cell growth rate by greater than 1.2 fold and soft agar colony formation by greater than 20% at a concentration of 15  $\mu\text{g/mL}$  (approximately 103 nM) (O'Brien et al., 2010). Nonetheless,  $\text{IC}_{50}$  values, the drug concentration needed to inhibit 50% of cellular proliferation, of trastuzumab and imetelstat were determined for both HCC1569 and HCC1954 cell lines. The ratio used in combination experiments was determined by dividing the  $\text{IC}_{50}$  value of imetelstat by the  $\text{IC}_{50}$  value of trastuzumab; therefore we treated HCC1569 cells with a 1:8 ratio of trastuzumab to imetelstat and HCC1954 cells with a 1:4 ratio of trastuzumab to imetelstat. In the HCC1569 cells, the combination decreased the concentration of both drugs needed to achieve the  $\text{IC}_{50}$  (Figure 3.15). Moreover, the combination index showed a synergistic effect ( $\text{CI} < 1$ ) of combination treatment at most concentrations tested (Table 3.2). Similarly, the combination in HCC1954 cells decreased the concentration of both drugs needed to achieve the  $\text{IC}_{50}$  (Figure 3.16). Likewise, the combination index showed a synergistic effect at most combination treatment concentrations studied (Table 3.3). Moreover, we tested different drug ratios in the HCC1954 cell line and found all ratios fell below the line of additivity on the isobologram, although 1:2 and 2:1 ratios (trastuzumab : imetelstat) may not be statistically below the line of additivity (Figure 3.16 C). Although these cells are reported to be innately

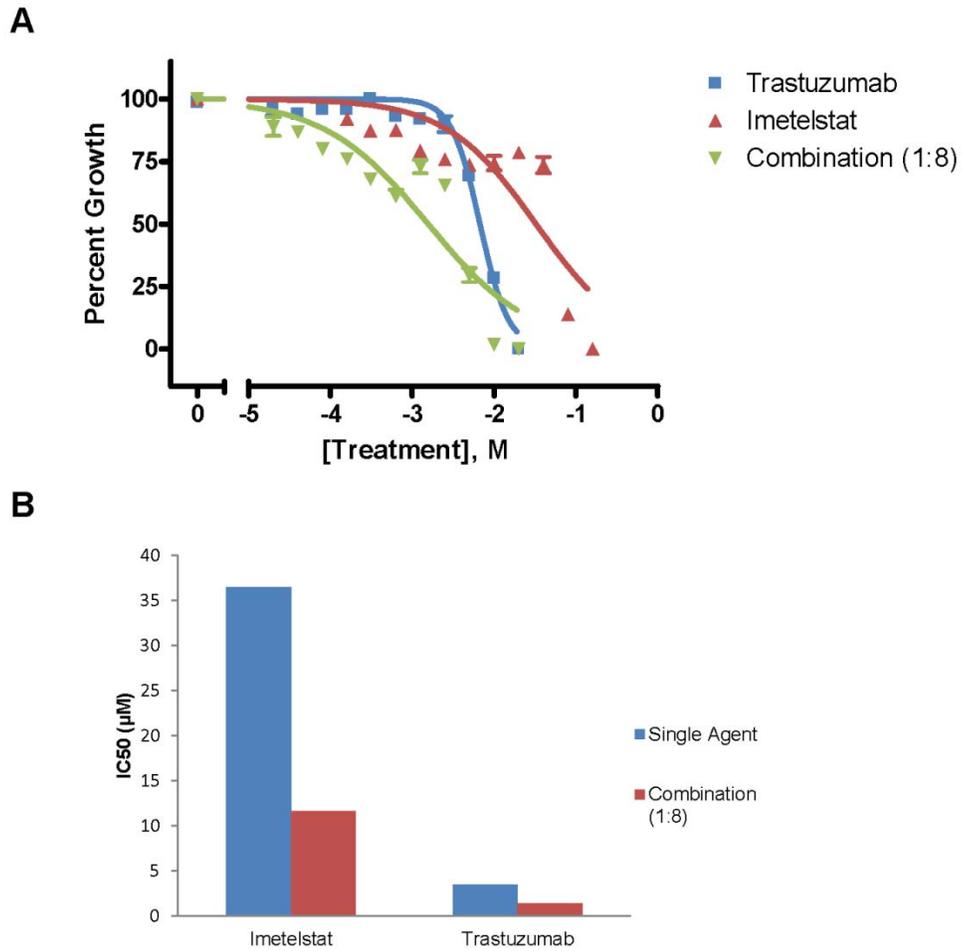


**Figure 3.15. Imetelstat Augments the Effects of Trastuzumab in HCC1569 Cells.** A) Representative dose-response curve of trastuzumab, imetelstat, and 1:8 combination treatment in HCC1569 cells. B) Average IC<sub>50</sub> value of each drug individually and in combination. n=3 experiments with 16–24 replicates each.

**Table 3.2. HCC1569 Combination Index.**

<b>Imetelstat (<math>\mu\text{M}</math>)</b>	<b>Trastuzumab (<math>\mu\text{M}</math>)</b>	<b>Combination Index</b>
0.156	0.020	0.466
0.313	0.039	0.908
0.625	0.078	0.554
1.25	0.156	0.334
2.5	0.313	0.295
5	0.625	0.313
10	1.25	1.148
20	2.5	9.013
40	5	0.327
80	10	0.060

Combination Index (CI) was calculated as described in Materials and Methods using Calcosyn Software. Synergism was defined as a CI value < 1.

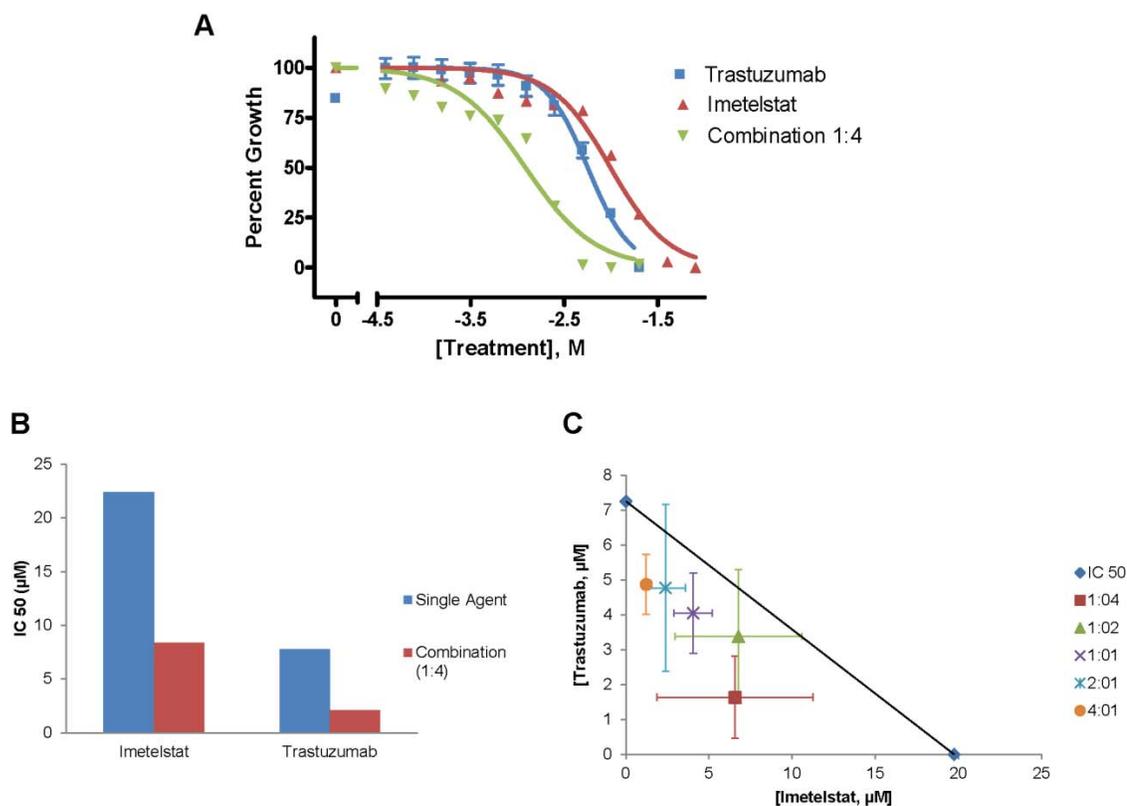


**Figure 3.16. Imetelstat Augments the Effects of Trastuzumab in HCC1954 Cells.** A) Representative dose-response curve of trastuzumab, imetelstat, and 1:4 combination treatment in HCC1954 cells. B) Average IC<sub>50</sub> value of each drug individually and in combination. n=3 experiments with 8–24 replicates each. C) Isobologram of HCC1954 cells treated with varying ratios of trastuzumab : imetelstat. Average IC<sub>50</sub> values are graphed. n=3 experiments with 6 replicates each.

**Table 3.3. HCC1954 Combination Index.**

<b>Imetelstat (<math>\mu\text{M}</math>)</b>	<b>Trastuzumab (<math>\mu\text{M}</math>)</b>	<b>Combination Index</b>
0.156	0.039	0.137
0.313	0.078	0.228
0.625	0.156	0.322
1.25	0.313	0.654
2.5	0.625	1.136
5	1.25	1.343
10	2.5	1.301
20	5	0.823
40	10	0.723
80	20	0.917

Combination Index (CI) was calculated as described in Materials and Methods using Calcosyn Software. Synergism was defined as a CI value < 1.

resistant to trastuzumab and we did notice little effect on cell proliferation at lower concentrations, we were able to determine  $IC_{50}$  values for trastuzumab and showed the combination treatment decreased the  $IC_{50}$  value for both trastuzumab and imetelstat. These combination studies suggest imetelstat can augment the effects of trastuzumab.

### **Imetelstat in Combination with Trastuzumab Decreases the CSC Population**

As imetelstat is used in combination with standard of care treatments like trastuzumab, we next wanted to determine the effect of imetelstat and trastuzumab combination treatment on the CSC population. For these combination studies, we used 2.5  $\mu$ M imetelstat, as this concentration is clinically relevant to the dose received by patients, and either 312.5 nM or 625 nM trastuzumab for the 1:8 or 1:4 ratio, respectively, used in our drug interaction studies above. Combination treatment statistically significantly decreased the  $CD44^+/CD24^-$  CSC population in the HCC1569 cell line ( $p < 0.05$  for 12–54 days of treatment) by approximately 25% or a 1.36 fold decrease (Figure 3.17). However, addition of trastuzumab had no effect on the percentage of  $CD44^+/CD24^-$  CSCs ( $p > 0.05$  for all time points).

Additionally, we determined the percentage of  $ALDH^+$  CSCs in the HCC1569, HCC1954, SKBR3, and SKBR3-R cells. As  $ALDH^+$  cells are determined by enzymatic activity (the removal of a hydrogen group on an aldehyde substrate), there is greater variability between samples than measuring surface marker expression for CD44 and CD24, which makes determining statistically significant differences difficult because the standard deviation is so large. In the HCC1569 cell line, imetelstat and combination treatment decreased the  $ALDH^+$  CSC population up to 80%, with a statistically significant decrease at 6, 18, and 24 days of treatment (Figure 3.18). In the HCC1954 cell line,

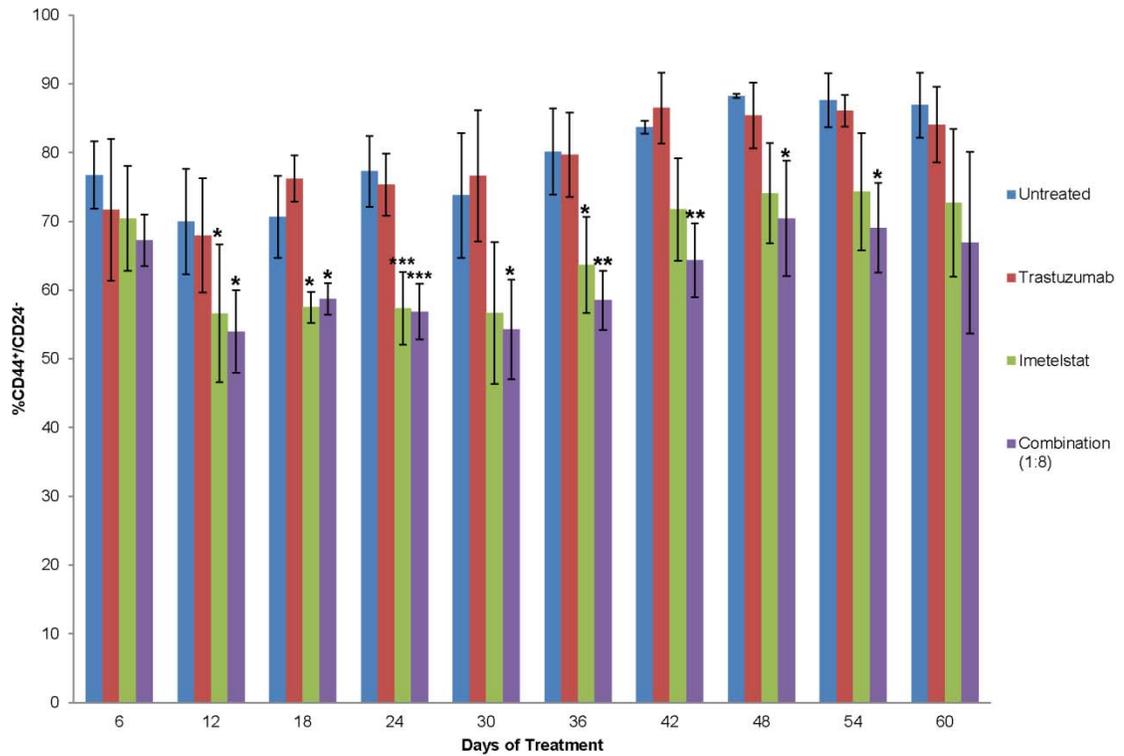


**Figure 3.17. Imetelstat Alone and in Combination with Trastuzumab Decreases the CD44<sup>+</sup>/CD24<sup>-</sup> CSC Population.** CSC marker expression analyzed by flow cytometry. Average percent CD44<sup>+</sup>/CD24<sup>-</sup>  $\pm$  SD, n=3, one-way ANOVA, \* p < 0.05, \*\* p < 0.01, \*\*\* p < 0.001

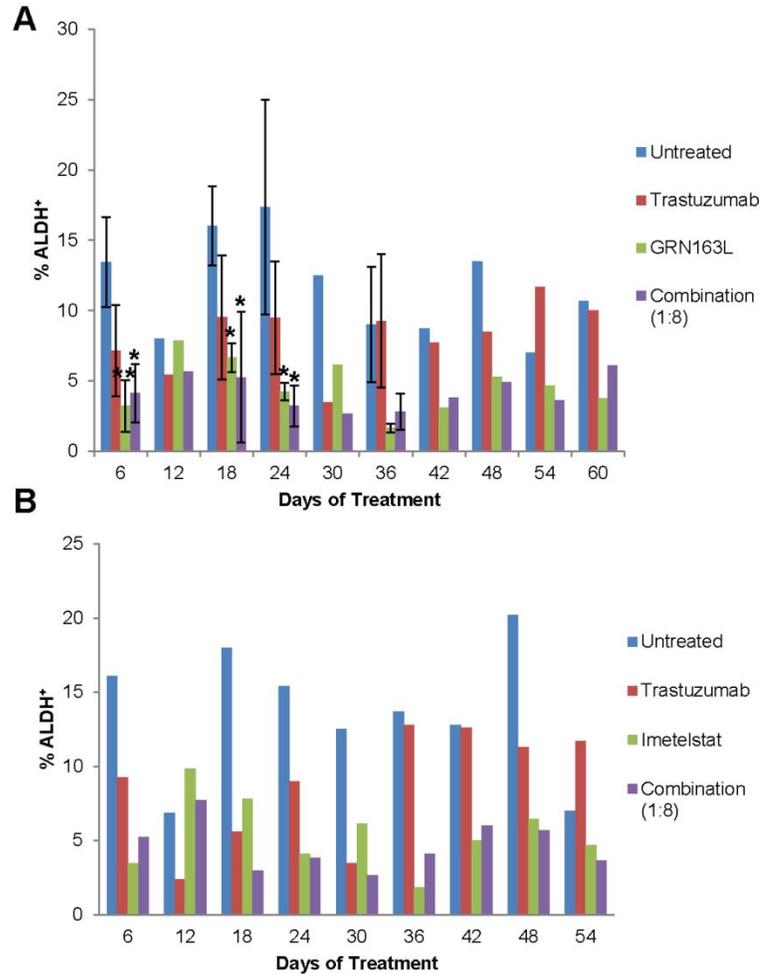


**Figure 3.18. Trastuzumab, Imetelstat, and Combination Treatment Decrease the ALDH<sup>+</sup> CSC Population in HCC1569 Cells.** A) ALDH enzymatic activity measured by flow cytometry. Average percent ALDH<sup>+</sup> ± SD when error bars are shown, n=2–3, one-way ANOVA, \* p < 0.05, \*\* p < 0.01. B) Representative ALDH enzymatic activity from one experiment.

trastuzumab, imetelstat, and combination treatment decreased the ALDH<sup>+</sup> CSC population by more than 50% when only one experiment is analyzed; however, there was no difference statistically due to the high variability in enzymatic activity when you analyze all three experiments together (Figure 3.19). Furthermore, in the SKBR3 cell line, trastuzumab, imetelstat, and combination treatment again decreased the ALDH<sup>+</sup> CSC population by up to 60% (Figure 3.20), although the treatments did not decrease the CSC population at every time point and again there was no difference statistically when you analyze all three experiments together due to the enzymatic activity variability. Additionally, we looked at the SKBR3-R cell line, which has an acquired resistance to trastuzumab due to continuous exposure to trastuzumab in cell culture (Nahta and Esteva, 2004). Indeed, 0.625  $\mu$ M trastuzumab decreased cellular proliferation in the SKBR3 cell line, but not the SKBR3-R cell line (Figure 3.21). In the SKBR3-R cells, imetelstat decreased the ALDH<sup>+</sup> CSC population at every time point and up to 60%, while trastuzumab and combination treatment decreased the CSC population at only half the time points when looking at one experiment (Figure 3.22). Interestingly, the time points with increased CSCs after trastuzumab treatment also had increased CSCs after combination treatment (Figure 3.22 B). In accordance with previous reports that showed trastuzumab decreased the percentage of ALDH<sup>+</sup> CSCs after 2-5 days of treatment, we also observed a decrease in the ALDH<sup>+</sup> CSC population after 6 days of trastuzumab treatment in all 4 cell lines (Korkaya et al., 2008). These results suggest imetelstat alone, and in combination with trastuzumab, is able to target the CSC population. Notably, in the HCC1569 cell line, combination treatment decreased both CD44<sup>+</sup>/CD24<sup>-</sup> and ALDH<sup>+</sup> CSCs (Figures 3.17 and 3.18).

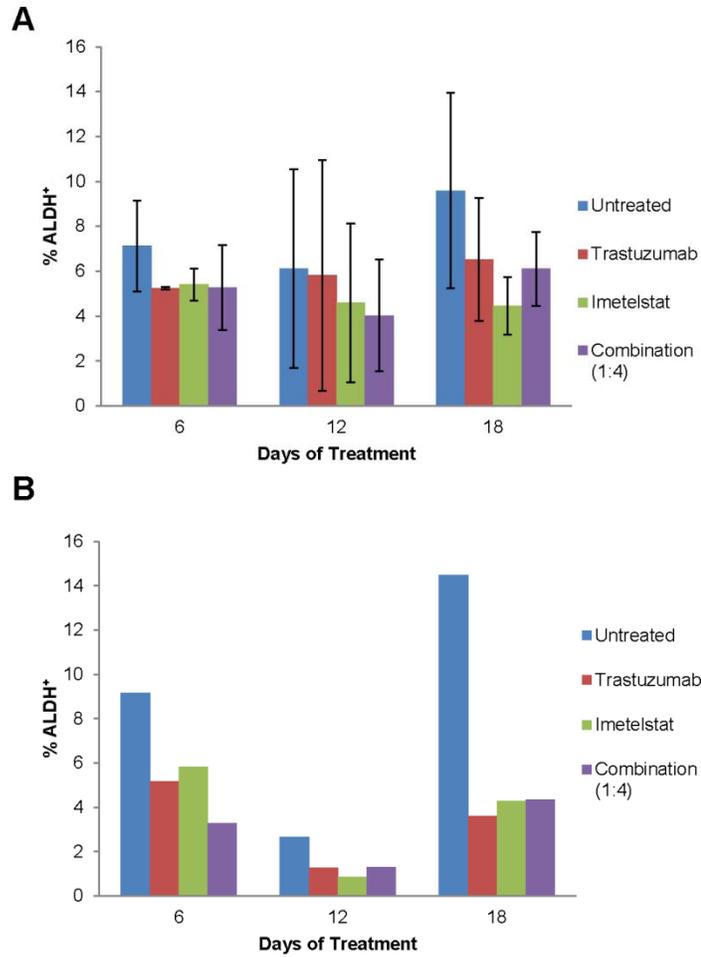


**Figure 3.19. Trastuzumab, Imetelstat, and Combination Treatment Decrease the ALDH<sup>+</sup> CSC Population in HCC1954 Cells.** A) ALDH enzymatic activity measured by flow cytometry. Average percent ALDH<sup>+</sup>  $\pm$  SD, n=3. B) Representative ALDH enzymatic activity from one experiment.

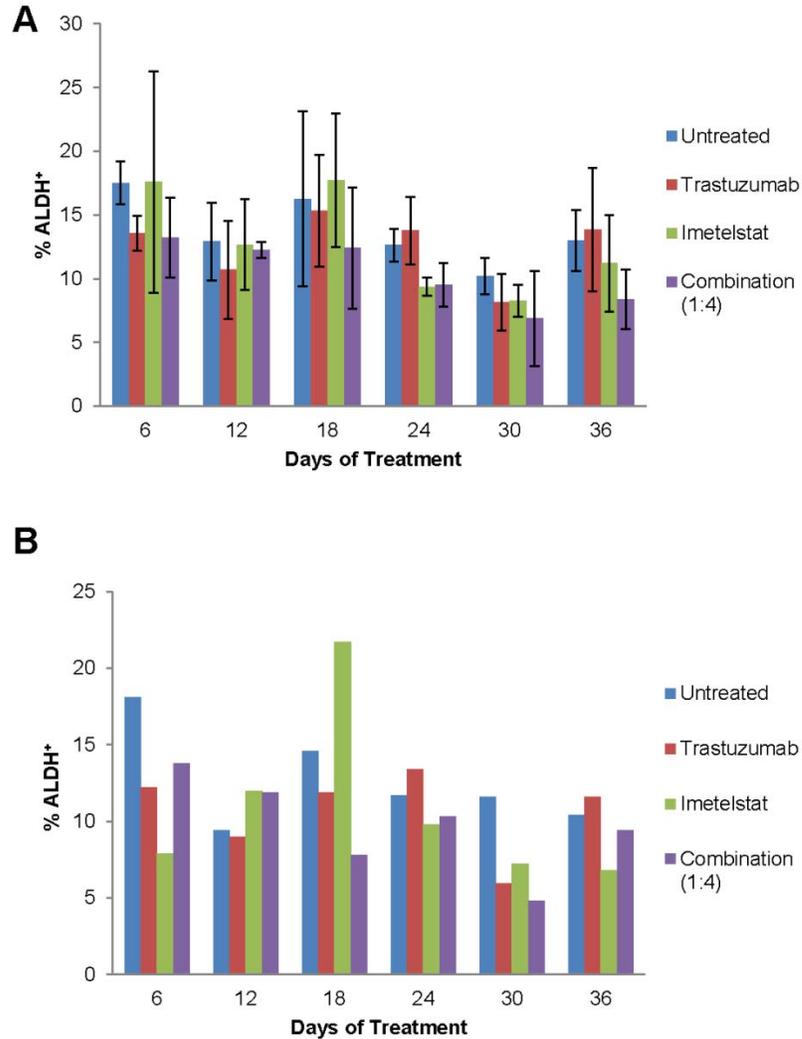


**Figure 3.20. Trastuzumab, Imetelstat, and Combination Treatment Decrease the ALDH<sup>+</sup> CSC Population in SKBR3 Cells.** A) ALDH enzymatic activity measured by flow cytometry. Average percent ALDH<sup>+</sup> ± SD, n=3. B) Representative ALDH enzymatic activity from one experiment.

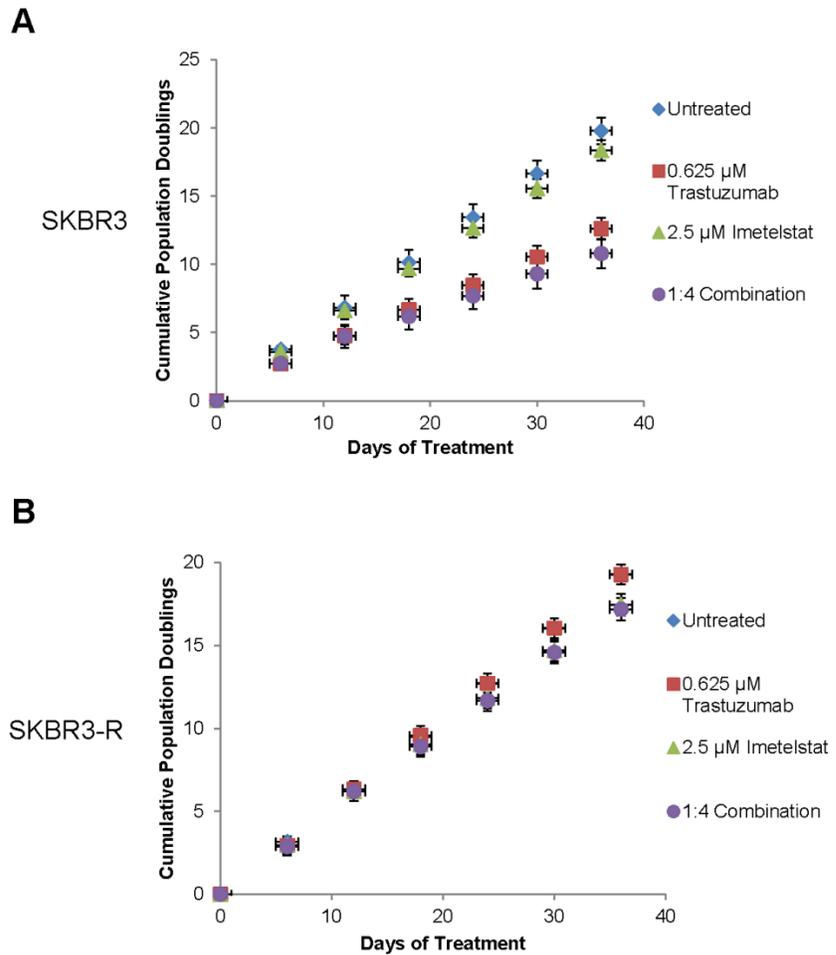


**Figure 3.21. Trastuzumab Limits Cellular Proliferation in SKBR3 Cells, But Not SKBR3-R Cells.** Cumulative population doubling graphs for A) SKBR3 and B) SKBR3-R cells.

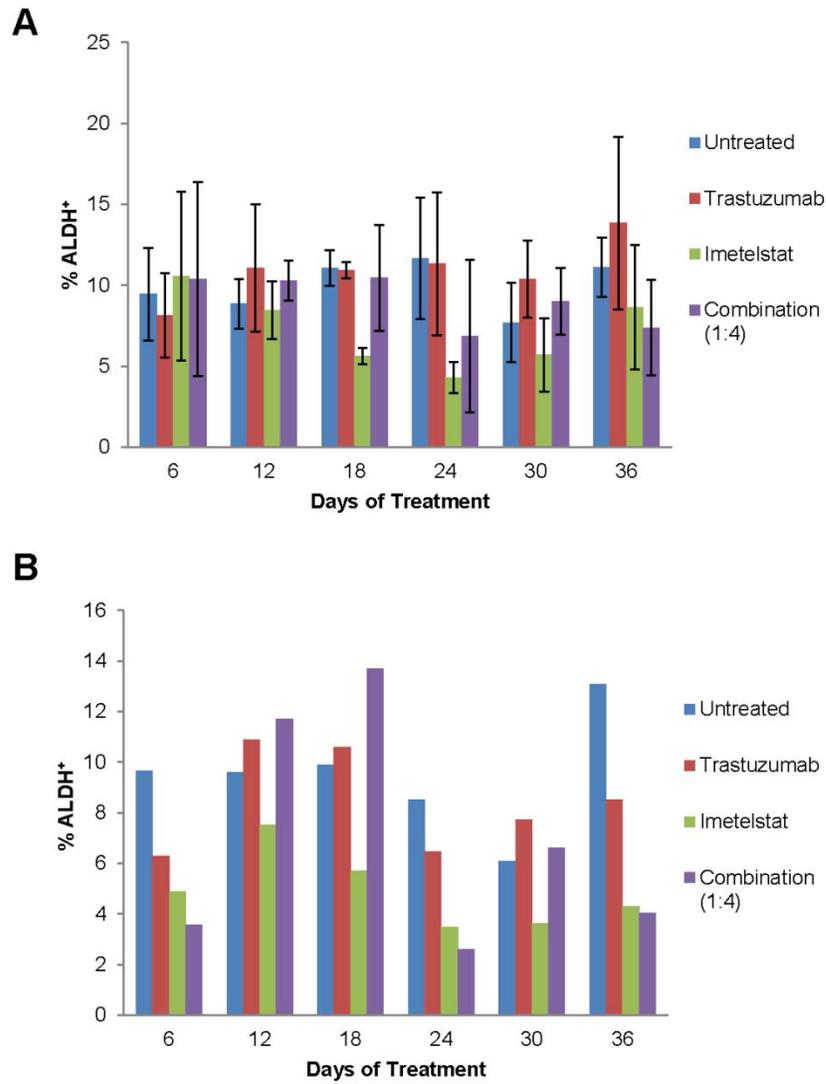


**Figure 3.22. Trastuzumab, Imetelstat, and Combination Treatment Decrease the ALDH+ CSC Population in SKBR3-R Cells.** A) ALDH enzymatic activity measured by flow cytometry. Average percent ALDH<sup>+</sup> ± SD, n=3. B) Representative ALDH enzymatic activity from one experiment.

## **Imetelstat in Combination with Trastuzumab Inhibits Self-renewal and Invasive Potential of CSCs**

We next wanted to determine if the decrease in the CSC population after imetelstat and combination treatment resulted in decreased functional ability of the CSCs. Pretreated cells were plated in non-adherent dishes using undifferentiating medium. Under these culture conditions, cells with self-renewal potential grow to form spheroids called mammospheres. We observed a significant decrease in mammosphere count following trastuzumab, imetelstat, and combination treatment after short term pretreatment (12 and 36 days) and long term pretreatment (90 days), suggesting CSC self-renewal is continually inhibited by these agents (Figure 3.23). Moreover, short term treatment with imetelstat does not lead to telomere shortening, but long term treatment does, suggesting imetelstat inhibits self-renewal potential of CSCs in telomere length dependent and independent mechanisms.

It has been reported that the CSC population has an increased invasive potential, an early step required for metastasis (Charafe-Jauffret et al., 2009; Sheridan et al., 2006). We performed *in vitro* invasion assays to determine if the decrease in CSCs following twelve days of imetelstat and/or trastuzumab treatment could also decrease invasive potential. While the invasive potential for the HER2<sup>+</sup> cell lines is much lower than other breast cancer cell lines, such as MDA-MD-231, we extended the length of the experiment (72 hours instead of 24 hours reported in other breast cancer cell lines) and were able to see some cells had invaded through the basement membrane and onto the bottom of the membrane insert (Neve et al., 2006). Ten random fields per well were counted. Imetelstat and combination treatment significantly decreased the invasive potential compared to untreated samples, with less than half as many cells invading in those treatment groups (Figure 3.24). These results suggest the decrease in CSCs

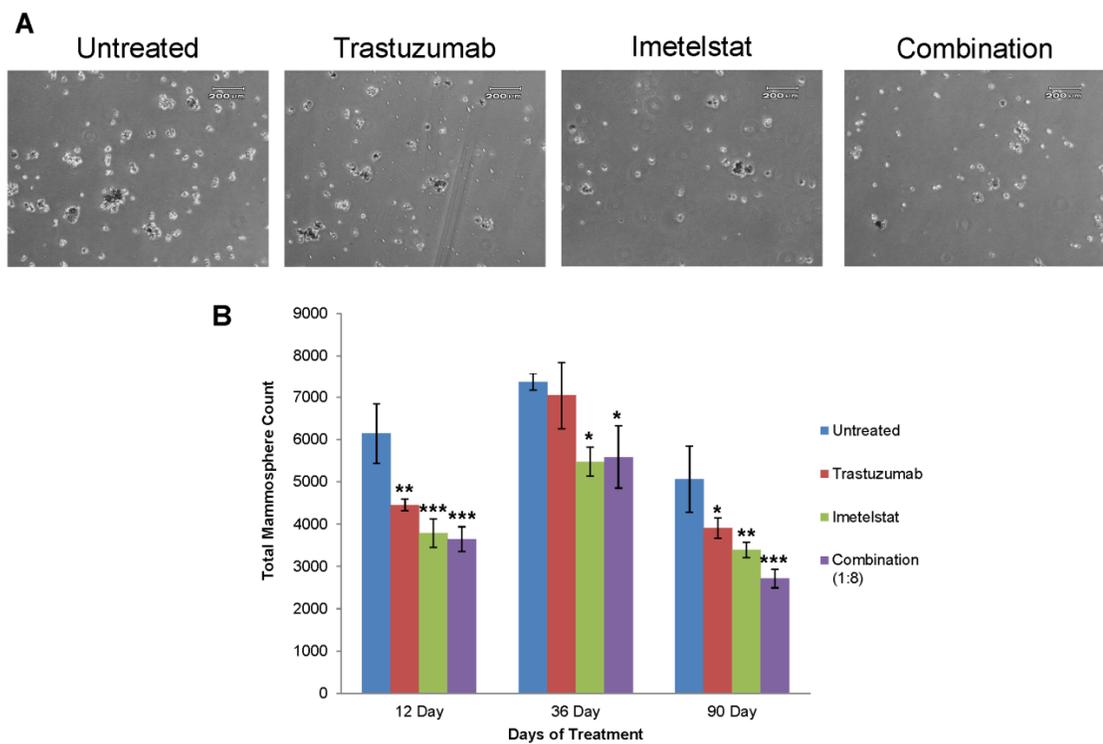


**Figure 3.23. Trastuzumab, Imetelstat, and Combination Treatment Inhibit Mammosphere Formation of HCC1569 Cells.** A) Representative Images of Primary Mammospheres cultured from HCC1569 cells. 4X Magnification, 200  $\mu\text{m}$  scale bar. B) Total mammosphere counts from 3 different pretreatment time points, Average  $\pm$  SD, n=3, one-way ANOVA, \* p < 0.05, \*\* p < 0.01, \*\*\* p < 0.001.

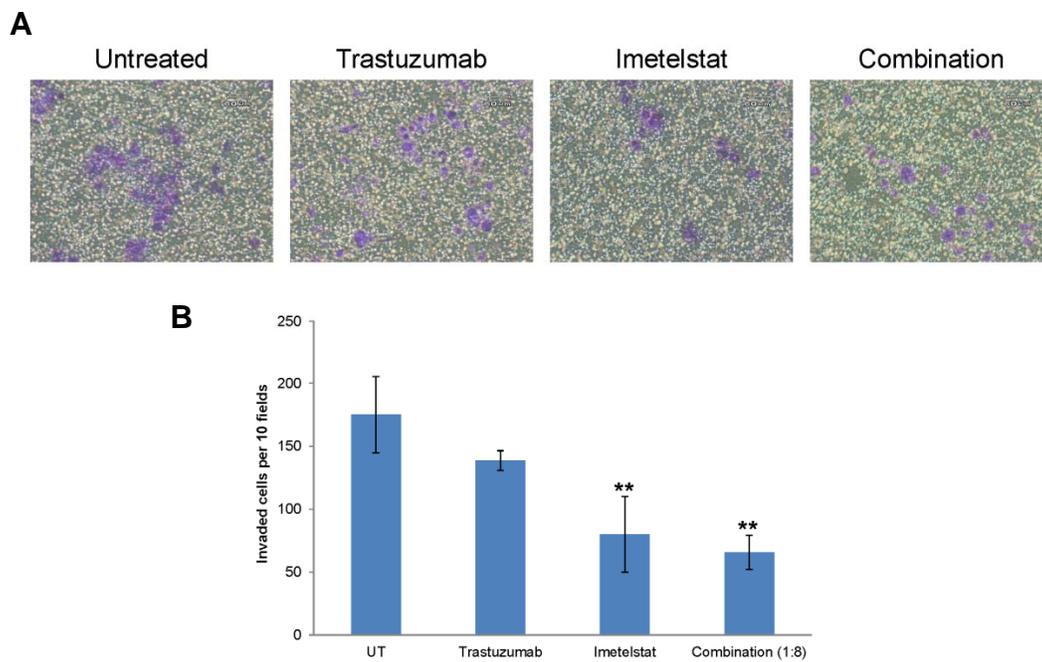


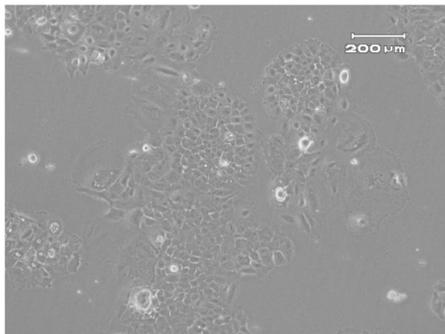
**Figure 3.24. Imetelstat Alone and in Combination with Trastuzumab Limits Invasion Potential of HCC1569 Cells.** A) Representative images of invaded cells in purple, 10X magnification, 60  $\mu\text{m}$  scale bar. B) Invaded cells in 10 random fields per well, Average  $\pm$  SD,  $n=3$ , one-way ANOVA, \*\*  $p < 0.01$ .

following imetelstat and combination treatment also inhibits the functional ability of the CSCs, shown by decreased self-renewal and invasive potentials.

### **Imetelstat and Trastuzumab Combination Treatment Decreases Primary Tumor Growth *In Vivo***

We and others have shown imetelstat treatment can decrease primary tumor growth in xenograft mouse models (Dikmen et al., 2005; Goldblatt et al., 2009b; Hochreiter et al., 2006; Shamma et al., 2008). However, the effect of imetelstat and trastuzumab combination treatment on xenograft tumor growth has not previously been studied. We chose to use the HCC1954 cell line for our animal model studies because these cells are ER<sup>-</sup>; therefore, addition of an estrogen pellet is not required and tumor formation via mammary fat pad inoculation has previously been reported (Korkaya et al., 2008). Initially, HCC1954 cells only formed tumors when injected subcutaneously and no tumor formation was observed after inoculation in the mammary fat pad of female, 5–7 week old NSG mice. We resected these subcutaneous tumors, mechanically digested them, and grew them as a monolayer culture. The xenograft HCC1954 cells, the cells that grew in culture from the xenograft tumors, are morphologically similar to the parental HCC1954 cells (Figure 3.25) and have overexpressed HER2 protein as shown by immunofluorescence (Figure 3.26), indicating our xenograft cell line was derived from the inoculated HCC1954 cells and not from murine cells. In a two animal pilot study, the xenograft HCC1954 cells were able to form tumors after mammary fat pad implantation in both mice and appeared to be forming metastatic lesions in the lungs as analyzed by H&E staining of lung tissue slides by a pathologist. Three to seven very small lesions of less than ten cells each were found in

Parental HCC1954



Xenograft HCC1954

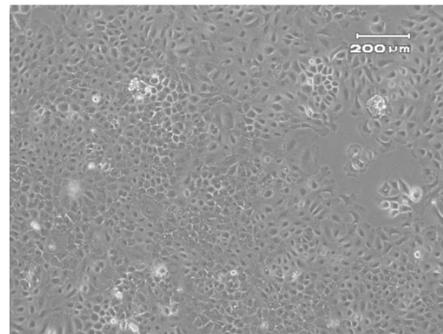


**Figure 3.25. Xenograft HCC1954 Cells have Similar Morphology to Parental Cell Line.** Xenograft mouse tumors were resected, digested, and grown as monolayer cells. Representative images of parental HCC1954 and xenograft HCC1954 cultures, 4X magnification, 200 μm scale bar.

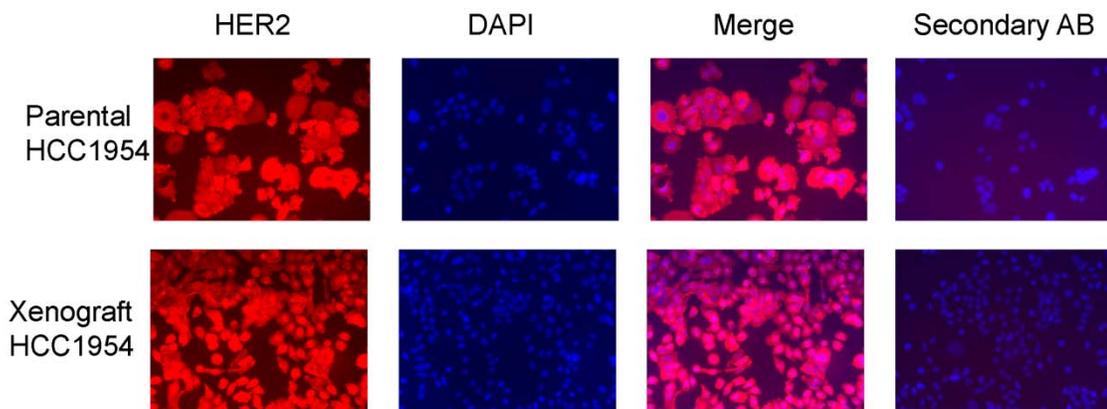


**Figure 3.26. Xenograft HCC1954 Cells Overexpress HER2 Protein.**

Immunofluorescence staining of Parental and Xenograft HCC1954 cells showing HER2 protein (red) is overexpressed in both cell lines, DAPI (blue) used as a nuclear stain, secondary antibody (AB) used as negative control for background staining, 20X magnification.

the lung tissue of both mice (summarized in Table 3.4 and Figure 3.27). It was recommended to extend our study for an additional week or two to allow the metastases to grow larger. Therefore, in our study, we chose to inject 750,000 cells instead of 1,000,000 cells, hoping we would be able to lengthen the study without the tumor burden hindering the well-being of the animals.

In our experimental study, we implanted 750,000 xenograft HCC1954 cells into the fourth mammary fat pad of female, 5–7 week old NSG mice and began treating with PBS (thrice weekly), imetelstat (thrice weekly), and/or trastuzumab (twice weekly) four days after the minor surgery. Trastuzumab and combination treatment delayed the onset of tumor formation and inhibited tumor growth (Figure 3.28 A). We found a significant decrease in primary tumor volume in the trastuzumab and combination treatment groups compared to the saline vehicle control group ( $p < 0.01$ ) (Figure 3.28 B). However, the study was concluded, due to burdensome tumor volume in the vehicle control group, before differences in tumor volume between the trastuzumab alone and combination group could be observed. The effects on tumor growth in the imetelstat only group lie between saline control and trastuzumab/combination groups. Final tumor volume was not statistically significantly different between saline control and imetelstat ( $p > 0.05$ ), as well as imetelstat and trastuzumab or combination ( $p > 0.05$  for both).

We determined tumor growth rates, calculated as the slope of the line of tumor volume versus days post inoculation, as an additional means of looking at tumor volume differences in our four sample groups (Figure 3.29). Tumor growth rates roughly doubled from combination to trastuzumab alone (6.0314 and 12.909, respectively). Tumor growth rates more than doubled between trastuzumab and imetelstat (12.909 and 30.94, respectively), but importantly saline control tumor growth rate was more than

**Table 3.4. Summary of Pilot Studies to Determine Metastatic Capability *In Vivo*.**

Cell Line	Fat Pad Injection (HBSS)	Tumor?	SubQ (1:1 SF media:matrigel)	Tumor?	Xenograft cell line
<b>1954</b>	1.00E+06	0/3	1.00E+06	3/3	X
	Fat Pad Injection (1 media: 1matrigel)	Tumor?	Mets?		Xenograft cell line
<b>1954 Xenograft</b>	1.00E+06	2/2	2/2 (3-7 small mets per lung, 11 weeks later)		X
	Fat pad injection	Tumor?	Mets?		
<b>1954 2nd xenograft</b>	1.00E+06	2/2	no matrigel mouse 25% matrigel mouse	Possibly a few cells (6.5 weeks) no evidence of mets (8 weeks)	
	Fat Pad Injection (1 media: 1matrigel)	Tumor?	Mets?		
<b>1954 Xenograft</b>	750,000	10/10	3/10 (10 weeks post injection)		

HCC1954 cells or xenograft HCC1954 cells were implanted into the mammary fat pad of 5-7 week old NSG mice under anesthesia. Tumor formation was evaluated as well as lung metastases.

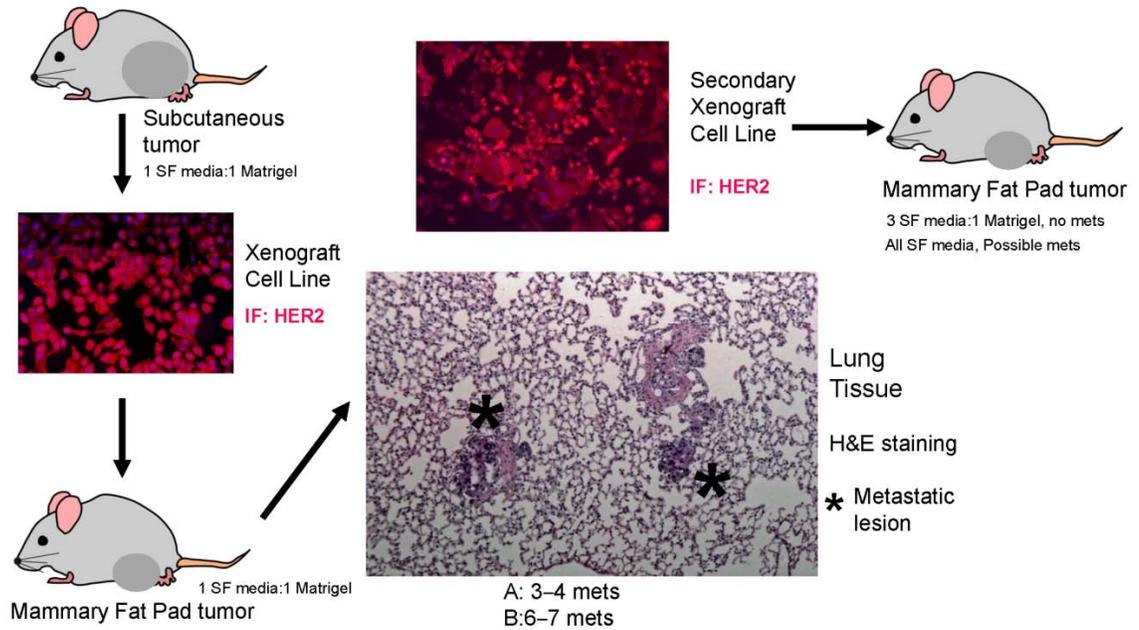


**Figure 3.27. Xenograft HCC1954 Cells Metastasize to the Lungs.** Xenograft HCC1954 cells formed tumors after implantation in the mammary fat pad of NSG mice and were able to colonize small metastatic lesions (less than 10 cells each) in the lungs. An additional passage in mice (Secondary Xenograft Cell Line) was potentially able to form metastases in the lungs, but these mice had to be sacrificed early due to tumor burden.

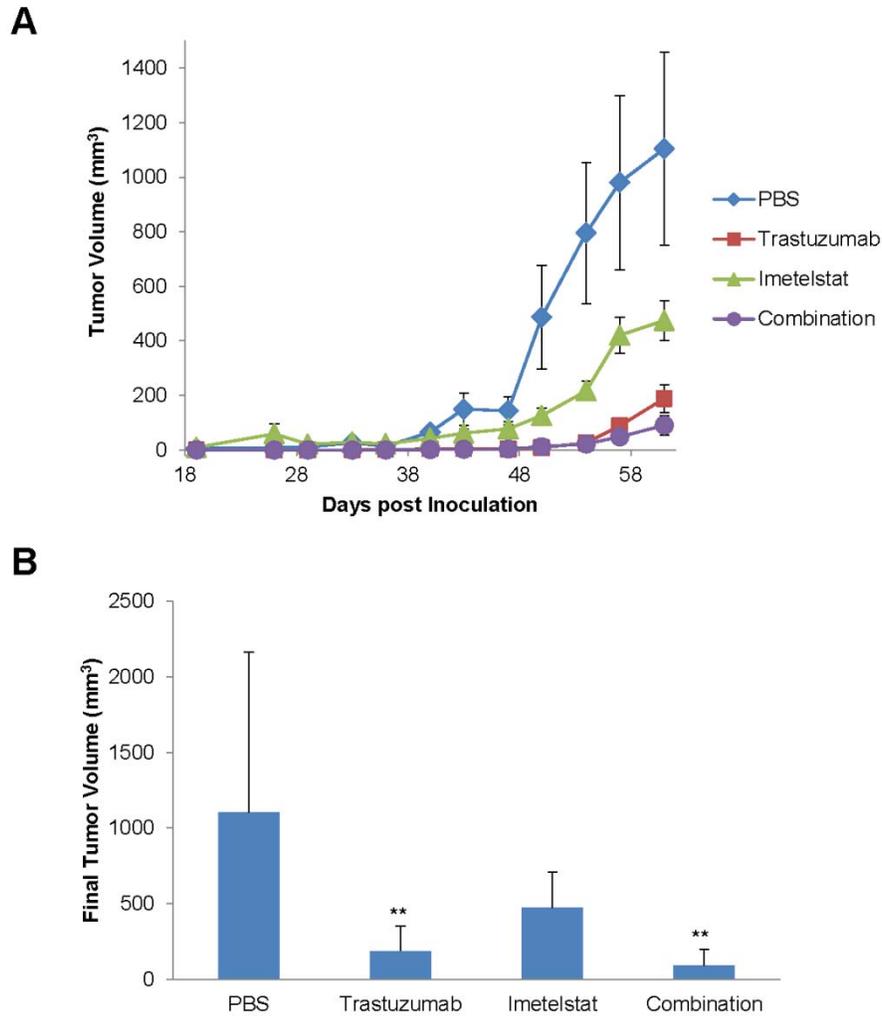


**Figure 3.28. Trastuzumab and Combination Treatment Inhibits Xenograft HCC1954 Primary Tumor Growth.** A) Tumor Volume (length x width<sup>2</sup>/2) was determined by caliper measurements twice weekly and graphed throughout the study. Average ± SEM, n=9–10 animals per group. B) Final Tumor volume for each sample group. Average + SD, n=9–10 animals per group, one-way ANOVA with Tukey's post-tests, \*\* p < 0.01.

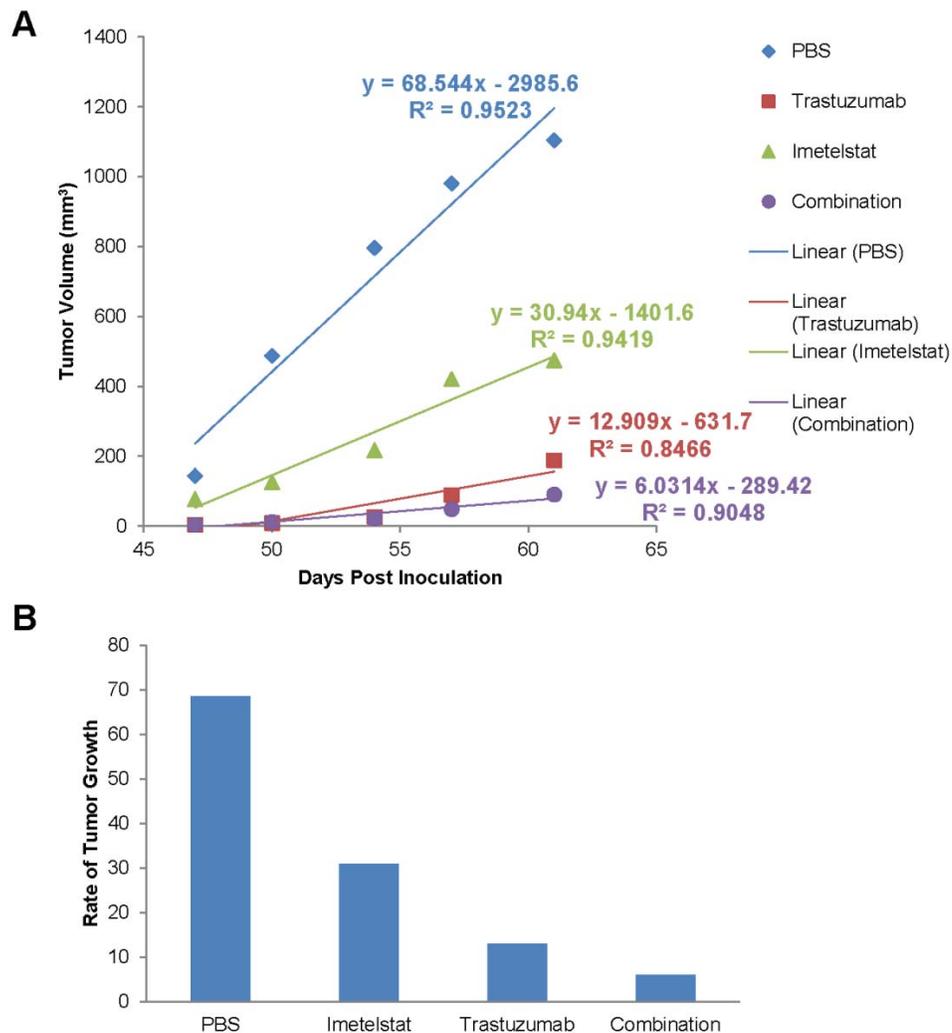


**Figure 3.29. Imetelstat, Trastuzumab, and Combination Treatment Decreases Xenograft HCC1954 Tumor Growth Rates.** A) Linear Regression was used to determine tumor growth rate (slope of the line, tumor volume per days post inoculation) for each sample group. B) Bar graph displaying Rate of Tumor Growth, as calculated in A) for each sample group.

double that of imetelstat (68.544 versus 30.94), suggesting imetelstat somewhat inhibits tumor growth by itself but not to the extent of trastuzumab or combination treatment. Different tumor growth rates between combination and trastuzumab alone groups suggest addition of imetelstat to trastuzumab can enhance the inhibitory effect of trastuzumab on tumor growth, supporting our *in vitro* data above (Figures 3.15 and 3.16) and previous report (Goldblatt et al., 2009a). Although we extended our study as long as possible so that metastatic lesions would be able to grow larger, we actually had to discontinue our study one week earlier than the pilot study due to large tumor burden impairing the animals of the saline control group (Table 3.4). H&E staining revealed the xenograft HCC1954 cells did not consistently metastasize in this study and only a few animals had any tumor cell infiltration into the lungs (Table 3.5).

### **Imetelstat Treated Xenograft Cells Have Decreased CSC Features**

We next wanted to determine whether the decrease we observed in the CSC population *in vitro* could also be observed *in vivo*. Imetelstat alone decreased the CSC population to levels similar as combination treatment (Figures 3.16–18) and we have previously shown imetelstat decreases lung metastases; therefore, we chose to use a cell line model which reliably metastasizes to the lungs without primary tumor resection, TMD-231 breast cancer cells, since we were unable to consistently observe metastasis with the HER2<sup>+</sup> HCC1954 xenograft cell line (Chen et al., 2013; Hochreiter et al., 2006). TMD-231 cells do not express HER2 amplification so trastuzumab is ineffective in these cells and was not studied. In accordance with our previous report, imetelstat significantly decreased tumor growth (Figure 3.30 A) and appeared to decrease lung metastases; although, lungs were too overtaken with tumor cells to quantitate the metastatic index

**Table 3.5. Xenograft HCC1954 Study Lung Metastases Observations.**

<b>Treatment Group</b>	<b>Observations</b>
<b>PBS</b>	Negative
	Negative
	5 tumor cells on edge
	Negative, congestion
	Negative
	Negative
	2 cells
	Tumor ball filling blood vessel, 4 mitotic figures
	Inflammation, congestion
	Negative
<b>Trastuzumab</b>	Negative, congestion
	Negative
	Negative, congestion
	Negative, congestion
	Negative
	Negative
	Mineral body
	Small tumor ball
	1 tumor cell, mitotic figure
Mineral body, inflammation	
<b>Imetelstat</b>	Negative
	Mineral body
	Small changes
	Macrophages
	Negative, congestion
	Negative
	Inflammation
	Negative
	2 tumor cells
	Inflammation
<b>Combination</b>	2 mineral bodies, tumor cells died
	Negative
	2-3 tumor cells
	3 yellow areas, blocked blood vessel with scar tissue, pulmonary emboli, dead, necrotic tissue
	Inflammation in blood
	Inflammation
	2-3 tumor cells
	Negative
	Inflammation

Animals were sacrificed after 10 weeks and lungs were resected, formalin fixed, paraffin embedded, and stained with H&E. Lung tissue slides were analyzed by a pathologist and observations were recorded.



(Figure 3.30 B). The primary tumor tissue from this study was mechanically and enzymatically digested to generate a single cell suspension. These primary xenograft tumor cells were then grown in monolayer culture or subjected to flow cytometry analysis of CSC marker expression. The PBS treated xenograft cells had a more mesenchymal-like phenotype characterized by the elongated morphology and reduced cell-cell contact, a phenotype typical of breast CSCs (Mani et al., 2008), whereas the imetelstat treated xenograft cells had more epithelial features, namely rounder morphology with more cell-cell contact (Figure 3.31 A). Furthermore, there was a trend of decreased CSC marker expression in imetelstat treated xenograft cells compared to vehicle control, but this decrease was not statistically significant due to higher variability in the PBS group with a near outlier and small sample size (Figure 3.31 B). These data suggest imetelstat can target the CSC population *in vivo*.

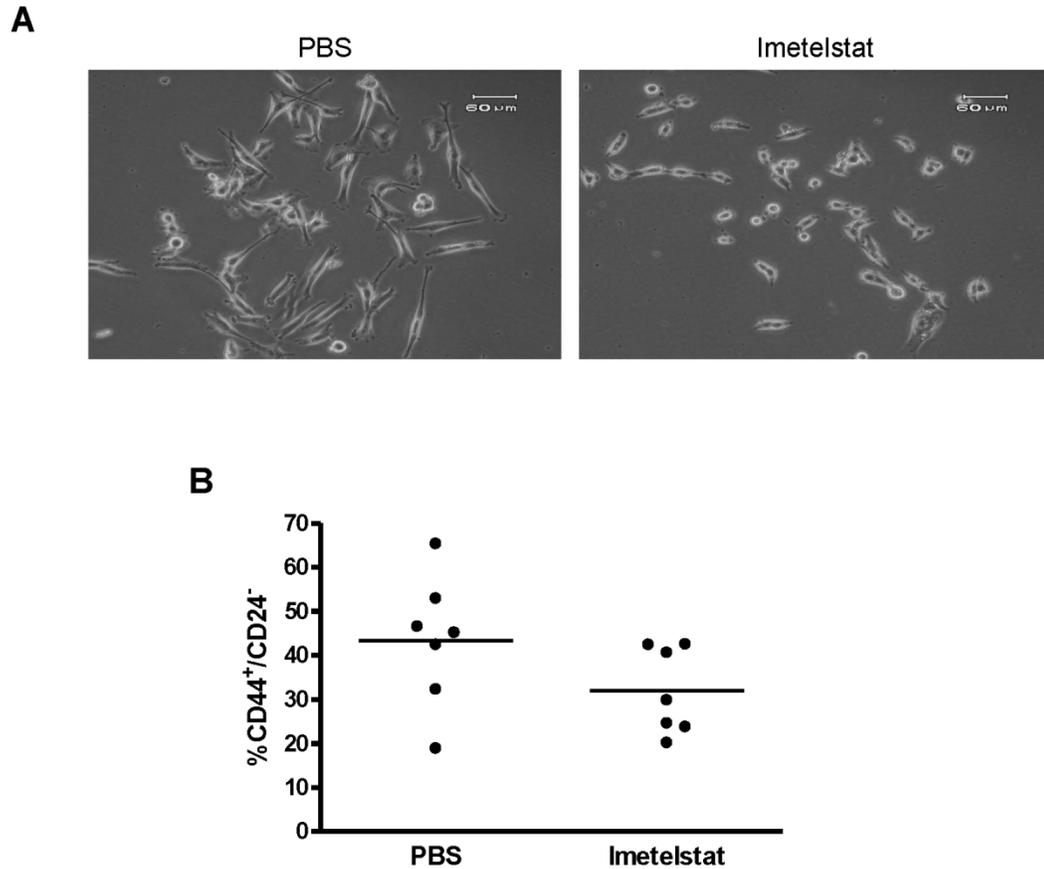


**Figure 3.31. Imetelstat Decreases TMD-231 CSC Features.** A) Resected primary TMD-231 tumors digested and cultured as xenograft cells. Imetelstat treated cells appear more epithelial while PBS treated cells have a predominately mesenchymal phenotype, 10X magnification, 60  $\mu$ m scale bar. B) Flow cytometry analysis of CSC marker expression of primary TMD-231 tumors from Figure 3.30. Average is lineated, Students t-test,  $p = 0.12$ .

## CHAPTER FOUR

### DISCUSSION

In this thesis, we show HER2<sup>+</sup> CSCs have active telomerase that can be inhibited by imetelstat treatment, leading to telomere shortening. Imetelstat treatment alone, and in combination with trastuzumab, decreased the number of CSCs, as well as their functional ability, as shown by decreased mammosphere count and invasive potential. Moreover, imetelstat was able to decrease the CSC population and mammosphere formation in a Triple Negative Breast Cancer cell line, TMD-231. We report the first *in vivo* study of imetelstat and trastuzumab combination, in which the combination treatment had a slower tumor growth rate than either drug alone. Additionally, we found a trend toward lower CSC marker expression in imetelstat treated xenograft cells compared to PBS control, although this was not statistically significant due to small sample size and a near outlier in the PBS group.

Imetelstat has previously been shown to decrease the CSC population (Castelo-Branco et al., 2011; Joseph et al., 2010; Marian et al., 2010a; Marian et al., 2010b). These studies mainly analyzed marker expression and spheroid formation following imetelstat treatment and did not investigate invasive and metastatic potential or combination with standard of care therapies. This study is the first to propose the decreased metastases and invasion following imetelstat treatment are due to decreased CSCs. Moreover, we are the first to investigate the effect of imetelstat and trastuzumab combination therapy on the CSC population.

Telomerase inhibition therapies have a long lag time from start of treatment to cell death or senescence due to their mechanism of action. Cells must undergo a large number of cell divisions before telomeres become critically short and signal a DNA

damage response or growth arrest, suggesting telomerase inhibitors would be most effective when used in combination with standard therapies that have a rapid inhibitory effect on tumor cells. Furthermore, telomerase inhibitors, like imetelstat, will be best tolerated when used in combination with agents that have different dose-limiting toxicities, such as targeted therapies like trastuzumab that have very few hematological side effects. Indeed, the dose-limiting toxicities of imetelstat and trastuzumab combination therapy have been studied in a Phase I clinical trial in refractory HER2<sup>+</sup> metastatic breast cancer patients (NCT01265927, [www.clinicaltrials.gov](http://www.clinicaltrials.gov)).

Interestingly, we observed a decrease in the CSC population following imetelstat treatment both prior to telomere shortening and after telomere shortening, suggesting the effect of imetelstat on the CSC population occurs in telomere length dependent and independent mechanisms, as also reported by Brennan and colleagues when looking at short and long-term treatment with imetelstat on the multiple myeloma CSC fraction (Brennan et al., 2010). In the study by Brennan, 72 hour treatment with imetelstat decreased mRNA expression of 5 genes important in CSC cell-fate decisions and self-renewal, suggesting imetelstat can target the CSC population by impacting essential stem cell pathways during stem cell-fate decisions independent of telomere length. Additionally, long-term treatment with imetelstat inhibited clonogenic survival of multiple myeloma CSCs, suggesting imetelstat modulates CSC growth and self-renewal through decreasing telomere length (Brennan et al., 2010). In our study, the CSC and non-CSC populations have similar telomerase activity and average telomere length, discounting the possibility that CSCs have shorter baseline telomeres and thus require less time to reach critically short lengths. However, it is possible that CSCs have one or a few very short telomeres that are sufficient to signal telomere uncapping after short-term telomerase inhibition. It is unlikely the decrease in the CSC population after just 12 days

of treatment is due to changes in telomere length, supporting the notion imetelstat can also work in telomere length independent mechanisms.

The noncanonical functions of telomerase have recently been investigated (reviewed in (Li and Tergaonkar, 2014)) and may elucidate how imetelstat impairs CSCs independent of telomere shortening. Distinct from its activity at telomeres, telomerase can activate NF- $\kappa$ B mediated transcription and regulate NF- $\kappa$ B target gene expression by binding to the p65 subunit of NF- $\kappa$ B and being recruited to NF- $\kappa$ B promoters such as IL-6, TNF- $\alpha$ , and metalloproteinases (Ding et al., 2013; Ghosh et al., 2012). Additionally, TERT serves as a transcriptional modulator of the Wnt/ $\beta$ -catenin signaling pathway by binding to the promoter of Wnt-dependent genes (Park et al., 2009). Furthermore, TERT, BRG1, and GNL3L/NS form a complex necessary to maintain the function of CSCs (Okamoto et al., 2011). Both NF- $\kappa$ B and Wnt are critical pathways in CSC maintenance. NF- $\kappa$ B regulates CSC self-renewal both cell autonomously and non-autonomously (Liu et al., 2010; Yamamoto et al., 2013). Wnt/ $\beta$ -catenin regulates self-renewal and proliferation of CSCs (Hallett et al., 2012; Liu et al., 2004). It could be possible the decrease we see in CSCs following imetelstat treatment is related to the transcriptional activity of telomerase on NF- $\kappa$ B and/or Wnt signaling independent of imetelstat causing shortening of telomeres. The inhibition of telomerase activity through imetelstat is more complex than simply shortening telomere length and warrants further investigation.

Another potential telomere independent mechanism to explain the effect of imetelstat on CSCs could be due to reversal of the epithelial mesenchymal transition (EMT). EMT activation is associated with maintenance of stem cell properties and acquisition of invasive and metastatic properties; EMT is able to generate CSCs (Gupta et al., 2009; Mani et al., 2008; Morel et al., 2008). The hallmarks of EMT are loss of E-

cadherin, which is associated with adherence junction disassembly, and expression of vimentin and fibronectin (Christiansen and Rajasekaran, 2006). We did observe a change in cellular phenotype of imetelstat treated xenograft cells compared to PBS treated (Figure 3.31 A). EMT is crucial for the initial steps of metastasis, including local invasion, intravasation, systemic transport, and extravasation; however, cells must then undergo a reversion of EMT termed MET to colonize a metastatic lesion (Tsai and Yang, 2013). Interestingly, a recent study investigated the off-target effects of imetelstat, including the cell rounding and loss of attachment frequently observed following imetelstat treatment. This study found imetelstat disrupts the cytoskeleton through changes in actin, tubulin, and intermediate filament organization; furthermore, imetelstat decreases MMP2 expression and subsequently invasive ability of lung cancer cells (Mender et al., 2013). Of note, this study also found imetelstat treatment resulted in a loss of E-cadherin, which could suggest cells have undergone EMT, but are unable to subsequently undergo MET and cannot adhere to colonize a metastatic lesion.

While EMT has been closely associated with CSCs, other studies suggest cells that undergo EMT are not the cells responsible for metastases (Tsuji et al., 2008). Studies were carried out by Liu and collaborators to better understand the relationship between EMT, MET, and CSCs and furthermore distinguish between CD44<sup>+</sup>/CD24<sup>-</sup> CSCs and ALDH<sup>+</sup> CSCs (Liu et al., 2014). Gene expression analysis using microarrays was performed on isolated CD44<sup>+</sup>/CD24<sup>-</sup> or ALDH<sup>+</sup> cell populations from primary breast cancer tissue. The researchers found many genes displayed reciprocal expression patterns between CD44<sup>+</sup>/CD24<sup>-</sup> and ALDH<sup>+</sup> cell populations; for example, mRNA transcripts elevated in CD44<sup>+</sup>/CD24<sup>-</sup> population were diminished in the ALDH<sup>+</sup> cell population. However, a set of transcripts expressed in CD44<sup>+</sup>/CD24<sup>-</sup> and ALDH<sup>+</sup> cell populations overlapped with spheroid-forming cells, likely representing genes involved in

stem cell function. These results suggest two stem cell compartments in human breast cancers are identified by CSC markers. Moreover, CD44<sup>+</sup>/CD24<sup>-</sup> CSCs were significantly enriched in EMT-associated genes and ALDH<sup>+</sup> CSCs were elevated in genes associated with the epithelial-like state (Liu et al., 2014). Furthermore, purified CD44<sup>+</sup>/CD24<sup>-</sup> or ALDH<sup>+</sup> cells were able to generate heterogeneous populations and recapitulate the CD44<sup>+</sup>/CD24<sup>-</sup> and ALDH<sup>+</sup> proportions present in the original cell line *in vitro*, suggesting CSCs display plasticity and are able to reversibly transition between the mesenchymal-like CD44<sup>+</sup>/CD24<sup>-</sup> CSC state and the epithelial-like ALDH<sup>+</sup> CSC state (Liu et al., 2014). This switching between two distinct EMT and non-EMT CSC populations is supported by work in squamous cell carcinoma in which CSCs behaved likewise (Biddle et al., 2011). Of note, it may be important to target both CSC populations as they can alternate between the two states (Liu et al., 2014). Importantly, in this thesis, we show imetelstat alone and in combination with trastuzumab is able to decrease CD44<sup>+</sup>/CD24<sup>-</sup> and ALDH<sup>+</sup> CSCs in a number of cell lines and most notably in the HCC1569 cell line, which displays both CSC populations.

The ability of cells to undergo EMT and MET and thus cross back and forth between epithelial and mesenchymal states is known as epithelial mesenchymal plasticity (EMP) (Pinto et al., 2013). Circulating tumor cells are thought to display EMP and share both epithelial and mesenchymal markers (Armstrong et al., 2011; Bednarz-Knoll et al., 2012). Furthermore, in a xenograft model using MDA-MB 468 cells, EMT is exhibited by cells at the tumor periphery while lymph node and lung metastases are mainly epithelial (Bonnomet et al., 2012). Additionally, metastases from a xenograft MDA-MD-231 model exhibited epithelial marker expression, while these cells are highly mesenchymal *in vitro* (Chao et al., 2010). Thus, the plasticity allowing cells to transition

between epithelial and mesenchymal-like states may play a critical role in metastasis formation (Liu et al., 2014).

In summary, our results show imetelstat treatment of HER2<sup>+</sup> breast cancer cells leads to telomerase inhibition and decreases the CSC population alone and in combination with trastuzumab. Markedly, imetelstat and trastuzumab combination is able to decrease the percentage of CD44<sup>+</sup>/CD24<sup>-</sup> and ALDH<sup>+</sup> CSCs in the same cell line, suggesting this combination would be effective in targeting CSCs because we are able to target both subsets and thus cells would not benefit from transitioning to the other CSC state, which could potentially occur if we were only able to target one CSC state. Imetelstat decreased the self-renewal potential as well as invasive potential of the CSC population alone and in combination with trastuzumab. CSCs are thought to be responsible for recurrent and metastatic disease and our study suggests adding imetelstat to trastuzumab treatment may provide a more durable clinical response for HER2<sup>+</sup> breast cancer patients.

## CHAPTER FIVE

### CONCLUSIONS AND FUTURE DIRECTIONS

The overall goal of this research project was to gain insight into the role of telomerase inhibition on the CSC population in breast cancer cells. Additionally, we wanted to expand our studies on imetelstat and trastuzumab combination treatment in additional cell lines, as well as *in vivo*. The work presented in this thesis demonstrates HER2<sup>+</sup> CSCs have active telomerase that can be inhibited by imetelstat treatment, leading to telomere length shortening. Additionally, we show imetelstat alone, and in combination with trastuzumab, can significantly decrease the CSC population and their self-renewal and invasive potentials. Moreover, we observed a significant inhibition of tumor growth in combination treated mice compared to saline control treated mice, as well as the slowest tumor growth rate in combination treated mice. Furthermore, cells from imetelstat treated xenograft tumors were morphologically different and exhibited a trend toward decreased CSC marker expression compared to cells from saline treated xenograft tumors.

This study is novel in that assessment of imetelstat in combination with a standard of care therapy on the CSC population has not previously been reported. One of the major concerns of telomerase inhibitors is the long lag period needed to shorten telomeres to critical levels before they undergo senescence or cell death. To overcome this obstacle, telomerase inhibition is combined with agents that have a swift mechanism of action on cancer cells, notably paclitaxel and trastuzumab in breast cancer patients. Imetelstat has previously been shown to target the CSC population as a single agent, but the effects of imetelstat in combination with other agents was unknown (Castelo-Branco et al., 2011; Joseph et al., 2010; Marian et al., 2010a; Marian et al., 2010b). In this study, we show imetelstat and trastuzumab combination treatment can inhibit the

CSC population as effectively as imetelstat alone and potentially enhanced at some study points. It would be interesting to determine the effects of imetelstat in combination with other therapeutic agents, such as paclitaxel and doxorubicin, on the CSC population. Standard chemotherapeutic agents have been shown to increase the CSC population and it would be interesting to see if combination with imetelstat is able to overturn the increase in CSCs (Li et al., 2008).

HER2 overexpression and/or amplification is a major driver of pathogenesis in breast cancer, and it is also becoming more apparent the importance of HER2 overexpression in other cancer types as well. Up to 30% of gastric cancers are HER2<sup>+</sup>, prompting the ToGA trial to determine the efficacy and safety of trastuzumab and subsequently FDA approval for the use of trastuzumab in advanced gastric cancers (Boku, 2014). HER2 overexpression has also been observed in up to 50% of uterine serous carcinomas and up to 30% of endometrial cancers, leading to clinical trials to test trastuzumab efficacy and safety in these cancer types (Diaz-Montes et al., 2006; Morrison et al., 2006). More recently, HER2 amplification was found in up to 20% of esophageal adenocarcinomas and the addition of trastuzumab to standard of care is being evaluated (Hu et al., 2011). It would be interesting to examine the use of imetelstat and trastuzumab combination therapy in these HER2<sup>+</sup> cancer subtypes and determine if imetelstat can augment the effects of trastuzumab similar to what we have demonstrated in breast cancer. Additionally, it may prove beneficial to examine the effect of trastuzumab and imetelstat combination treatment on the CSC populations of these cancer subtypes as well.

Telomerase plays a critical role in normal stem cell self-renewal and differentiation (Choi et al., 2008). It has been reported that alterations in CSC number correlates with changes in expression of stem cell related genes, suggesting differentiation of CSCs when they are targeted (Brennan et al., 2010; Korkaya et al.,

2008). As we have shown a decrease in CSCs after imetelstat and combination treatment with trastuzumab in this study, it is important to determine what results from this decrease. To determine if our treatments are inducing differentiation of CSCs, we would perform real-time PCR to measure mRNA expression of stem cell related genes, for example, *OCT3/4*, *SOX2*, *NANOG*, *BMI1*, *JAG1*, and *GLI1*. Alternatively, the decrease in CSCs could be due to induction of cell death. To determine if our treatments are inducing apoptosis of CSCs, we would measure Annexin V and propidium iodine staining by flow cytometry and perform western blotting to determine caspase cleavage.

In this study, we also show imetelstat alone and in combination with trastuzumab decreases invasive potential of HCC1569 cells. While the invasive potential for HCC1569 cells is much lower than other breast cancer cell lines, such as MDA-MD-231, we extended the length of the experiment and were able to see some cells had invaded through the basement membrane invasion assay (Neve et al., 2006). To further explore the effects of imetelstat and combination with trastuzumab on invasive and metastatic potential, it would be useful to measure changes in invasion and metastasis associated proteins. We would use real-time PCR to analyze mRNA expression of matrix metalloproteinases (*MMP2*, *MMP3*, and *MMP9*) used to break down extracellular matrix and the metastasis associated proteins (*MTA1*, *MTA2*, and *MTA3*).

This study is the first to report a significant inhibition of tumor formation in a xenograft animal model using imetelstat and trastuzumab combination treatment. We were unable to distinguish tumor volume differences between trastuzumab treated mice and combination treated mice due to cessation of the study because of tumor burden in the saline treated animals. To determine whether combination treatment can inhibit tumor formation better than trastuzumab alone, it would be important to perform modified survival studies *in vivo*, where animals are sacrificed once tumors reach a set volume,

as has previously been used to study other agents in combination with trastuzumab (Garrett et al., 2013). Additionally, use of a less immunocompromised mouse strain, such as athymic nude mice which still have Natural Killer (NK) cells, would provide a better model of primary tumor growth response to trastuzumab and combination treatment, as antibody-dependent cell cytotoxicity mediated through NK cells is thought to be a main mechanism of trastuzumab action (Bianchini and Gianni, 2014).

While we show decreased lung metastases using the TNBC cell line TMD-231 following imetelstat treatment, we were unable to consistently form metastatic lesions using the HER2<sup>+</sup> breast cancer cell line HCC1954 and therefore could not study the effect of imetelstat and trastuzumab combination on metastasis formation. Developing a representative metastatic model has proven difficult in HER2<sup>+</sup> breast cancers, although a few have been described. Infection of a metastatic cell line, such as TMD-231, with a lentivirus containing *HER2*, would generate a HER2<sup>+</sup> metastatic model, but could lack the relevant pathology of this subtype due to exogenous overexpression of HER2. Yu and colleagues were able to generate lung metastases and liver metastases (80% and 60% incidence rates, respectively) after tertiary serial passage *in vivo* of the HER2<sup>+</sup> breast cancer cell line SKBR3 (Yu et al., 2007). Additionally, Nanni and collaborators developed a model of multiorgan metastases of HER2<sup>+</sup> human breast cancer cells using highly immunodeficient Rag2<sup>-/-</sup>;Il2rg<sup>-/-</sup> (also called Rag2<sup>-/-</sup>;gamma<sup>-/-</sup>) mice and orthotopic implantation of 10<sup>7</sup> MDA-MD 453 or BT474 with metastatic incidences of 100% and 67%, respectively (Nanni et al., 2012). It would be beneficial to determine the effect of trastuzumab and imetelstat combination on metastatic potential and one of the above models could help us do so.

As discussed in Chapter Four, telomerase can activate NF-κB mediated transcription and regulate NF-κB target gene expression, as well as serve as a transcriptional modulator of the Wnt/β-catenin signaling pathway (Ding et al., 2013;

Ghosh et al., 2012; Park et al., 2009). As NF- $\kappa$ B and Wnt signaling pathways are essential in CSC maintenance, it is possible inhibition of telomerase by imetelstat impacts regulation of these signaling pathways and may explain the decrease in CSCs after imetelstat treatment. It is worthwhile to investigate whether binding of TERT to the NF- $\kappa$ B p65 subunit is altered after imetelstat treatment. Additionally, investigating gene expression of NF- $\kappa$ B dependent genes before and after imetelstat treatment would be of interest as telomerase regulates expression of these genes, many of which are important in cancer progression. Moreover, TERT activates the Wnt pathway by acting as a cofactor in a  $\beta$ -catenin transcriptional complex, although recent work suggests this may be cell type and experimental system dependent (Listerman et al., 2014). Nonetheless, in a study of esophageal cancer, telomerase variants found in patient samples decreased telomere length, depleted  $\beta$ -catenin, down regulated canonical Wnt signaling, and significantly decreased tumorigenicity of esophageal cancer cells (Zhang et al., 2014). It would be interesting to investigate Wnt pathway activation after imetelstat treatment.

As telomerase plays an important role in normal stem cell function, another serious concern of telomerase inhibition used as an anti-cancer therapeutic is the effect on normal stem cells. The most common toxicities of patients receiving imetelstat are neutropenia, thrombocytopenia, and lymphopenia and in the only clinical trial data published, 2 of 6 patients had dose-limiting myelosuppression (Thompson et al., 2013). As Hematopoietic Stem Cells (HSCs) are one of the most rapidly dividing cells in the body, it is not surprising patients develop low blood cell counts after receiving telomerase inhibitors. Indeed, telomerase deficient murine HSCs can be serially transplanted less than half as many rounds as wild-type HSCs and have approximately a 2-fold increase in rate of telomere shortening, suggesting telomerase maintains replicative capacity of HSCs by countering telomere shortening that occurs with every

cell division (Allsopp et al., 2003). It would be interesting to investigate the consequences of telomerase inhibition therapy on HSCs and hematopoietic progenitor cells. HSCs are defined as CD34<sup>+</sup>, CD59<sup>-</sup>, Thy1/CD90<sup>+</sup>, CD38<sup>-</sup>, C-kit/CD117<sup>+</sup>, lin<sup>-</sup>. Flow cytometry could be used to measure the percentage of HSCs after imetelstat treatment. Notably, bone marrow aspirates were collected from patients enrolled in the Phase I study of imetelstat and trastuzumab combination in refractory HER2<sup>+</sup> metastatic breast cancer and could be used for these studies. Studying the effect of telomerase inhibition on the normal HSC compartment would provide insight into the toxicities observed in patients receiving imetelstat.

In conclusion, we report here imetelstat treatment decreases the CSC population alone and in combination with trastuzumab. Strikingly, imetelstat and trastuzumab combination is able to decrease the percentage of CD44<sup>+</sup>/CD24<sup>-</sup> (mesenchymal-like CSCs) and ALDH<sup>+</sup> (epithelial-like CSCs) populations in the HCC1569 cell line, suggesting this combination would be highly effective in targeting CSCs. Both epithelial-like CSCs and mesenchymal-like CSCs are decreased; thus, cells would have no advantage or escape route by transitioning to the other CSC state, which could potentially occur if we were only able to target one CSC state. Imetelstat decreased the self-renewal potential as well as invasive potential of HCC1569 cells alone and in combination with trastuzumab. CSCs are thought to be responsible for recurrent and metastatic disease, which leads to most cancer deaths. Our study suggests adding imetelstat to trastuzumab treatment may provide a more durable clinical response in HER2<sup>+</sup> breast cancer patients.

## REFERENCES

- Agarwal, M., Pandita, S., Hunt, C.R., Gupta, A., Yue, X., Khan, S., Pandita, R.K., Pratt, D., Shay, J.W., Taylor, J.S., *et al.* (2008). Inhibition of telomerase activity enhances hyperthermia-mediated radiosensitization. *Cancer Res* 68, 3370-3378.
- Akiyama, T., Sudo, C., Ogawara, H., Toyoshima, K., and Yamamoto, T. (1986). The product of the human c-erbB-2 gene: a 185-kilodalton glycoprotein with tyrosine kinase activity. *Science* 232, 1644-1646.
- Al-Hajj, M., Wicha, M.S., Benito-Hernandez, A., Morrison, S.J., and Clarke, M.F. (2003). Prospective identification of tumorigenic breast cancer cells. *Proc Natl Acad Sci U S A* 100, 3983-3988.
- Allsopp, R.C., and Harley, C.B. (1995). Evidence for a critical telomere length in senescent human fibroblasts. *Exp Cell Res* 219, 130-136.
- Allsopp, R.C., Morin, G.B., DePinho, R., Harley, C.B., and Weissman, I.L. (2003). Telomerase is required to slow telomere shortening and extend replicative lifespan of HSCs during serial transplantation. *Blood* 102, 517-520.
- Armstrong, A.J., Marengo, M.S., Oltean, S., Kemeny, G., Bitting, R.L., Turnbull, J.D., Herold, C.I., Marcom, P.K., George, D.J., and Garcia-Blanco, M.A. (2011). Circulating tumor cells from patients with advanced prostate and breast cancer display both epithelial and mesenchymal markers. *Mol Cancer Res* 9, 997-1007.
- Artandi, S.E., Chang, S., Lee, S.L., Alson, S., Gottlieb, G.J., Chin, L., and DePinho, R.A. (2000). Telomere dysfunction promotes non-reciprocal translocations and epithelial cancers in mice. *Nature* 406, 641-645.
- Asai, A., Oshima, Y., Yamamoto, Y., Uochi, T.A., Kusaka, H., Akinaga, S., Yamashita, Y., Pongracz, K., Pruzan, R., Wunder, E., *et al.* (2003). A novel telomerase template antagonist (GRN163) as a potential anticancer agent. *Cancer Res* 63, 3931-3939.
- Awada, A., Bozovic-Spasojevic, I., and Chow, L. (2012). New therapies in HER2-positive breast cancer: a major step towards a cure of the disease? *Cancer Treat Rev* 38, 494-504.
- Badve, S., and Nakshatri, H. (2012). Breast-cancer stem cells-beyond semantics. *Lancet Oncol* 13, e43-48.
- Balic, M., Lin, H., Young, L., Hawes, D., Giuliano, A., McNamara, G., Datar, R.H., and Cote, R.J. (2006). Most early disseminated cancer cells detected in bone marrow of breast cancer patients have a putative breast cancer stem cell phenotype. *Clin Cancer Res* 12, 5615-5621.
- Bao, S., Wu, Q., McLendon, R.E., Hao, Y., Shi, Q., Hjelmeland, A.B., Dewhirst, M.W., Bigner, D.D., and Rich, J.N. (2006). Glioma stem cells promote radioresistance by preferential activation of the DNA damage response. *Nature* 444, 756-760.

- Bapat, S.A., Mali, A.M., Koppikar, C.B., and Kurrey, N.K. (2005). Stem and progenitor-like cells contribute to the aggressive behavior of human epithelial ovarian cancer. *Cancer Res* 65, 3025-3029.
- Baselga, J., Cortes, J., Kim, S.B., Im, S.A., Hegg, R., Im, Y.H., Roman, L., Pedrini, J.L., Pienkowski, T., Knott, A., *et al.* (2012). Pertuzumab plus trastuzumab plus docetaxel for metastatic breast cancer. *N Engl J Med* 366, 109-119.
- Baum, C.M., Weissman, I.L., Tsukamoto, A.S., Buckle, A.M., and Peault, B. (1992). Isolation of a candidate human hematopoietic stem-cell population. *Proc Natl Acad Sci U S A* 89, 2804-2808.
- Bednarz-Knoll, N., Alix-Panabieres, C., and Pantel, K. (2012). Plasticity of disseminating cancer cells in patients with epithelial malignancies. *Cancer Metastasis Rev* 31, 673-687.
- Begus-Nahrman, Y., Hartmann, D., Kraus, J., Eshraghi, P., Scheffold, A., Grieb, M., Rasche, V., Schirmacher, P., Lee, H.W., Kestler, H.A., *et al.* (2012). Transient telomere dysfunction induces chromosomal instability and promotes carcinogenesis. *J Clin Invest* 122, 2283-2288.
- Bhatia, M., Wang, J.C., Kapp, U., Bonnet, D., and Dick, J.E. (1997). Purification of primitive human hematopoietic cells capable of repopulating immune-deficient mice. *Proc Natl Acad Sci U S A* 94, 5320-5325.
- Bianchini, G., and Gianni, L. (2014). The immune system and response to HER2-targeted treatment in breast cancer. *Lancet Oncol* 15, e58-68.
- Biddle, A., Liang, X., Gammon, L., Fazil, B., Harper, L.J., Emich, H., Costea, D.E., and Mackenzie, I.C. (2011). Cancer stem cells in squamous cell carcinoma switch between two distinct phenotypes that are preferentially migratory or proliferative. *Cancer Res* 71, 5317-5326.
- Blackburn, E.H. (1991). Structure and function of telomeres. *Nature* 350, 569-573.
- Blackburn, E.H. (2005). Telomeres and telomerase: their mechanisms of action and the effects of altering their functions. *FEBS Lett* 579, 859-862.
- Bodnar, A.G., Ouellette, M., Frolkis, M., Holt, S.E., Chiu, C.P., Morin, G.B., Harley, C.B., Shay, J.W., Lichtsteiner, S., and Wright, W.E. (1998). Extension of life-span by introduction of telomerase into normal human cells. *Science* 279, 349-352.
- Boku, N. (2014). HER2-positive gastric cancer. *Gastric cancer* 17, 1-12.
- Bonnet, D., and Dick, J.E. (1997). Human acute myeloid leukemia is organized as a hierarchy that originates from a primitive hematopoietic cell. *Nat Med* 3, 730-737.
- Bonnomet, A., Syne, L., Brysse, A., Feyereisen, E., Thompson, E.W., Noel, A., Foidart, J.M., Birembaut, P., Polette, M., and Gilles, C. (2012). A dynamic in vivo model of epithelial-to-mesenchymal transitions in circulating tumor cells and metastases of breast cancer. *Oncogene* 31, 3741-3753.

Boultonwood, J., Fidler, C., Kusec, R., Rack, K., Elliott, P.J., Atoyebi, O., Chapman, R., Oscier, D.G., and Wainscoat, J.S. (1997). Telomere length in myelodysplastic syndromes. *Am J Hematol* 56, 266-271.

Brennan, S.K., Wang, Q., Tressler, R., Harley, C., Go, N., Bassett, E., Huff, C.A., Jones, R.J., and Matsui, W. (2010). Telomerase inhibition targets clonogenic multiple myeloma cells through telomere length-dependent and independent mechanisms. *PLoS One* 5.

Bria, E., Cuppone, F., Fornier, M., Nistico, C., Carlini, P., Milella, M., Sperduti, I., Terzoli, E., Cognetti, F., and Giannarelli, D. (2008). Cardiotoxicity and incidence of brain metastases after adjuvant trastuzumab for early breast cancer: the dark side of the moon? A meta-analysis of the randomized trials. *Breast Cancer Res Treat* 109, 231-239.

Burchett, K.M., Yan, Y., and Ouellette, M.M. (2014). Telomerase inhibitor Imetelstat (GRN163L) limits the lifespan of human pancreatic cancer cells. *PLoS One* 9, e85155.

Buzdar, A.U., Ibrahim, N.K., Francis, D., Booser, D.J., Thomas, E.S., Theriault, R.L., Puzstai, L., Green, M.C., Arun, B.K., Giordano, S.H., *et al.* (2005). Significantly higher pathologic complete remission rate after neoadjuvant therapy with trastuzumab, paclitaxel, and epirubicin chemotherapy: results of a randomized trial in human epidermal growth factor receptor 2-positive operable breast cancer. *J Clin Oncol* 23, 3676-3685.

Castelo-Branco, P., Zhang, C., Lipman, T., Fujitani, M., Hansford, L., Clarke, I., Harley, C.B., Tressler, R., Malkin, D., Walker, E., *et al.* (2011). Neural tumor-initiating cells have distinct telomere maintenance and can be safely targeted for telomerase inhibition. *Clin Cancer Res* 17, 111-121.

Chao, Y.L., Shepard, C.R., and Wells, A. (2010). Breast carcinoma cells re-express E-cadherin during mesenchymal to epithelial reverting transition. *Mol Cancer* 9, 179.

Charafe-Jauffret, E., Ginestier, C., Iovino, F., Wicinski, J., Cervera, N., Finetti, P., Hur, M.H., Diebel, M.E., Monville, F., Dutcher, J., *et al.* (2009). Breast cancer cell lines contain functional cancer stem cells with metastatic capacity and a distinct molecular signature. *Cancer Res* 69, 1302-1313.

Chen, D., Bhat-Nakshatri, P., Goswami, C., Badve, S., and Nakshatri, H. (2013). ANTXR1, a stem cell-enriched functional biomarker, connects collagen signaling to cancer stem-like cells and metastasis in breast cancer. *Cancer Res* 73, 5821-5833.

Chin, L., Artandi, S.E., Shen, Q., Tam, A., Lee, S.L., Gottlieb, G.J., Greider, C.W., and DePinho, R.A. (1999). p53 deficiency rescues the adverse effects of telomere loss and cooperates with telomere dysfunction to accelerate carcinogenesis. *Cell* 97, 527-538.

Chiu, C.P., Dragowska, W., Kim, N.W., Vaziri, H., Yui, J., Thomas, T.E., Harley, C.B., and Lansdorf, P.M. (1996). Differential expression of telomerase activity in hematopoietic progenitors from adult human bone marrow. *Stem Cells* 14, 239-248.

Cho, R.W., and Clarke, M.F. (2008). Recent advances in cancer stem cells. *Curr Opin Genet Dev* 18, 48-53.

Choi, J., Southworth, L.K., Sarin, K.Y., Venteicher, A.S., Ma, W., Chang, W., Cheung, P., Jun, S., Artandi, M.K., Shah, N., *et al.* (2008). TERT promotes epithelial proliferation through transcriptional control of a Myc- and Wnt-related developmental program. *PLoS Genet* 4, e10.

Chou, T.C., and Talalay, P. (1984). Quantitative analysis of dose-effect relationships: the combined effects of multiple drugs or enzyme inhibitors. *Adv Enzyme Regul* 22, 27-55.

Christiansen, J.J., and Rajasekaran, A.K. (2006). Reassessing epithelial to mesenchymal transition as a prerequisite for carcinoma invasion and metastasis. *Cancer Res* 66, 8319-8326.

Chute, J.P., Muramoto, G.G., Whitesides, J., Colvin, M., Safi, R., Chao, N.J., and McDonnell, D.P. (2006). Inhibition of aldehyde dehydrogenase and retinoid signaling induces the expansion of human hematopoietic stem cells. *Proc Natl Acad Sci U S A* 103, 11707-11712.

Clark, G.M., Osborne, C.K., Levitt, D., Wu, F., and Kim, N.W. (1997). Telomerase activity and survival of patients with node-positive breast cancer. *J Natl Cancer Inst* 89, 1874-1881.

Collins, A.T., Berry, P.A., Hyde, C., Stower, M.J., and Maitland, N.J. (2005). Prospective identification of tumorigenic prostate cancer stem cells. *Cancer Res* 65, 10946-10951.

Cong, Y.S., Wright, W.E., and Shay, J.W. (2002). Human telomerase and its regulation. *Microbiol Mol Biol Rev* 66, 407-425.

d'Adda di Fagagna, F., Reaper, P.M., Clay-Farrace, L., Fiegler, H., Carr, P., Von Zglinicki, T., Saretzki, G., Carter, N.P., and Jackson, S.P. (2003). A DNA damage checkpoint response in telomere-initiated senescence. *Nature* 426, 194-198.

Dalerba, P., Cho, R.W., and Clarke, M.F. (2007). Cancer stem cells: models and concepts. *Annu Rev Med* 58, 267-284.

de Lange, T. (2005). Shelterin: the protein complex that shapes and safeguards human telomeres. *Genes Dev* 19, 2100-2110.

Denchi, E.L. (2009). Give me a break: how telomeres suppress the DNA damage response. *DNA Repair* 8, 1118-1126.

Diaz-Montes, T.P., Ji, H., Smith Sehdev, A.E., Zahurak, M.L., Kurman, R.J., Armstrong, D.K., and Bristow, R.E. (2006). Clinical significance of Her-2/neu overexpression in uterine serous carcinoma. *Gynecol Oncol* 100, 139-144.

Dikmen, Z.G., Gellert, G.C., Jackson, S., Gryaznov, S., Tressler, R., Dogan, P., Wright, W.E., and Shay, J.W. (2005). In vivo inhibition of lung cancer by GRN163L: a novel human telomerase inhibitor. *Cancer Res* 65, 7866-7873.

Dikmen, Z.G., Wright, W.E., Shay, J.W., and Gryaznov, S.M. (2008). Telomerase targeted oligonucleotide thio-phosphoramidates in T24-luc bladder cancer cells. *J Cell Biochem* 104, 444-452.

- Ding, D., Xi, P., Zhou, J., Wang, M., and Cong, Y.S. (2013). Human telomerase reverse transcriptase regulates MMP expression independently of telomerase activity via NF-kappaB-dependent transcription. *FASEB J* 27, 4375-4383.
- Djojotubroto, M.W., Chin, A.C., Go, N., Schaezlein, S., Manns, M.P., Gryaznov, S., Harley, C.B., and Rudolph, K.L. (2005). Telomerase antagonists GRN163 and GRN163L inhibit tumor growth and increase chemosensitivity of human hepatoma. *Hepatology* 42, 1127-1136.
- Dontu, G., Al-Hajj, M., Abdallah, W.M., Clarke, M.F., and Wicha, M.S. (2003). Stem cells in normal breast development and breast cancer. *Cell proliferation* 36 *Suppl 1*, 59-72.
- Ewer, M.S., Vooletich, M.T., Durand, J.B., Woods, M.L., Davis, J.R., Valero, V., and Lenihan, D.J. (2005). Reversibility of trastuzumab-related cardiotoxicity: new insights based on clinical course and response to medical treatment. *J Clin Oncol* 23, 7820-7826.
- Fang, D., Nguyen, T.K., Leishear, K., Finko, R., Kulp, A.N., Hotz, S., Van Belle, P.A., Xu, X., Elder, D.E., and Herlyn, M. (2005). A tumorigenic subpopulation with stem cell properties in melanomas. *Cancer Res* 65, 9328-9337.
- Feng, J., Funk, W.D., Wang, S.S., Weinrich, S.L., Avilion, A.A., Chiu, C.P., Adams, R.R., Chang, E., Allsopp, R.C., Yu, J., *et al.* (1995). The RNA component of human telomerase. *Science* 269, 1236-1241.
- Fillmore, C.M., and Kuperwasser, C. (2008). Human breast cancer cell lines contain stem-like cells that self-renew, give rise to phenotypically diverse progeny and survive chemotherapy. *Breast Cancer Res* 10, R25.
- Garrett, J.T., Sutton, C.R., Kuba, M.G., Cook, R.S., and Arteaga, C.L. (2013). Dual blockade of HER2 in HER2-overexpressing tumor cells does not completely eliminate HER3 function. *Clin Cancer Res* 19, 610-619.
- Ge, Z., Liu, C., Bjorkholm, M., Gruber, A., and Xu, D. (2006). Mitogen-activated protein kinase cascade-mediated histone H3 phosphorylation is critical for telomerase reverse transcriptase expression/telomerase activation induced by proliferation. *Mol Cell Biol* 26, 230-237.
- Ghosh, A., Saginc, G., Leow, S.C., Khattar, E., Shin, E.M., Yan, T.D., Wong, M., Zhang, Z., Li, G., Sung, W.K., *et al.* (2012). Telomerase directly regulates NF-kappaB-dependent transcription. *Nat Cell Biol* 14, 1270-1281.
- Gibbs, C.P., Kukekov, V.G., Reith, J.D., Tchigrinova, O., Suslov, O.N., Scott, E.W., Ghivizzani, S.C., Ignatova, T.N., and Steindler, D.A. (2005). Stem-like cells in bone sarcomas: implications for tumorigenesis. *Neoplasia* 7, 967-976.
- Ginestier, C., Hur, M.H., Charafe-Jauffret, E., Monville, F., Dutcher, J., Brown, M., Jacquemier, J., Viens, P., Kleer, C.G., Liu, S., *et al.* (2007). ALDH1 is a marker of normal and malignant human mammary stem cells and a predictor of poor clinical outcome. *Cell Stem Cell* 1, 555-567.

- Goldblatt, E.M., Erickson, P.A., Gentry, E.R., Gryaznov, S.M., and Herbert, B.S. (2009a). Lipid-conjugated telomerase template antagonists sensitize resistant HER2-positive breast cancer cells to trastuzumab. *Breast Cancer Res Treat* 118, 21-32.
- Goldblatt, E.M., Gentry, E.R., Fox, M.J., Gryaznov, S.M., Shen, C., and Herbert, B.S. (2009b). The telomerase template antagonist GRN163L alters MDA-MB-231 breast cancer cell morphology, inhibits growth, and augments the effects of paclitaxel. *Mol Cancer Ther* 8, 2027-2035.
- Gomez-Millan, J., Goldblatt, E.M., Gryaznov, S.M., Mendonca, M.S., and Herbert, B.S. (2007). Specific telomere dysfunction induced by GRN163L increases radiation sensitivity in breast cancer cells. *Int J Radiat Oncol Biol Phys* 67, 897-905.
- Goueli, B.S., and Janknecht, R. (2004). Upregulation of the Catalytic Telomerase Subunit by the Transcription Factor ER81 and Oncogenic HER2/Neu, Ras, or Raf. *Mol Cell Biol* 24, 25-35.
- Greider, C.W., and Blackburn, E.H. (1987). The telomere terminal transferase of Tetrahymena is a ribonucleoprotein enzyme with two kinds of primer specificity. *Cell* 51, 887-898.
- Griffith, J.D., Comeau, L., Rosenfield, S., Stansel, R.M., Bianchi, A., Moss, H., and de Lange, T. (1999). Mammalian telomeres end in a large duplex loop. *Cell* 97, 503-514.
- Gryaznov, S.M. (2010). Oligonucleotide 3'→5' phosphoramidates and thio-phosphoramidates as potential therapeutic agents. *Chemistry & biodiversity* 7, 477-493.
- Guglin, M., Cutro, R., and Mishkin, J.D. (2008). Trastuzumab-induced cardiomyopathy. *J Card Fail* 14, 437-444.
- Gunes, C., and Rudolph, K.L. (2013). The role of telomeres in stem cells and cancer. *Cell* 152, 390-393.
- Gupta, P.B., Onder, T.T., Jiang, G., Tao, K., Kuperwasser, C., Weinberg, R.A., and Lander, E.S. (2009). Identification of selective inhibitors of cancer stem cells by high-throughput screening. *Cell* 138, 645-659.
- Hahn, W.C., Counter, C.M., Lundberg, A.S., Beijersbergen, R.L., Brooks, M.W., and Weinberg, R.A. (1999). Creation of human tumour cells with defined genetic elements. *Nature* 400, 464-468.
- Hallett, R.M., Kondratyev, M.K., Giacomelli, A.O., Nixon, A.M., Girgis-Gabardo, A., Ilieva, D., and Hassell, J.A. (2012). Small molecule antagonists of the Wnt/beta-catenin signaling pathway target breast tumor-initiating cells in a Her2/Neu mouse model of breast cancer. *PLoS One* 7, e33976.
- Hanahan, D., and Weinberg, R.A. (2000). The hallmarks of cancer. *Cell* 100, 57-70.
- Hanahan, D., and Weinberg, R.A. (2011). Hallmarks of cancer: the next generation. *Cell* 144, 646-674.

- Haraguchi, N., Utsunomiya, T., Inoue, H., Tanaka, F., Mimori, K., Barnard, G.F., and Mori, M. (2006). Characterization of a side population of cancer cells from human gastrointestinal system. *Stem Cells* 24, 506-513.
- Harley, C.B. (2008). Telomerase and cancer therapeutics. *Nat Rev Cancer* 8, 167-179.
- Harley, C.B., Futcher, A.B., and Greider, C.W. (1990). Telomeres shorten during ageing of human fibroblasts. *Nature* 345, 458-460.
- Harley, C.B., Vaziri, H., Counter, C.M., and Allsopp, R.C. (1992). The telomere hypothesis of cellular aging. *Exp Gerontol* 27, 375-382.
- Hayflick, L., and Moorhead, P.S. (1961). The serial cultivation of human diploid cell strains. *Exp Cell Res* 25, 585-621.
- Helbig, G., Christopherson, K.W., 2nd, Bhat-Nakshatri, P., Kumar, S., Kishimoto, H., Miller, K.D., Broxmeyer, H.E., and Nakshatri, H. (2003). NF-kappaB promotes breast cancer cell migration and metastasis by inducing the expression of the chemokine receptor CXCR4. *J Biol Chem* 278, 21631-21638.
- Henson, J.D., Hannay, J.A., McCarthy, S.W., Royds, J.A., Yeager, T.R., Robinson, R.A., Wharton, S.B., Jellinek, D.A., Arbuckle, S.M., Yoo, J., *et al.* (2005). A robust assay for alternative lengthening of telomeres in tumors shows the significance of alternative lengthening of telomeres in sarcomas and astrocytomas. *Clin Cancer Res* 11, 217-225.
- Herbert, B.S., Gellert, G.C., Hochreiter, A., Pongracz, K., Wright, W.E., Zielinska, D., Chin, A.C., Harley, C.B., Shay, J.W., and Gryaznov, S.M. (2005). Lipid modification of GRN163, an N3'-->P5' thio-phosphoramidate oligonucleotide, enhances the potency of telomerase inhibition. *Oncogene* 24, 5262-5268.
- Herbert, B.S., Hochreiter, A.E., Wright, W.E., and Shay, J.W. (2006). Nonradioactive detection of telomerase activity using the telomeric repeat amplification protocol. *Nat Protoc* 1, 1583-1590.
- Herbert, B.S., Shay, J.W., and Wright, W.E. (2003). Analysis of telomeres and telomerase. *Curr Protoc Cell Biol Chapter 18*, Unit 18 16
- Hochreiter, A.E., Xiao, H., Goldblatt, E.M., Gryaznov, S.M., Miller, K.D., Badve, S., Sledge, G.W., and Herbert, B.S. (2006). Telomerase template antagonist GRN163L disrupts telomere maintenance, tumor growth, and metastasis of breast cancer. *Clin Cancer Res* 12, 3184-3192.
- Hoos, A., Hepp, H.H., Kaul, S., Ahlert, T., Bastert, G., and Wallwiener, D. (1998). Telomerase activity correlates with tumor aggressiveness and reflects therapy effect in breast cancer. *Int J Cancer* 79, 8-12.
- Hope, K.J., Jin, L., and Dick, J.E. (2004). Acute myeloid leukemia originates from a hierarchy of leukemic stem cell classes that differ in self-renewal capacity. *Nature Immunol* 5, 738-743.

- Hu, Y., Bandla, S., Godfrey, T.E., Tan, D., Luketich, J.D., Pennathur, A., Qiu, X., Hicks, D.G., Peters, J.H., and Zhou, Z. (2011). HER2 amplification, overexpression and score criteria in esophageal adenocarcinoma. *Mod Pathol* 24, 899-907.
- Joseph, I., Tressler, R., Bassett, E., Harley, C., Buseman, C.M., Pattamatta, P., Wright, W.E., Shay, J.W., and Go, N.F. (2010). The telomerase inhibitor imetelstat depletes cancer stem cells in breast and pancreatic cancer cell lines. *Cancer Res* 70, 9494-9504.
- Ju, Z., and Rudolph, K.L. (2006). Telomeres and telomerase in cancer stem cells. *Eur J Cancer* 42, 1197-1203.
- Kabir, S., Sfeir, A., and de Lange, T. (2010). Taking apart Rap1: an adaptor protein with telomeric and non-telomeric functions. *Cell Cycle* 9, 4061-4067.
- Kelland, L. (2007). Targeting the limitless replicative potential of cancer: the telomerase/telomere pathway. *Clin Cancer Res* 13, 4960-4963.
- Kim, N.W., Piatyszek, M.A., Prowse, K.R., Harley, C.B., West, M.D., Ho, P.L., Coviello, G.M., Wright, W.E., Weinrich, S.L., and Shay, J.W. (1994). Specific association of human telomerase activity with immortal cells and cancer. *Science* 266, 2011-2015.
- Korkaya, H., Paulson, A., Iovino, F., and Wicha, M.S. (2008). HER2 regulates the mammary stem/progenitor cell population driving tumorigenesis and invasion. *Oncogene* 27, 6120-6130.
- Korkaya, H., and Wicha, M.S. (2013). HER2 and breast cancer stem cells: more than meets the eye. *Cancer Res* 73, 3489-3493.
- Lapidot, T., Sirard, C., Vormoor, J., Murdoch, B., Hoang, T., Caceres-Cortes, J., Minden, M., Paterson, B., Caligiuri, M.A., and Dick, J.E. (1994). A cell initiating human acute myeloid leukaemia after transplantation into SCID mice. *Nature* 367, 645-648.
- Levy, M.Z., Allsopp, R.C., Futcher, A.B., Greider, C.W., and Harley, C.B. (1992). Telomere end-replication problem and cell aging. *J Mol Biol* 225, 951-960.
- Li, C., Heidt, D.G., Dalerba, P., Burant, C.F., Zhang, L., Adsay, V., Wicha, M., Clarke, M.F., and Simeone, D.M. (2007). Identification of pancreatic cancer stem cells. *Cancer Res* 67, 1030-1037.
- Li, S.G., and Li, L. (2013). Targeted therapy in HER2-positive breast cancer. *Biomed Rep* 1, 499-505.
- Li, X., Lewis, M.T., Huang, J., Gutierrez, C., Osborne, C.K., Wu, M.F., Hilsenbeck, S.G., Pavlick, A., Zhang, X., Chamness, G.C., *et al.* (2008). Intrinsic resistance of tumorigenic breast cancer cells to chemotherapy. *J Natl Cancer Inst* 100, 672-679.
- Li, Y., and Tergaonkar, V. (2014). Noncanonical functions of telomerase: implications in telomerase-targeted cancer therapies. *Cancer Res* 74, 1639-1644.
- Lin, N.U., and Winer, E.P. (2007). Brain metastases: the HER2 paradigm. *Clin Cancer Res* 13, 1648-1655.

- Listerman, I., Gazzaniga, F.S., and Blackburn, E.H. (2014). An investigation of the effects of the core protein telomerase reverse transcriptase on Wnt signaling in breast cancer cells. *Mol Cell Biol* 34, 280-289.
- Liu, B.Y., McDermott, S.P., Khwaja, S.S., and Alexander, C.M. (2004). The transforming activity of Wnt effectors correlates with their ability to induce the accumulation of mammary progenitor cells. *Proc Natl Acad Sci U S A* 101, 4158-4163.
- Liu, D. (2011). Analysis of average telomere length in cultured human cells. *Methods Mol Biol* 735, 13-19.
- Liu, M., Sakamaki, T., Casimiro, M.C., Willmarth, N.E., Quong, A.A., Ju, X., Ojeifo, J., Jiao, X., Yeow, W.S., Katiyar, S., *et al.* (2010). The canonical NF-kappaB pathway governs mammary tumorigenesis in transgenic mice and tumor stem cell expansion. *Cancer Res* 70, 10464-10473.
- Liu, R., Wang, X., Chen, G.Y., Dalerba, P., Gurney, A., Hoey, T., Sherlock, G., Lewicki, J., Shedden, K., and Clarke, M.F. (2007). The prognostic role of a gene signature from tumorigenic breast-cancer cells. *N Engl J Med* 356, 217-226.
- Liu, S., Cong, Y., Wang, D., Sun, Y., Deng, L., Liu, Y., Martin-Trevino, R., Shang, L., McDermott, S.P., Landis, M.D., *et al.* (2014). Breast Cancer Stem Cells Transition between Epithelial and Mesenchymal States Reflective of their Normal Counterparts. *Stem cell reports* 2, 78-91.
- Looi, L.M., Ng, M.H., and Cheah, P.L. (2007). Telomerase activation in neoplastic cell immortalization and tumour progression. *Malays J Pathol* 29, 33-35.
- Lu, Y., Zi, X., Zhao, Y., Mascarenhas, D., and Pollak, M. (2001). Insulin-like growth factor-I receptor signaling and resistance to trastuzumab (Herceptin). *J Natl Cancer Inst* 93, 1852-1857.
- Magnifico, A., Albano, L., Campaner, S., Delia, D., Castiglioni, F., Gasparini, P., Sozzi, G., Fontanella, E., Menard, S., and Tagliabue, E. (2009). Tumor-initiating cells of HER2-positive carcinoma cell lines express the highest oncoprotein levels and are sensitive to trastuzumab. *Clin Cancer Res* 15, 2010-2021.
- Maida, Y., Kyo, S., Kanaya, T., Wang, Z., Yatabe, N., Tanaka, M., Nakamura, M., Ohmichi, M., Gotoh, N., Murakami, S., *et al.* (2002). Direct activation of telomerase by EGF through Ets-mediated transactivation of TERT via MAP kinase signaling pathway. *Oncogene* 21, 4071-4079.
- Makarov, V.L., Hirose, Y., and Langmore, J.P. (1997). Long G tails at both ends of human chromosomes suggest a C strand degradation mechanism for telomere shortening. *Cell* 88, 657-666.
- Mani, S.A., Guo, W., Liao, M.J., Eaton, E.N., Ayyanan, A., Zhou, A.Y., Brooks, M., Reinhard, F., Zhang, C.C., Shipitsin, M., *et al.* (2008). The epithelial-mesenchymal transition generates cells with properties of stem cells. *Cell* 133, 704-715.

- Marian, C.O., Cho, S.K., McEllin, B.M., Maher, E.A., Hatanpaa, K.J., Madden, C.J., Mickey, B.E., Wright, W.E., Shay, J.W., and Bachoo, R.M. (2010a). The telomerase antagonist, imetelstat, efficiently targets glioblastoma tumor-initiating cells leading to decreased proliferation and tumor growth. *Clin Cancer Res* 16, 154-163.
- Marian, C.O., Wright, W.E., and Shay, J.W. (2010b). The effects of telomerase inhibition on prostate tumor-initiating cells. *Int J Cancer* 127, 321-331.
- Maser, R.S., and DePinho, R.A. (2002). Connecting chromosomes, crisis, and cancer. *Science* 297, 565-569.
- Matsui, W., Huff, C.A., Wang, Q., Malehorn, M.T., Barber, J., Tanhehco, Y., Smith, B.D., Civin, C.I., and Jones, R.J. (2004). Characterization of clonogenic multiple myeloma cells. *Blood* 103, 2332-2336.
- Meeker, A.K., and Argani, P. (2004). Telomere shortening occurs early during breast tumorigenesis: a cause of chromosome destabilization underlying malignant transformation? *J Mammary Gland Biol Neoplasia* 9, 285-296.
- Meeker, A.K., Hicks, J.L., Gabrielson, E., Strauss, W.M., De Marzo, A.M., and Argani, P. (2004). Telomere shortening occurs in subsets of normal breast epithelium as well as in situ and invasive carcinoma. *Am J Pathol* 164, 925-935.
- Mehta, A.I., Brufsky, A.M., and Sampson, J.H. (2013). Therapeutic approaches for HER2-positive brain metastases: circumventing the blood-brain barrier. *Cancer Treat Rev* 39, 261-269.
- Mender, I., Senturk, S., Ozgunes, N., Akcali, K.C., Kletsas, D., Gryaznov, S., Can, A., Shay, J.W., and Dikmen, Z.G. (2013). Imetelstat (a telomerase antagonist) exerts offtarget effects on the cytoskeleton. *Int J Oncol* 42, 1709-1715.
- Miller, K.D. (2004). The role of ErbB inhibitors in trastuzumab resistance. *Oncologist* 9 Suppl 3, 16-19.
- Moasser, M.M. (2007). Targeting the function of the HER2 oncogene in human cancer therapeutics. *Oncogene* 26, 6577-6592.
- Mohd Sharial, M.S., Crown, J., and Hennessy, B.T. (2012). Overcoming resistance and restoring sensitivity to HER2-targeted therapies in breast cancer. *Ann Oncol* 23, 3007-3016.
- Morel, A.P., Lievre, M., Thomas, C., Hinkal, G., Ansieau, S., and Puisieux, A. (2008). Generation of breast cancer stem cells through epithelial-mesenchymal transition. *PLoS One* 3, e2888.
- Morin, G.B. (1989). The human telomere terminal transferase enzyme is a ribonucleoprotein that synthesizes TTAGGG repeats. *Cell* 59, 521-529.

- Morrison, C., Zanagnolo, V., Ramirez, N., Cohn, D.E., Kelbick, N., Copeland, L., Maxwell, G.L., and Fowler, J.M. (2006). HER-2 is an independent prognostic factor in endometrial cancer: association with outcome in a large cohort of surgically staged patients. *J Clin Oncol* 24, 2376-2385.
- Moyzis, R.K., Buckingham, J.M., Cram, L.S., Dani, M., Deaven, L.L., Jones, M.D., Meyne, J., Ratliff, R.L., and Wu, J.R. (1988). A highly conserved repetitive DNA sequence, (TTAGGG)<sub>n</sub>, present at the telomeres of human chromosomes. *Proc Natl Acad Sci U S A* 85, 6622-6626.
- Muezzinler, A., Zaineddin, A.K., and Brenner, H. (2013). A systematic review of leukocyte telomere length and age in adults. *Ageing research reviews* 12, 509-519.
- Mukohara, T. (2011). Mechanisms of resistance to anti-human epidermal growth factor receptor 2 agents in breast cancer. *Cancer Sci* 102, 1-8.
- Nabetani, A., and Ishikawa, F. (2011). Alternative lengthening of telomeres pathway: recombination-mediated telomere maintenance mechanism in human cells. *J Biochem* 149, 5-14.
- Nahta, R., and Esteva, F.J. (2004). In vitro effects of trastuzumab and vinorelbine in trastuzumab-resistant breast cancer cells. *Cancer Chemother Pharmacol* 53, 186-190.
- Nahta, R., and Esteva, F.J. (2006). HER2 therapy: molecular mechanisms of trastuzumab resistance. *Breast Cancer Res* 8, 215.
- Nahta, R., and O'Regan, R.M. (2012). Therapeutic implications of estrogen receptor signaling in HER2-positive breast cancers. *Breast Cancer Res Treat* 135, 39-48.
- Nahta, R., Yu, D., Hung, M.C., Hortobagyi, G.N., and Esteva, F.J. (2006). Mechanisms of disease: understanding resistance to HER2-targeted therapy in human breast cancer. *Nat Clin Pract Oncol* 3, 269-280.
- Nahta, R., Yuan, L.X., Zhang, B., Kobayashi, R., and Esteva, F.J. (2005). Insulin-like growth factor-I receptor/human epidermal growth factor receptor 2 heterodimerization contributes to trastuzumab resistance of breast cancer cells. *Cancer Res* 65, 11118-11128.
- Nanni, P., Nicoletti, G., Palladini, A., Croci, S., Murgo, A., Ianzano, M.L., Grosso, V., Stivani, V., Antognoli, A., Lamolinara, A., *et al.* (2012). Multiorgan metastasis of human HER-2+ breast cancer in Rag2<sup>-/-</sup>;Il2rg<sup>-/-</sup> mice and treatment with PI3K inhibitor. *PloS One* 7, e39626.
- Neve, R.M., Chin, K., Fridlyand, J., Yeh, J., Baehner, F.L., Fevr, T., Clark, L., Bayani, N., Coppe, J.P., Tong, F., *et al.* (2006). A collection of breast cancer cell lines for the study of functionally distinct cancer subtypes. *Cancer Cell* 10, 515-527.
- O'Brien, N.A., Browne, B.C., Chow, L., Wang, Y., Ginther, C., Arboleda, J., Duffy, M.J., Crown, J., O'Donovan, N., and Slamon, D.J. (2010). Activated phosphoinositide 3-kinase/AKT signaling confers resistance to trastuzumab but not lapatinib. *Mol Cancer Ther* 9, 1489-1502.

Okamoto, N., Yasukawa, M., Nguyen, C., Kasim, V., Maida, Y., Possemato, R., Shibata, T., Ligon, K.L., Fukami, K., Hahn, W.C., *et al.* (2011). Maintenance of tumor initiating cells of defined genetic composition by nucleostemin. *Proc Natl Acad Sci U S A* *108*, 20388-20393.

Oliver, M.H., Harrison, N.K., Bishop, J.E., Cole, P.J., and Laurent, G.J. (1989). A rapid and convenient assay for counting cells cultured in microwell plates: application for assessment of growth factors. *J Cell Sci* *92 ( Pt 3)*, 513-518.

Ouellette, M.M., Wright, W.E., and Shay, J.W. (2011). Targeting telomerase-expressing cancer cells. *J Cell Mol Med* *15*, 1433-1442.

Ozcelik, C., Erdmann, B., Pilz, B., Wettschureck, N., Britsch, S., Hubner, N., Chien, K.R., Birchmeier, C., and Garratt, A.N. (2002). Conditional mutation of the ErbB2 (HER2) receptor in cardiomyocytes leads to dilated cardiomyopathy. *Proc Natl Acad Sci U S A* *99*, 8880-8885.

Palm, W., and de Lange, T. (2008). How shelterin protects mammalian telomeres. *Annu Rev Genet* *42*, 301-334.

Papanikolaou, V., Athanassiou, E., Dubos, S., Dimou, I., Papathanasiou, I., Kitsiou-Tzeli, S., Kappas, C., and Tsezou, A. (2011). hTERT regulation by NF-kappaB and c-myc in irradiated HER2-positive breast cancer cells. *Int J Radiat Biol* *87*, 609-621.

Park, J.I., Venteicher, A.S., Hong, J.Y., Choi, J., Jun, S., Shkreli, M., Chang, W., Meng, Z., Cheung, P., Ji, H., *et al.* (2009). Telomerase modulates Wnt signalling by association with target gene chromatin. *Nature* *460*, 66-72.

Perou, C.M., Sorlie, T., Eisen, M.B., van de Rijn, M., Jeffrey, S.S., Rees, C.A., Pollack, J.R., Ross, D.T., Johnsen, H., Akslén, L.A., *et al.* (2000). Molecular portraits of human breast tumours. *Nature* *406*, 747-752.

Pestalozzi, B.C., Zahrieh, D., Price, K.N., Holmberg, S.B., Lindtner, J., Collins, J., Crivellari, D., Fey, M.F., Murray, E., Pagani, O., *et al.* (2006). Identifying breast cancer patients at risk for Central Nervous System (CNS) metastases in trials of the International Breast Cancer Study Group (IBCSG). *Ann Oncol* *17*, 935-944.

Pinto, C.A., Widodo, E., Waltham, M., and Thompson, E.W. (2013). Breast cancer stem cells and epithelial mesenchymal plasticity - Implications for chemoresistance. *Cancer Lett* *341*, 56-62.

Ponti, D., Costa, A., Zaffaroni, N., Pratesi, G., Petrangolini, G., Coradini, D., Pilotti, S., Pierotti, M.A., and Daidone, M.G. (2005). Isolation and in vitro propagation of tumorigenic breast cancer cells with stem/progenitor cell properties. *Cancer Res* *65*, 5506-5511.

Prince, M.E., Sivanandan, R., Kaczorowski, A., Wolf, G.T., Kaplan, M.J., Dalerba, P., Weissman, I.L., Clarke, M.F., and Ailles, L.E. (2007). Identification of a subpopulation of cells with cancer stem cell properties in head and neck squamous cell carcinoma. *Proc Natl Acad Sci U S A* *104*, 973-978.

- Reese, D.M., and Slamon, D.J. (1997). HER-2/neu signal transduction in human breast and ovarian cancer. *Stem Cells* 15, 1-8.
- Ricci-Vitiani, L., Lombardi, D.G., Pilozzi, E., Biffoni, M., Todaro, M., Peschle, C., and De Maria, R. (2007). Identification and expansion of human colon-cancer-initiating cells. *Nature* 445, 111-115.
- Roger, L., Jones, R.E., Heppel, N.H., Williams, G.T., Sampson, J.R., and Baird, D.M. (2013). Extensive telomere erosion in the initiation of colorectal adenomas and its association with chromosomal instability. *J Natl Cancer Inst* 105, 1202-1211.
- Ross, J.S., Slodkowska, E.A., Symmans, W.F., Pusztai, L., Ravdin, P.M., and Hortobagyi, G.N. (2009). The HER-2 receptor and breast cancer: ten years of targeted anti-HER-2 therapy and personalized medicine. *Oncologist* 14, 320-368.
- Roth, A., Harley, C.B., and Baerlocher, G.M. (2010). Imetelstat (GRN163L)--telomerase-based cancer therapy. *Recent Results Cancer Res* 184, 221-234.
- Ruden, M., and Puri, N. (2013). Novel anticancer therapeutics targeting telomerase. *Cancer Treat Rev* 39, 444-456.
- Rudolph, K.L., Chang, S., Lee, H.W., Blasco, M., Gottlieb, G.J., Greider, C., and DePinho, R.A. (1999). Longevity, stress response, and cancer in aging telomerase-deficient mice. *Cell* 96, 701-712.
- Rudolph, K.L., Millard, M., Bosenberg, M.W., and DePinho, R.A. (2001). Telomere dysfunction and evolution of intestinal carcinoma in mice and humans. *Nat Genet* 28, 155-159.
- Scaltriti, M., Eichhorn, P.J., Cortes, J., Prudkin, L., Aura, C., Jimenez, J., Chandarlapaty, S., Serra, V., Prat, A., Ibrahim, Y.H., *et al.* (2011). Cyclin E amplification/overexpression is a mechanism of trastuzumab resistance in HER2+ breast cancer patients. *Proc Natl Acad Sci U S A* 108, 3761-3766.
- Sfeir, A., and de Lange, T. (2012). Removal of shelterin reveals the telomere end-protection problem. *Science* 336, 593-597.
- Shammas, M.A., Koley, H., Bertheau, R.C., Neri, P., Fulciniti, M., Tassone, P., Blotta, S., Protopopov, A., Mitsiades, C., Batchu, R.B., *et al.* (2008). Telomerase inhibitor GRN163L inhibits myeloma cell growth in vitro and in vivo. *Leukemia* 22, 1410-1418.
- Shay, J.W., and Wright, W.E. (2005). Senescence and immortalization: role of telomeres and telomerase. *Carcinogenesis* 26, 867-874.
- Shay, J.W., and Wright, W.E. (2006). Telomerase therapeutics for cancer: challenges and new directions. *Nat Rev Drug Discov* 5, 577-584.
- Shay, J.W., and Wright, W.E. (2010). Telomeres and telomerase in normal and cancer stem cells. *FEBS Lett* 584, 3819-3825.

Sheridan, C., Kishimoto, H., Fuchs, R.K., Mehrotra, S., Bhat-Nakshatri, P., Turner, C.H., Goulet, R., Jr., Badve, S., and Nakshatri, H. (2006). CD44+/CD24- breast cancer cells exhibit enhanced invasive properties: an early step necessary for metastasis. *Breast Cancer Res* 8, R59.

Singh, S.K., Clarke, I.D., Terasaki, M., Bonn, V.E., Hawkins, C., Squire, J., and Dirks, P.B. (2003). Identification of a cancer stem cell in human brain tumors. *Cancer Res* 63, 5821-5828.

Slamon, D.J., Clark, G.M., Wong, S.G., Levin, W.J., Ullrich, A., and McGuire, W.L. (1987). Human breast cancer: correlation of relapse and survival with amplification of the HER-2/neu oncogene. *Science* 235, 177-182.

Slamon, D.J., Godolphin, W., Jones, L.A., Holt, J.A., Wong, S.G., Keith, D.E., Levin, W.J., Stuart, S.G., Udove, J., Ullrich, A., *et al.* (1989). Studies of the HER-2/neu proto-oncogene in human breast and ovarian cancer. *Science* 244, 707-712.

Slamon, D.J., Leyland-Jones, B., Shak, S., Fuchs, H., Paton, V., Bajamonde, A., Fleming, T., Eiermann, W., Wolter, J., Pegram, M., *et al.* (2001). Use of chemotherapy plus a monoclonal antibody against HER2 for metastatic breast cancer that overexpresses HER2. *N Engl J Med* 344, 783-792.

Sorlie, T., Perou, C.M., Tibshirani, R., Aas, T., Geisler, S., Johnsen, H., Hastie, T., Eisen, M.B., van de Rijn, M., Jeffrey, S.S., *et al.* (2001). Gene expression patterns of breast carcinomas distinguish tumor subclasses with clinical implications. *Proc Natl Acad Sci U S A* 98, 10869-10874.

Spangrude, G.J., Heimfeld, S., and Weissman, I.L. (1988). Purification and characterization of mouse hematopoietic stem cells. *Science* 241, 58-62.

Spector, N.L., and Blackwell, K.L. (2009). Understanding the mechanisms behind trastuzumab therapy for human epidermal growth factor receptor 2-positive breast cancer. *J Clin Oncol* 27, 5838-5847.

Stemmler, H.J., Schmitt, M., Willems, A., Bernhard, H., Harbeck, N., and Heinemann, V. (2007). Ratio of trastuzumab levels in serum and cerebrospinal fluid is altered in HER2-positive breast cancer patients with brain metastases and impairment of blood-brain barrier. *Anticancer Drugs* 18, 23-28.

Tallarida, R.J. (2011). Quantitative methods for assessing drug synergism. *Genes Cancer* 2, 1003-1008.

Tamakawa, R.A., Fleisig, H.B., and Wong, J.M. (2010). Telomerase inhibition potentiates the effects of genotoxic agents in breast and colorectal cancer cells in a cell cycle-specific manner. *Cancer Res* 70, 8684-8694.

Tanaka, H., Abe, S., Huda, N., Tu, L., Beam, M.J., Grimes, B., and Gilley, D. (2012). Telomere fusions in early human breast carcinoma. *Proc Natl Acad Sci U S A* 109, 14098-14103.

- Thompson, P.A., Drissi, R., Muscal, J.A., Panditharatna, E., Fouladi, M., Ingle, A.M., Ahern, C.H., Reid, J.M., Lin, T., Weigel, B.J., *et al.* (2013). A phase I trial of imetelstat in children with refractory or recurrent solid tumors: a Children's Oncology Group Phase I Consortium Study (ADV1112). *Clin Cancer Res* 19, 6578-6584.
- Tirino, V., Desiderio, V., Paino, F., De Rosa, A., Papaccio, F., La Noce, M., Laino, L., De Francesco, F., and Papaccio, G. (2013). Cancer stem cells in solid tumors: an overview and new approaches for their isolation and characterization. *FASEB J* 27, 13-24.
- Tiwari, R.K., Borgen, P.I., Wong, G.Y., Cordon-Cardo, C., and Osborne, M.P. (1992). HER-2/neu amplification and overexpression in primary human breast cancer is associated with early metastasis. *Anticancer Res* 12, 419-425.
- Tsai, J.H., and Yang, J. (2013). Epithelial-mesenchymal plasticity in carcinoma metastasis. *Genes Dev* 27, 2192-2206.
- Tsuji, T., Ibaragi, S., Shima, K., Hu, M.G., Katsurano, M., Sasaki, A., and Hu, G.F. (2008). Epithelial-mesenchymal transition induced by growth suppressor p12CDK2-AP1 promotes tumor cell local invasion but suppresses distant colony growth. *Cancer Res* 68, 10377-10386.
- Vageli, D., Ioannou, M.G., and Koukoulis, G.K. (2009). Transcriptional activation of hTERT in breast carcinomas by the Her2-ER81-related pathway. *Oncol Res* 17, 413-423.
- Verma, S., Miles, D., Gianni, L., Krop, I.E., Welslau, M., Baselga, J., Pegram, M., Oh, D.Y., Dieras, V., Guardino, E., *et al.* (2012). Trastuzumab emtansine for HER2-positive advanced breast cancer. *N Engl J Med* 367, 1783-1791.
- Visvader, J.E., and Lindeman, G.J. (2008). Cancer stem cells in solid tumours: accumulating evidence and unresolved questions. *Nat Rev Cancer* 8, 755-768.
- Visvader, J.E., and Lindeman, G.J. (2012). Cancer stem cells: current status and evolving complexities. *Cell Stem Cell* 10, 717-728.
- Watanabe, M., Yu, S.K., Sawafuji, M., Kawamura, M., Horinouchi, H., Mukai, M., and Kobayashi, K. (2002). Enhanced expression of telomerase activity in thymoma and thymic carcinoma tissues: a clinicopathologic study. *Cancer* 94, 240-244.
- Wei, C., and Price, M. (2003). Protecting the terminus: t-loops and telomere end-binding proteins. *Cell Mol Life Sci* 60, 2283-2294.
- Wicha, M.S., Liu, S., and Dontu, G. (2006). Cancer stem cells: an old idea--a paradigm shift. *Cancer Res* 66, 1883-1890; discussion 1895-1886.
- Wright, W.E., Piatyszek, M.A., Rainey, W.E., Byrd, W., and Shay, J.W. (1996). Telomerase activity in human germline and embryonic tissues and cells. *Dev Genet* 18, 173-179.
- Wright, W.E., and Shay, J.W. (1992). The two-stage mechanism controlling cellular senescence and immortalization. *Exp Gerontol* 27, 383-389.

Wright, W.E., Shay, J.W., and Piatyszek, M.A. (1995). Modifications of a telomeric repeat amplification protocol (TRAP) result in increased reliability, linearity and sensitivity. *Nucleic Acids Res* 23, 3794-3795.

Wu, Y., Amonkar, M.M., Sherrill, B.H., O'Shaughnessy, J., Ellis, C., Baselga, J., Blackwell, K.L., and Burstein, H.J. (2011). Impact of lapatinib plus trastuzumab versus single-agent lapatinib on quality of life of patients with trastuzumab-refractory HER2+ metastatic breast cancer. *Ann Oncol* 22, 2582-2590.

Xia, W., Bacus, S., Hegde, P., Husain, I., Strum, J., Liu, L., Paulazzo, G., Lyass, L., Trusk, P., Hill, J., *et al.* (2006). A model of acquired autoresistance to a potent ErbB2 tyrosine kinase inhibitor and a therapeutic strategy to prevent its onset in breast cancer. *Proc Natl Acad Sci U S A* 103, 7795-7800.

Yamamoto, M., Taguchi, Y., Ito-Kureha, T., Semba, K., Yamaguchi, N., and Inoue, J. (2013). NF-kappaB non-cell-autonomously regulates cancer stem cell populations in the basal-like breast cancer subtype. *Nat Commun* 4, 2299.

Yarden, Y. (2001). Biology of HER2 and its importance in breast cancer. *Oncology* 61 *Suppl 2*, 1-13.

Yu, F., Yao, H., Zhu, P., Zhang, X., Pan, Q., Gong, C., Huang, Y., Hu, X., Su, F., Lieberman, J., *et al.* (2007). let-7 regulates self renewal and tumorigenicity of breast cancer cells. *Cell* 131, 1109-1123.

Zelnak, A.B., and Wisinski, K.B. (2014). Management of patients with HER2-positive metastatic breast cancer: Is there an optimal sequence of HER2-directed approaches? *Cancer*.

Zhang, X., and Munster, P.N. (2014). New protein kinase inhibitors in breast cancer: afatinib and neratinib. *Expert Opin Pharmacother* 15, 1277-1288.

Zhang, Y., Calado, R., Rao, M., Hong, J.A., Meeker, A.K., Dumitriu, B., Atay, S., McCormick, P.J., Garfield, S.H., Wangsa, D., *et al.* (2014). Telomerase variant A279T induces telomere dysfunction and inhibits non-canonical telomerase activity in esophageal carcinomas. *PloS One* 9, e101010.

## **CURRICULUM VITAE**

**Jillian Elizabeth Koziel**

### **Education**

2009-2015 Ph.D., Indiana University, Department of Medical and Molecular Genetics, Cancer Biology Minor, Indianapolis, IN  
2005-2009 B.A., Hanover College, Department of Biology, Chemistry Minor, Hanover, IN

### **Research/Work Experience**

2009-2015 Graduate research assistant (Mentor: Dr. Brittney-Shea Herbert, IU)  
My dissertation work focuses on inhibition of telomerase using a template antagonistic oligonucleotide (imetelstat) as a therapeutic agent for breast cancer. I am particularly interested in the effect of this agent on the cancer stem cell population and its use in combination with trastuzumab in HER2<sup>+</sup> breast cancer.

2008-2009 Undergraduate independent study (Mentor: Dr. Jennifer Osterhage, Hanover College)  
My project was to study the relationship between a vacuolar protein in yeast (Ape3p) and telomere length regulation.

2004-2008 Clerical Assistant, St. Joseph Physician Network, Kokomo, IN

### **Laboratory Skills**

- Cell Culture- cell proliferation, cell viability, clonogenic survival, drug interactions, mammosphere cultures, and cell line generation
- Flow Cytometry
- TRAP Assay
- DNA extraction
- PCR and real-time PCR
- Western Blotting
- Southern Blotting
- Small animal handling and injections
- Subcutaneous and mammary fat pad *in vivo* tumor models
- Immunofluorescence and fluorescent microscopy
- Computer software: Microsoft Office, Endnote, GraphPad Prism, Calcusyn, Adobe Photoshop and Illustrator, FlowJo, Cell Quest, and ImageJ

### **Grants, Awards, and Memberships**

2013-2014 NIH/NIAID T32 Training Grant (full stipend and tuition)  
2013 IU Simon Cancer Center AACR Travel Award  
2012 IUSM Graduate Student Organization Travel Award

2012-present American Association for Cancer Research, Associate Member, Women in Cancer Research Member  
2012 Department of Medical and Molecular Genetics Seminar Attendance Award  
2010-2011 IU Simon Cancer Center Cancer Biology Training Program Predoctoral Fellowship (full stipend and tuition)  
2008- 2009 Walne Grant (Hanover College Undergraduate Research Grant)  
2005 Hanover College Presidential Scholarship  
2005 Hanover College Dr. Agust Eiriksson Faculty Scholarship

### **Scientific Publications**

**Koziel JE** and Herbert B-S. (2015) The telomerase inhibitor imetelstat alone, and in combination with trastuzumab, decreases the cancer stem cell population and self-renewal of HER2<sup>+</sup> breast cancer cells. Accepted to *Breast Cancer Research and Treatment*.

Sauder CAM, **Koziel JE**, Choi M, Fox MJ, Grimes BR, Badve S, Blosser RJ, Radovich M, Lam C, Vaughan M, Herbert B-S, Clare SE. (2014) Phenotypic Plasticity in Normal Breast Derived Epithelial Cells. *BMC Cell Biol.* 15(1):20.

**Koziel JE**, Fox, MJ, Steding CE, Sprouse AA, Herbert, B-S. (2011) Medical Genetics and Epigenetics of Telomerase. *J Cell Mol Med.* 15:457-67.

### **Abstracts and Presentations**

**Koziel JE** and Herbert B-S. Targeting Telomerase in HER2 Positive Breast Cancer: Role of Cancer Stem Cells. 2013 Medical and Molecular Genetics Department Poster Session

**Koziel JE** and Herbert B-S. Targeting Telomerase in HER2 Positive Breast Cancer: Role of Cancer Stem Cells. 2013 Cancer Research Day, IU Simon Cancer Center

**Koziel JE**, Gryaznov S, Herbert B-S. (2013) Targeting Telomerase in HER2 Positive Breast Cancer: Role of Cancer Stem Cells. 2013 American Association for Cancer Research Annual Meeting: 2188

**Koziel JE** and Herbert B-S. Targeting Telomerase in HER2 Positive Breast Cancer: Role of Cancer Stem Cells. 2012 Medical and Molecular Genetics Department Poster Session

Sauder CAM, **Koziel JE**, Choi M, Fox MJ, Badve S, Blosser RJ, Mathieson T, Rufenbarger CA, Henry JE, Storniolo AMV, Herbert B-S, Clare SE. Phenotypic Plasticity in the Normal Breast. 2012 American Association for Cancer Research Annual Meeting: 3322

Sauder CAM, **Koziel JE**, Choi M, Fox MJ, Badve S, Blosser RJ, Mathieson T, Rufenbarger CA, Henry JE, Storniolo AMV, Herbert B-S, Clare SE. Phenotypic Plasticity in the Normal Breast. 2011 San Antonio Breast Cancer Symposium (SABCS): P5-05-02

**Koziel, JE**, Gentry E, and Herbert B-S. Targeting Telomerase in Recurrent and Metastatic Breast Cancer. 2011 Cancer Research Day, IU Simon Cancer Center  
**Koziel JE**, Brandau E, Shewmaker S, Lubrano A, Osterhage J. (2009) Investigating the Relationship Between Vacuolar Proteins and Telomere Length Regulation in *Saccharomyces cerevisiae*. Butler Undergraduate Research Conference.

### **Conferences and Workshops Attended**

- Amelia Project for Breast Cancer Research (Indiana University, February 2011)
- Breast Cancer Discovery Group Retreat (Purdue University, May 2011)
- Mammary Stem Cell Training Course (Jackson Laboratory, June 2011)
- San Antonio Breast Cancer Symposium (San Antonio, TX, December 2012)
- American Association for Cancer Research Annual Meeting (Washington, D.C., April 2013)